STRONG COUPLING PROBLEMS IN GAUGE THEORIES

Thesis

Submitted by

MARIFI GÜLER

for the degree of

DOCTOR OF PHILOSOPHY

Department of Physics

University of Edinburgh

OCTOBER, 1986.

I dedicate this thesis to the memory of

my Father

ACKNOWLEDGEMENTS

I would like to thank Professor D.J. Wallace for his guidance and encouragement during the course of my research.

It is also a great pleasure to thank all the staff and students in the Theory group for the support, discussions and friendship, particularly Alasdair Brown, David Chalmers, Stephen Goodyear, Alan McKane, Richard Kenway, David Scott and Charlie Wall. I am also indebted to those friends outside the department for their support and friendship throughout my stay in Edinburgh.

Thanks are also due to Mrs. Chester for her patient and efficient typing of this thesis.

I am grateful for the NATO grant given by the Scientific and Technical Research Council of Turkey.

ABSTRACT

This thesis is concerned with two topics: O(N) symmetric (abelian) scalar electrodynamics, and pure SU(3) lattice gauge theory in the two parameter fundamental-adjoint coupling plane.

The N component massive scalar electrodynamics is renormalized to one-loop in arbitrary d dimensions. It is shown that the infrared divergence problem can be avoided by the introduction of a gauge field mass equal to the scalar field mass. The renormalization group structure is studied in three dimensions, and the value of N, where the stability of the superconducting fixed points changes, is calculated. The ε expansion results are also reproduced.

The lattice formulation of gauge theories without matter fields is reviewed with particular reference to the strong coupling expansions.

The SU(3) fundamental-adjoint mixed action is used to calculate the strong coupling series for the string tension and mass gap to eighth and third orders respectively, in β and β_A. The constant string tension and mass gap lines in the fundamental-adjoint plane are drawn. The results and their Padé approximations are used to study the behaviour of $m/\sqrt{K}$ and the renormalization group function along the lines with various fixed β_A/β angles. $m/\sqrt{K}$ is found to behave universally in the negative adjoint plane but not for the non-negative values of β_A. It is also found that $m/\sqrt{K}$ shows a better scaling in the negative adjoint plane, and becomes smaller as more positive values of β_A are approached. The renormalization group function is found to become suppressed as the critical endpoint in the positive adjoint plane is approached.

CONTENTS

C O N T E N T S (Contd.)

CHAPTER 1

INTRODUCTION

Ever since the phenomenal success of quantum electrodynamics (QED), gauge theories have played the central role in the description of sub-atomic interactions. The $SU(2) \times U(1)$ gauge theory put forward by Glashow (1961), Salam (1968) and Weinberg (1967) as a unified theory of electromagnetic and weak interactions has been experimentally verified, firstly with the discovery of weak neutral currents [Hasert et al. (1973)] and more recently with the spectacular discovery of the $W^{\pm}$ and Z^{o} bosons [Arnison et al. (1983a,b); Banner et al. (1983); Bagnaia et al. (1983)]. The strong nuclear force is also thought to be described by a gauge theory, known as Quantum Chromodynamics (QCD). Its history began with a proposal that hadrons should be looked upon as bound states of localised but weakly interacting objects called quarks [Gell-Mann (1964); Zweig (1964)]. Gell-Man's so-called 'eightfold way' then accounted for the patterns seen in the hadronic spectrum. However, in order to satisfy the generalised Pauli exclusion principle, it was necessary to endow these objects with a new hidden quantum number which had three possible values. This new quantum number became known as colour. Initial evidence for the physical reality of quarks came from deep inelastic lepton-nucleon scattering experiments. It was found that the cross-sections satisfied Bjorken scaling [Bjorken (1969)]. All the aspects of hadronic physics are tied together in the

present model of QCD [Gross and Wilczek (1973a,b); Politzer (1973)] where the gauge group is SU(3) in colour space and the eight massless gauge particles are referred to as gluons.

The first non-abelian gauge theory was suggested by Yang and Mills (1954), which we shall look at in order to get a feeling for the properties of Yang-Mills systems. Consider the fermionic isospin doublet

$$\psi = \begin{pmatrix} \psi_1 \\ \psi_2 \end{pmatrix} \tag{1.1}$$

with the following free lagrangian

$$\mathcal{L}_o = \bar{\psi}(x) \{ i \gamma^\mu \partial_\mu - m \} \psi(x) \quad . \tag{1.2}$$

The global SU(2) transformation

$$\psi(x) \rightarrow U(\theta)\psi(x) = e^{-\frac{i}{2} \underline{\tau} \cdot \underline{\theta}} \psi(x) \tag{1.3}$$

leaves this lagrangian invariant. Here $\underline{\tau} = (\tau^1, \tau^2, \tau^3)$ are the Pauli matrices and $\underline{\theta}(\theta_1, \theta_2, \theta_3)$ are space-time independent parameters. We want to modify the lagrangian in such a way that it will be invariant under local transformations. By a local transformation we mean a transformation where $\underline{\theta}$ is space-time dependent. The modified lagrangian can be obtained in the following way. Firstly, we introduce vector gauge fields A_μ^i , $i = 1,2,3$ (one for each group generator) and then employ a substitution

$$\partial_\mu \rightarrow D_\mu = \partial_\mu - i \frac{g}{2} \tau^i A_\mu^i \quad . \tag{1.4}$$

After this substitution the lagrangian is invariant under the local transformations provided that $A^i_\mu(x)$ transforms as

$$A^i_\mu(x) \rightarrow A^i_\mu(x) + \frac{1}{2}\partial_\mu \theta_i(x) + \varepsilon_{ijk}\theta^j(x) A^k_\mu(x) \qquad (1.5)$$

Thus, the modified lagrangian describes the interaction between the SU(2) matter fields ψ and the gauge fields A^i_μ. Addition of the pure gauge term $-\frac{1}{4} F^i_{\mu\nu} F^{i\mu\nu}$ yields the complete Lagrangian of the theory

$$\mathcal{L} = -\frac{1}{4} F^i_{\mu\nu} F^{i\mu\nu} + i\bar{\psi}\gamma^\mu D_\mu \psi - m\bar{\psi}\psi \qquad (1.6)$$

where

$$F^i_{\mu\nu} = \partial_\mu A^i_\nu - \partial_\nu A^i_\mu + g\,\varepsilon^{ijk} A^j_\mu A^k_\nu \quad . \qquad (1.7)$$

Here g is the coupling constant of the theory. Note that the pure gauge term contains factors which are trilinear and quadrilinear in A_μ which correspond to self interactions of the non-abelian gauge fields. These prove to be the fundamental ingredient which give non-abelian gauge theories their rich structure.

One important feature of gauge theories is that they are renormalizable as long as no terms (like mass terms for the gauge particles) which break the gauge invariance, are added to the lagrangian. This situation posed some problems for the $SU(2) \times U(1)$ model where one needs only one massless gauge particle instead of four. That is because the particles responsible for carrying the

the weak force must be very massive because of the short range of interaction. This difficulty was circumvented in applying the ideas of spontaneous symmetry breaking (already known in the context of superconductivity to gauge theories [Higgs (1964a,b; 1966)]. By the addition of scalar fields to the lagrangian in a fully gauge invariant way but with a potential which has a degenerate vacuum state, the $SU(2) \times U(1)$ theory is spontaneously broken to the U(1) gauge theory of QED. Hence, three of the massless vector bosons become massive.

A better understanding of the origin of spontaneous symmetry breaking can be found in the work of Coleman and Weinberg (1973). They have studied self-interacting neutral scalar fields and scalar electrodynamics, U(1) gauge theory of self-interacting charged scalar fields, with corresponding lagrangians

$$\mathcal{L} = \frac{1}{2} \partial_\mu \phi \, \partial^\mu \phi - \frac{1}{2} m^2 \phi^2 - \frac{g}{4!} \phi^4 \tag{1.8}$$

and

$$\mathcal{L} = -\frac{1}{4} F_{\mu\nu} F^{\mu\nu} + \partial_\mu \phi \, \partial^\mu \phi^\dagger - m^2 \phi^\dagger \phi + ie\phi \, A^\mu \partial_\mu \phi^\dagger - ie\phi^\dagger \, A^\mu \partial_\mu \phi$$
$$+ e^2 \, A_\mu A^\mu \, \phi^\dagger \phi - \frac{g}{4} (\phi^\dagger \phi)^2 \tag{1.9}$$

respectively. Using the functional integral methods the effective potential, V_{eff}, was calculated to one-loop in perturbation theory. It was found to be

$$V_{eff} = \frac{g}{4!} \phi_c^4 + \frac{g^2 \, \phi_c^4}{256 \, \pi^2} \left[\log \frac{\phi_c^2}{M^2} - \frac{25}{6} \right] \tag{1.10}$$

for the massless version of the self-interacting neutral theory. Here M is some number with the dimensions of a mass and the classical field ϕ_c is given by

$$\phi_c(x) = \frac{<0^+|\phi(x)|0^->}{<0^+|0^->} \quad . \tag{1.11}$$

Even though the classical potential (tree level) has its minimum at the origin the one-loop potential has developed a minimum away from the origin and the origin has become a maximum. Thus, radiative corrections to the effective potential have caused spontaneous symmetry breaking. The effect of radiative corrections on the massless scaler electrodynamics is the same as the occurrence of the Higgs phenomenon. The only difference is that the driving mechanism of the instability is not a negative mass term in the lagrangian, but certain effects of higher-order processes involving virtual photons. On the other hand, radiative corrections do not cause the Higgs phenomenon to occur for the massive scalar electrodynamics. It stays as the conventional massive scalar electrodynamics.

The effective potential given by eqn. (1.10) seems to depend on one arbitrary scale M^2 but it really does not, because, considering the renormalized coupling constant g is defined by

$$g \equiv \left.\frac{d^4V_{eff}}{d\phi_c^4}\right|_{\phi_c = M} , \tag{1.12}$$

if we change the scale from M^2 to M'^2, we have to change at the same time g to g', where

$$g' = g + \frac{3g^2}{16\pi^2} \log \frac{M'}{M} \quad . \tag{1.13}$$

Hence, the effective potential is form invariant under this reparametrization:

$$V_{eff}(g', M') = V_{eff}(g, M) \quad . \tag{1.14}$$

This shows that the physics does not change, only our way of interpreting the constants. This statement can be expressed as an equation

$$(M \frac{\partial}{\partial M} + \beta \frac{\partial}{\partial g} + n\omega)\Gamma^{(n)}(x_1, \ldots, x_n) = 0 \tag{1.15}$$

for an appropriate choice of the coefficients β and ω. Here $\Gamma^{(n)}$ is the one-particle-irreducible Green's function with n external legs. By dimensional analysis, β and ω can depend only on g. Note that eqn. (1.15) is the renormalization group equation of Gell-Mann and Low (1954). Also note that the renormalization group function β plays an important role in extracting physics from the theory.

The functional integration method used in the calculation of effective potential is one of the most powerful methods of contemporary theoretical physics, enabling us to simplify, accelerate, and gain a deeper understanding of the process. The idea of introducing path integrals via the superposition principle in quantum mechanics originates in the work of Dirac (1933), and was developed by Feynman (1948). Feynman constructed a new formulation of QED, based on the method of path integration, and developed the famous diagram technique of perturbation theory. This new theory has substantially

simplified calculations and has developed to construct the theory of renormalization. Schwinger (1951) developed an equivalent approach based on functional differentiation. This work has proved to be the most flexible tool in suggesting new developments in quantum field theory, and extended to the study of spontaneous symmetry breaking and effective potential [Jona-Lasinio (1964)].

A particularly fruitful field of applications of functional integrals was found in the quantization of non-abelian gauge fields [Faddeev and Popov (1967); De Witt (1967a,b)]. The method developed by Faddeev and Popov is based on the following idea. As an example, consider the SO(n) gauge theory of scalar field ϕ with n neutral components. The problem arises due to the gauge invariance. The action $S[\phi, A^{i\mu}]$ takes the same value on a large space (infinite dimensional manifold) of field configurations. Consequently the generating functional

$$Z = \int \{d\phi\}\{dA^{i\mu}\}\, e^{iS[\phi,\, A^{i\mu}]} \tag{1.16}$$

will diverge. Here the integral denotes functional integration over all possible field configurations. The classes of those fields which can be obtained from other fields through gauge transformations should be counted only once. In other words, the action should be a functional defined over all inequivalent classes. It can be accomplished if the integration is taken over the surface in the manifold of all fields whose elements intersect each of those classes once. Then each class will have exactly one representative on that surface. The integration measure arising on such surfaces changes

with the variation of the surface, but all physical results must be independent of the choice of the surface. After these considerations the generating functional picks up an additional δ-functional and a Jacobian factor as follows:

$$Z = \int \{d\phi\}\{dA^{i\mu}\}\, e^{iS[\phi,A^{i\mu}]}\delta[H_i]\det\left(\frac{\delta H_i}{\delta\theta_j}\right) \tag{1.17}$$

where i, j are group labels, θ_j are group parameters, and the functional H_i defines gauge conditions

$$H_i[A^{j\mu}] = 0 \ . \tag{1.18}$$

The δ-functional is cancelled out if one makes a replacement of the action

$$S \rightarrow S - \frac{1}{2\alpha}\sum_i \int d^4x(\partial_\mu A^{i\mu})^2 \ , \tag{1.19}$$

where α is a gauge parameter. The Jacobian factor can also be replaced by a modification of the lagrangian using the functional integration techniques

$$\det\left(\frac{\delta H_i}{\delta\theta_j}\right) = \int\{d\bar{\eta}\}\{d\eta\}\exp\left(-i\int d^4x\, d^4y\, \bar{\eta}^i(x)\,\frac{\delta H_i(x)}{\delta\theta_j(y)}\,\eta^j(y)\right) \tag{1.20}$$

where the fields η and $\bar{\eta}$ are, spatially, scalars. They transform under the adjoint representation of the group. However, they must be anticommuting variables. That is because, otherwise, the Jacobian factor has a negative power. This seems to violate the spin statistics theorem. Nevertheless, these particles do not occur as external

particles; they are fictitious particles which only occur as internal lines in Feynman diagrams in order to produce the effect of the Jacobian factor. They are referred to as ghost particles.

The final form of the generating functional reads

$$Z = \int \{d\eta\}\{d\bar{\eta}\}\{d\phi\}\{dA^{i\mu}\}\, e^{i S_{eff}} \tag{1.21}$$

where

$$S_{eff} = \int d^4x \Big[-\frac{1}{4} F^i_{\mu\nu} F^{i\mu\nu} + \frac{1}{2}(D_\mu \phi)^2 - V(\phi) - \frac{1}{2\alpha} \sum_i (\partial_\mu A^{i\mu})^2 + \partial^\mu \bar{\eta} D_\mu \eta \Big] \tag{1.22}$$

which gives us the Feynman rules.

Functional integral formulation of quantum theory reveals deep connections with statistical mechanics. That is basically because of the fact that both the generating functional of quantum theory and the partition function of statistical physics are path integrals. In general, a d-space-time dimensional quantum field theory is equivalent to a d-Euclidean dimensional classical statistical system. Quantum statistical mechanics can also be related to quantum field theory using the transfer matrix. Thus, quantum field theory can be expressed in the language of statistical mechanics and vice versa.

As a simple example, consider the self-interacting field theory given by lagrangian (1.8). If we force the mass to vanish the system undergoes spontaneous symmetry breaking. In statistical physics language, that is to say that a ferromagnet undergoes a second order phase transition as the temperature lowered to the

critical value. By a second order phase transition we mean that the second order derivative of the free energy is discontinuous. In general, n^{th} order phase transition means that the n^{th} derivative (but not $(n-1)^{th}$) of the free energy, is discontinuous.

Theoretical understanding of critical phenomena and phase transitions has greatly advanced since the introduction of the renormalization group to the subject [Wilson (1972)] and the use of field theory in which the lattice model of statistical mechanics is transformed into a representation by continuous classical fields [Brézin et al. (1973a,b)].

In order to study a critical phenomena problem using the renormalization group techniques, one must describe quantitatively the asymptotic behaviour near its critical point. One has to determine the position of the fixed points in the space of coupling constant parameters and classify them according to the type of renormalization group flow attraction they exhibit. Then, one can calculate various quantities, like the critical exponents, at least, near four dimensions [Wilson and Fisher (1972)] as an expansion in $\varepsilon = 4 - d$. The type of phase transition the system undergoes is also related to the structure of the renormalization group flows.

We now turn to QCD and underline some of its aspects which will be relevant to the work in Chapters 3 and 4.

The features which QCD exhibits are tightly connected to the fact that it is an unbroken non-abelian theory. It was shown [Gross and Wilczek (1973a,b); Politzer (1973)] in weak coupling

perturbation theory, $\beta(g)$, the function which controls the evolution of the effective coupling at different energies [Callan (1970); Symanzik (1970)] is given by

$$\beta(g) = -\frac{1}{16\pi^2}(11 - \frac{2}{3}n_f)g^3 + O(g^5) \qquad (1.23)$$

in the presence of n_f quark flavours. Thus the β function has a negative gradient at the origin provided there are no more than sixteen flavours of quarks. The evolution of the effective coupling at momentum scale Q is then governed by the differential equation

$$Q\frac{\partial}{\partial Q}\, g(Q^2) = \beta(g) \qquad (1.24)$$

which has a solution given by

$$\frac{g^2}{4\pi} = \frac{6}{33 - 2n_f}\,\frac{1}{\log(Q^2/\Lambda^2)} \qquad (1.25)$$

where Λ is the fundamental momentum scale. Thus g^2 decreases as Q^2 increases, a property which is known as asymptotic freedom. Therefore, weak coupling perturbation theory becomes more reliable at shorter distances. Hence, QCD can be used perturbatively to calculate physical processes when all the quarks involved are in the deep Euclidean region; this regime applies in high energy e^+e^- annihilation and lepton-hadron scattering, where perturbative results can be successfully interpreted in terms of jets. However at low energies (large distances) the effective coupling will become large and we will reach a point where perturbation theory will inevitably break down. But if QCD is a complete description of the strong interactions

between quarks, this is precisely the regime in which it should be possible to calculate the hadron spectrum from first principles. Furthermore no experiments, except for that of La Rue et al. (1981) which is still surrounded by controversy, have been able to find free quarks and so it appears that quarks and gluons are always bound together in such a way that they are permanently confined to lie within overall SU(3) colour singlet states. It is clear that to be able to explore the full range of the physics described by QCD some form of calculation scheme, which does not involve a regularization procedure that is tied down to weak coupling perturbation theory, is needed, so that we are able to perform calculations in the strong coupling constant region. Such a non-perturbative calculation scheme was introduced by Wilson (1974) when he formulated gauge theories on a discrete space-time lattice. An alternative but equivalent formulation, introduced by Kogut and Susskind (1975), uses the Hamiltonian on a discrete three dimensional space with a continuous time variable.

On a lattice, the theory becomes mathematically well-defined and can be studied in various ways. Lattice perturbation theory, although somewhat awkward, recovers all the conventional results of other regularization schemes. Discrete space-time, however, is particularly well-suited for a strong coupling expansion. Confinement is natural in the strong coupling limit of the lattice theory; however, this is not the region of direct physical interest, for which a continuum limit is necessary. The coupling constant on the lattice represents a bare coupling at a length scale of the lattice spacing. As a consequence of the asymptotic freedom

in non-abelian gauge theories, the bare coupling must be taken to zero as the lattice spacing decreases towards the continuum limit. Thus we are inevitably led out of the strong coupling regime and into a weak coupling domain. Along the way confinement might be lost. That is because, since lattice gauge theory is a quantum theory, it can be expressed in the language of statistical mechanics and in a general statistical system one might expect to encounter phase transitions.

Even abelian gauge theories, like QED, formulated on the lattice, yields confinement in the strong coupling region. However, there exists a phase transition [De Grand and Toussaint (1980); Lautrup and Nauenberg (1980a)] separating the strong coupling confining phase from a phase with massless photons, which gives rise to the usual Coulomb force law between electrons. However, as will be discussed in Chapter 3, it does not appear that non-abelian lattice gauge theories exhibit such a deconfining phase transition.

In Chapter 2 we will study scalar electrodynamics perturbatively as a problem in quantum field theory and as a model for the study of phase transitions in liquid crystals and superconductors. We will see that the deeper understanding of the problem requires a non-perturbative calculation such that strong coupling effects are included. In Chapter 3 our subject will be pure (without matter fields) lattice gauge theories and techniques which provide us with a strong coupling expansion. In Chapter 4 we will study pure SU(3) lattice gauge theory in the so-called fundamental-adjoint plane. Finally in Chapter 5 we will summarise the results and conclusions.

CHAPTER 2

SCALAR ELECTRODYNAMICS

In this chapter we study the infrared divergence problem of massive scalar electrodynamics and renormalize the theory to one-loop in arbitrary d dimensions. We find the β functions and the fixed points of the theory with N scalar components, draw the renormalization group flows in 3 dimensions and discuss the relevance to phase transitions in superconductors. We also reproduce the results already found by using the expansion in $\varepsilon = 4 - d$.

2.1 A Brief Introduction

As we mentioned in the introduction there are several reasons to study scalar electrodynamics and one of them is its relevance to the character of phase transitions in superconductors and liquid crystals. Fluctuation-corrected mean-field theory and an expansion in $\varepsilon = 4 - d$ were used to show that phase transitions in superconductors [Halperin et al. (1974)] and liquid crystals [Halperin and Lubensky (1974)] may actually be first order in character. The feature which led to these predictions was the coupling of the order parameter to a gauge field such as the vector potential in a superconductor, or the director in a liquid crystal. Hence these systems can be studied in terms of scalar electrodynamics defined by the lagrangian (1.9). However, for a generalized superconductor, one has to consider a theory with arbitrary N real scalar fields rather than two. The ε expansion of the N component theory

suggests that the phase transition, which occurs as the scalar field mass m passes through a critical value $m_c(g,e)$, is driven to first order by fluctuations whenever $N < N_0 = 365.9$, while for $N > N_0$ it may be second order for $g \gtrsim \text{constant} \times e^2$ [Chen et al. (1978)]. The first order character is inferred essentially from the absence or inaccessibility of an infrared-stable fixed point of the renormalization group. However, the construction of a free energy which explicitly verifies such behaviour can be carried through in practice only when the electric charge e is sufficiently small [Lawrie (1982)]. For further discussion we refer the reader to Chen et al. (1978) and more references therein.

A Monte Carlo simulation of a lattice version of the two-component model ($N = 2$) in three dimensions was carried out, which provides no evidence for a first-order transition [Dasgupta and Halperin (1981)]. This suggests that the ε expansion is correct only near four dimensions and not applicable in three dimensions (i.e. $\varepsilon = 1$); hence, one has to do a perturbative calculation in three dimensions rather than an expansion in ε to make a comparison with the Monte Carlo result, or else that N_0 in three dimensions is actually less than two. It could also be that, at least for the value of the charge used in the simulation, some mechanism inaccessible to perturbation theory is responsible for the continuous nature of the transition. To investigate these questions further we do a perturbative calculation in three dimensions to one-loop. As we will see, the way we overcome the infrared divergence problem is also of interest.

2.2 The Infrared Divergence Problem

We shall consider the two-component model given by lagrangian (1.9) and solve the infrared divergence problem which arises, due to the fact that the gauge field is massless; we consider the N-component model later on.

However, before we discuss the problem for scalar electrodynamics we shall consider the problem for QED and indicate how it was solved in the literature. One approach to the problem uses dimensional regularization ['t Hooft and Veltman (1972)], where the infrared divergence appears as a pole in the dimension plane, just like the ultraviolet divergence and can be cured by arranging the renormalization to cancel out the divergences in the $d \to 4$ limit [Gastmans and Meuldermans (1973)]. It is also possible to solve the problem by including a photon mass term in the action. Before we introduce a photon mass we shall note that in a gauge theory (abelian or non-abelian), because of the local gauge invariance, not all the Green's functions are independent. They are related by Ward identities, as described in any text-book on gauge theories. However, as we mentioned in the introduction, to quantize gauge theories one defines an effective action by introducing into the original action a gauge fixing term and ghost fields. The gauge fixing term is not gauge invariant and hence raises the question of the validity of the Ward identities. The question was solved by restoring the invariance of the effective action by using a special gauge transformation under which variation of the gauge fields and the matter fields depend on Grassmann parameters rather than the usual commuting parameters [Becchi, Rouet and Stora (1974)].

Invariance of the effective action under BRS transformation imposes a set of functional constraint equations on the generating functional, from which one can extract the Ward identities. If one introduces a gauge field mass term into the effective action, that breaks BRS invariance, hence we must expect it to spoil the Ward identities. However, that is not the case for QED because we can still maintain BRS invariance, even in the presence of a photon mass term, provided that the ghost acquires the same mass which decouples anyway.

For scalar electrodynamics we apply a gauge transformation similar to BRS of QED. The effective action in d dimensions is given as

$$S_{eff} = \int d^d x \{ \mathcal{L} - \frac{1}{2\alpha} (\partial \cdot A)^2 + i(\partial_\mu \bar{\eta})(\partial^\mu \eta) \} \qquad (2.1)$$

where $\mathcal{L}$ is lagrangian (1.9). The second term in (2.1) is the gauge fixing term and the third term is the ghost kinetic energy term. Note that η is a Grassmann variable. The gauge transformation

$$\begin{aligned} A_\mu &\to A_\mu - \frac{1}{e} \chi \partial_\mu (\eta + \bar{\eta}) \\ \phi &\to \phi - i\chi(\eta + \bar{\eta})\phi \\ \eta &\to \eta - \frac{i}{e\alpha} (\partial \cdot A)\chi \end{aligned} \qquad (2.2)$$

leaves S_{eff} invariant. Here χ is a space-time independent real Grassmann variable. Note that $\chi^2 = 0$ and $\chi\eta = -\eta\chi$ as a property

of Grassmann variables. Suppose we include a photon mass term $\frac{1}{2} r^2 A_\mu A^\mu$ in the action. The variation of this term under (2.2) will be

$$\delta(\tfrac{1}{2} r^2 A_\mu A^\mu) = -\frac{1}{e} r^2 \chi A^\mu \partial_\mu (\eta + \bar{\eta}) \quad . \tag{2.3}$$

One can also show that

$$\delta(-ir^2 \bar{\eta} \eta) = -\frac{1}{e\alpha} r^2 \chi A_\mu \partial^\mu (\eta + \bar{\eta}) \quad . \tag{2.4}$$

That is to say, in the presence of the photon mass term, one can still obtain an invariant effective action provided the ghost acquires a mass αr^2. Since the ghost decouples in our theory the presence of the photon mass term does not spoil the Ward identities. Note that this procedure can not be applied to non-abelian gauge theories. The reason is, of course, that the ghost field and the gauge field couple in these theories.

2.3 Renormalization

Any quantum field theory needs to be renormalized and the basis of renormalization is to obtain a renormalized lagrangian by substituting the quantities in the original lagrangian with the bare ones. In our theory (including the photon mass term) the bare parameters can be expressed in terms of the renormalized ones as

$$\phi_B = Z_2^{1/2}\phi, \qquad A_\mu^B = Z_3^{1/2}A_\mu, \qquad \mu^2 = \bar{Z}\, Z_2^{-1}\, m^2$$

$$e_B = Z_1 Z_2^{-1}\, Z_3^{-\frac{1}{2}}\, e, \qquad \lambda = Z_o Z_2^{-2}\, g, \qquad r_o^2 = Z_r\, Z_3^{-1}\, r^2. \tag{2.5}$$

Note that for a complete renormalization of the theory one also needs to consider the gauge fixing term and renormalize α as well. However, for our purposes that is not needed.

One can show that the Ward identity for scalar electrodynamics is given by

$$Z_2 = Z_1 \tag{2.6}$$

as in QED. Because of that identity some terms in (2.5) reduce to

$$\phi_B = Z_1^{\frac{1}{2}}\,\phi, \qquad \mu^2 = \bar{Z}\, Z_1^{-1}\, m^2, \qquad e_B = Z_3^{-\frac{1}{2}}\, e, \tag{2.7}$$

$$\lambda = Z_o\, Z_1^{-2}\, g.$$

In a quantum field theory, the renormalized lagrangian is related to the original one by the addition of some counterterms, which can be obtained, in our theory, if we rewrite the renormalization constants as

$$Z_1 = 1 + B, \quad \bar{Z} = 1 + C, \quad Z_3 = 1 + D, \quad Z_o = 1 + E$$

$$Z_r = 1 + H \tag{2.8}$$

where B, C, D, E and H are to be decided by the choice of a renormalization scheme. However, before we specify a scheme we shall note that the interaction part of the renormalized lagrangian in

momentum space then reads

$$\begin{aligned}\mathcal{L}_{\text{Int.}}^{\text{Ren}} = & - e(1 + B)(k + k')^{\mu} A_{\mu} \phi^{+}(-k)\phi(k') \\ & + 2e^2(1 + B)g^{\mu\nu} \frac{A_{\mu}A_{\nu}}{2} \phi^{+}\phi - \frac{g}{4}(1 + E)(\phi^{+}\phi)^2 \\ & + [(p^2 g^{\mu\nu} - p^{\mu}p^{\nu})D - g^{\mu\nu} r^2 H] \frac{A_{\mu}(p)A_{\nu}(p)}{2} \\ & - (k^2 B + m^2 C)\ \phi^{+}(k)\phi(k) \quad .\end{aligned} \tag{2.9}$$

We are interested in calculation of one-particle irreducible Green's functions of the form $\Gamma^{\mu_1,\ldots,\mu_N\ (M,N)}(k_1,\ldots, k_M; p_1,\ldots, p_N)$ with M external scalar field legs and N external photon legs, as described in Fig. 2.1.

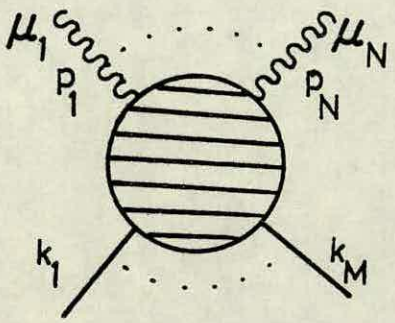

Fig. 2.1.

To calculate the Green's functions we need to know the two propagators (photon and scalar field) which are given in Fig. 2.2

and the Feynman rules which can be concluded from the lagrangian (2.9), as given in Fig. 2.3 and Fig. 2.4. The counterterm diagrams given in Fig. 2.4 arise due to the counterterms in the renormalized lagrangian and they are needed to get a renormalized theory. However, the ultimate goal of the renormalization procedure is to evaluate the renormalization constants and even after consideration of the counterterm diagrams, these constants are still arbitrary. The well-known procedure to overcome this arbitrariness in a quantum field theory goes through the specification of a renormalization scheme. A renormalization scheme consists of a set of equations that the Green's functions should satisfy to the lowest order, so as to fix unambiguously the renormalization constants to higher orders.

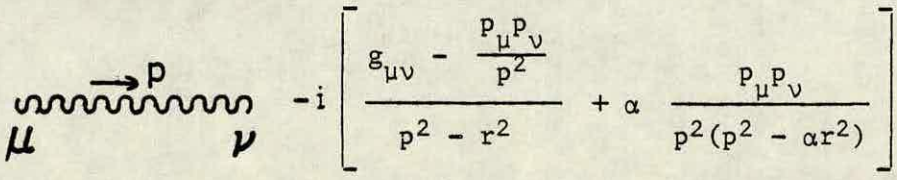

$$-i\left[\frac{g_{\mu\nu} - \frac{p_\mu p_\nu}{p^2}}{p^2 - r^2} + \alpha\,\frac{p_\mu p_\nu}{p^2(p^2 - \alpha r^2)}\right]$$

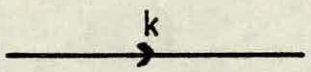

$$\frac{i}{k^2 - m^2}$$

Fig. 2.2. The photon and the scalar field propagators with momentum p and k and with mass r and m respectively. α in the photon propagator is the gauge parameter.

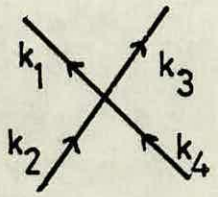

$$- ig\, \delta(k_2 + k_4 - k_1 - k_3)$$

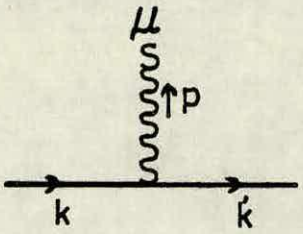

$$- ie(k + k')^{\mu}\, \delta(k - k' - p)$$

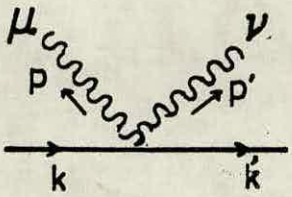

$$2ie^2\, g^{\mu\nu}\, \delta(k - k' - p - p')$$

Fig. 2.3. The Feynman rules of the scalar electrodynamics.

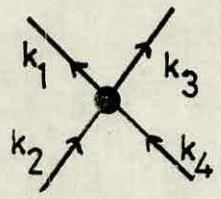

$$- igE\delta(k_2 + k_4 - k_1 - k_3)$$

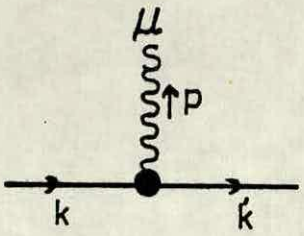

$$- ie\, B(k + k')^{\mu}\, \delta(k - k' - p)$$

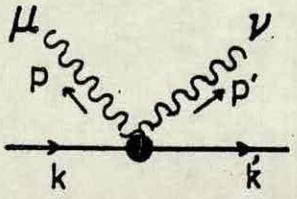

$$2ie^2\, g^{\mu\nu} B\, \delta(k - k' - p - p')$$

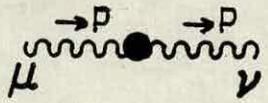

$$i[(p^2\, g^{\mu\nu} - p^{\mu}p^{\nu})D - g^{\mu\nu}\, r^2\, H]$$

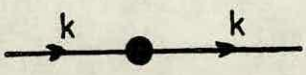

$$- i(k^2 B + m^2 C)$$

Fig. 2.4. The Feynman rules corresponding to the counter-terms in lagrangian (2.9).

Of course, we also require that the scheme should preserve the Lorentz invariance and the gauge invariance. The final but important condition that we want to be fulfilled is that the Ward identity (2.6) should be satisfied to every order by the choice of the scheme. Any renormalization scheme which does not realize these conditions is not sensible and should not be adopted. It is possible to specify a consistent scheme as follows:

$$\Gamma^{(4,0)}(k_1 = k_2 = k_3 = k_4 = 0) = -g \tag{2.10}$$

$$\Gamma^{(2,0)}(k = 0) = -m^2 \tag{2.11}$$

$$\frac{\partial}{\partial k^2}\,\Gamma^{(2,0)}(k)\Big|_{k=0} = 1 \tag{2.12}$$

$$\frac{\partial}{\partial k^\mu}\,\Gamma^{\mu(2,1)}(k' = k,\ p = 0)\Big|_{k=0} = -2de \tag{2.13}$$

$$g_{\mu\nu}\,\Gamma^{\mu\nu(2,2)}(k = k' = p = p' = 0) = 2de^2 \tag{2.14}$$

$$g_{\mu\nu}\Gamma^{\mu\nu(0,2)}(p = 0) = g_{\mu\nu}\Big[\ \mu \sim\sim\sim\sim\sim\sim \nu\ \Big]\Big|_{p=0} \tag{2.15}$$

$$\frac{\partial}{\partial p^2}\,g_{\mu\nu}\,\Gamma^{\mu\nu(0,2)}(p)\Big|_{p=0} = \frac{\partial}{\partial p^2}\,g_{\mu\nu}\,\Big[\ \mu \sim\sim\sim\sim\sim\sim \nu\ \Big]\Big|_{p=0}\ . \tag{2.16}$$

Here $\Big[\ \mu \sim\sim\sim\sim\sim\sim \nu\ \Big]$ is defined as the matrix inverse of the propagator

$$\Big[\ \mu \sim\sim\sim\sim\sim\sim \nu\ \Big] \times \mu \sim\sim\sim\sim\sim\sim \nu = i\ ;$$

it arises due to the fact that we are dealing with one-particle irreducible Green's functions which do not get propagators attached to their external legs. However one does not need the explicit expression for 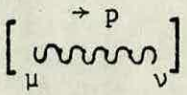 in the calculations. The equations are sufficient to calculate the renormalization constants, which is the subject of the next section, and they clearly fulfil the conditions we specified except that they might violate the Ward identity. We will discuss this particular point in great detail in the following section. The final remark of this section is that in the renormalization scheme we chose the external momenta are set to be zero because the integrals are easier to evaluate with a vanishing momentum. In fact, one can choose the external momenta to be any value, the choice is totally arbitrary; the physics is not dependent on the choice of the renormalization points. That is because the change in the renormalization points will be compensated by the change in the renormalized parameters to leave the physics invariant, which is of course the meaning of renormalization group invariance.

2.4 The Renormalization Constants

So far, we have completed the essential material for the calculation of the renormalization constants. However, as was mentioned, we are rather interested in the N-component theory; hence, we shall generalise the procedure and calculate those constants for the generalised theory. Consider the interaction part of lagrangian

(1.9) and make the substitution

$$\phi \rightarrow \frac{1}{\sqrt{2}} (\phi_1 + i\phi_2)$$
$$\phi^+ \rightarrow \frac{1}{\sqrt{2}} (\phi_1 - i\phi_2) \qquad (2.17)$$

to get

$$\mathcal{L}_{int} = - e(k + k')^\mu A_\mu (\frac{\phi_1^2}{2} + \frac{\phi_2^2}{2})$$
$$+ 2e^2 g^{\mu\nu} \frac{A_\mu A_\nu}{2} (\frac{\phi_1^2}{2} + \frac{\phi_2^2}{2})$$
$$- g (\frac{\phi_1^4}{4!} + \frac{\phi_2^4}{4!}) - \frac{g}{3} (\frac{\phi_1^2}{2} \frac{\phi_2^2}{2}) . \qquad (2.18)$$

This two-component lagrangian can be generalised to N-component one (i.e. O(N) symmetry case) as follows:

$$\mathcal{L}_{int} = -e(k + k')^\mu A_\mu \sum_{i=1}^{N} \frac{\phi_i^2}{2}$$
$$+ 2e^2 g^{\mu\nu} \frac{A_\mu A_\nu}{2} \sum_{i=1}^{N} \frac{\phi_i^2}{2}$$
$$- g \sum_{i=1}^{N} \frac{\phi_i^4}{4!} - \frac{g}{3} \sum_{\substack{j=1 \\ i>j}}^{N} \frac{\phi_i^2}{2} \frac{\phi_j^2}{2} . \qquad (2.19)$$

Comparison of (2.18) and (2.19) indicates that the Feynman rules and the renormalization for the two-component model and the N-component model are exactly the same except that the symmetry

factors of some Feynman diagrams will be different. The symmetry factor calculation for the O(N) symmetric scalar electrodynamics is very similar to the O(N) symmetric ϕ^4 model which is discussed by various authors. See, for example, Balian and Toulouse (1973) and Fisher (1973). In practice, one can calculate the symmetry factors by fixing the external legs to a certain label, while running the internal legs from 1 to N. In Fig. 2.5 we present the symmetry factors of some diagrams.

We shall continue the section with the calculation of the renormalization constants to one-loop. Note that it is possible to calculate the renormalization constant B from three different equations, namely (2.12), (2.13) and (2.14). If we get the three calculations to give the same result, that will mean that we are preserving the Ward identity at least to one-loop in perturbation theory; otherwise, it is not preserved. Let us calculate B via equation (2.14) first. The diagrams which contribute to $\Gamma^{\mu\nu(2,2)}$ to one-loop are given in Fig. 2.6. Our choice of gauge will be the Landau gauge, i.e. $\alpha = 0$ in the photon propagator. The reason for that choice is that, because in our scheme external momenta are set to zero, the momentum of the internal scalar field is the same as that of the internal photon and vanishes when it is contracted with the photon propagator leading to the contribution from some of the diagrams to vanish. Four of the diagrams in Fig. 2.6 do not contribute to $\Gamma^{\mu\nu(2,2)}(k = k' = p = p' = 0)$ for that reason. Hence one can easily derive

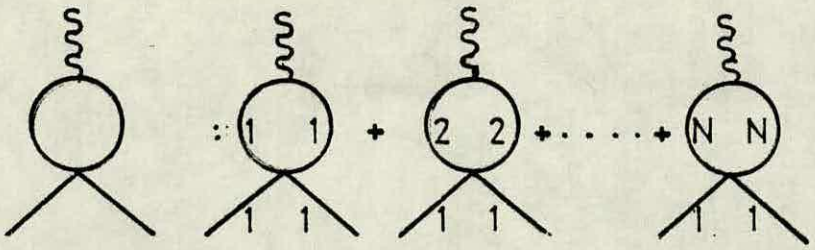

$$: \quad \frac{1}{2} \quad + \quad \frac{1}{2} \times \frac{1}{3} \quad + \ldots\ldots + \frac{1}{2} \times \frac{1}{3} \quad = \quad \frac{1}{2} + \frac{1}{6}(N-1) \quad = \quad \frac{N+2}{6}$$

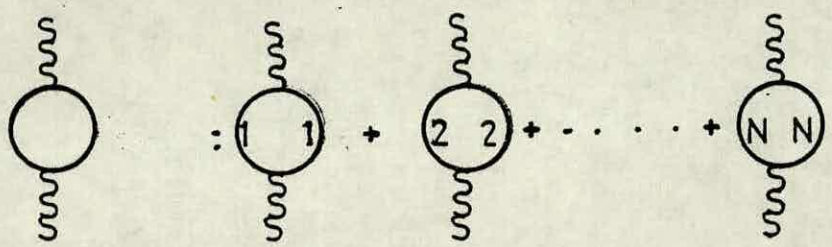

$$: \quad \frac{1}{2} \quad + \quad \frac{1}{2} \quad + \ldots\ldots + \quad \frac{1}{2} \quad = \quad \frac{N}{2}$$

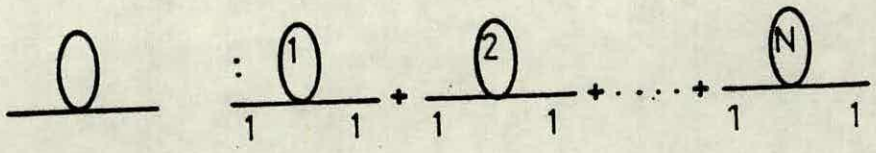

$$: \quad \frac{1}{2} \quad + \quad \frac{1}{2} \times \frac{1}{3} \quad + \ldots\ldots + \quad \frac{1}{2} \times \frac{1}{3} \quad = \quad \frac{1}{2} + \frac{1}{6}\,(N-1) \quad = \quad \frac{N+2}{6}$$

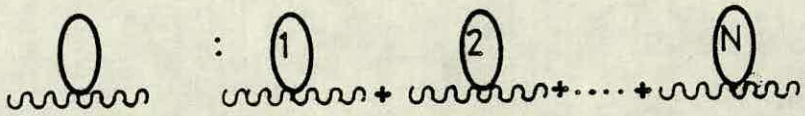

$$: \quad \frac{1}{2} \quad + \quad \frac{1}{2} \quad + \ldots\ldots + \quad \frac{1}{2} \quad = \quad \frac{N}{2}$$

Fig. 2.5 (see over): Symmetry factor calculation for the N-component model.

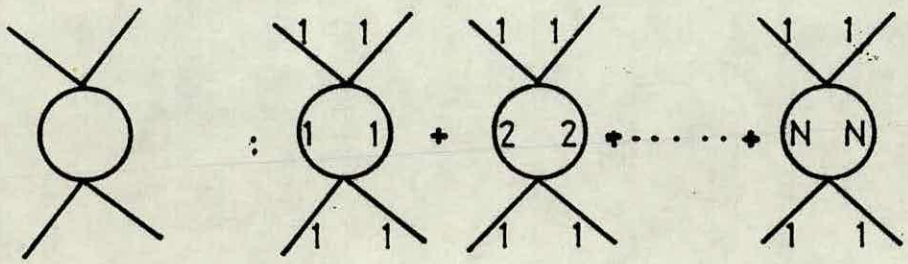

$$: \quad \frac{3}{2} \quad + \quad \frac{3}{2}\times\frac{1}{3}\times\frac{1}{3} \quad + \ldots\ldots + \frac{3}{2}\times\frac{1}{3}\times\frac{1}{3}$$

$$= \quad \frac{3}{2} + \frac{1}{6}(N-1) = \frac{N+8}{6}$$

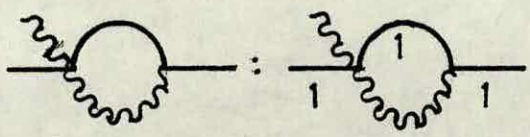

$$: \quad 1$$

Fig. 2.5.

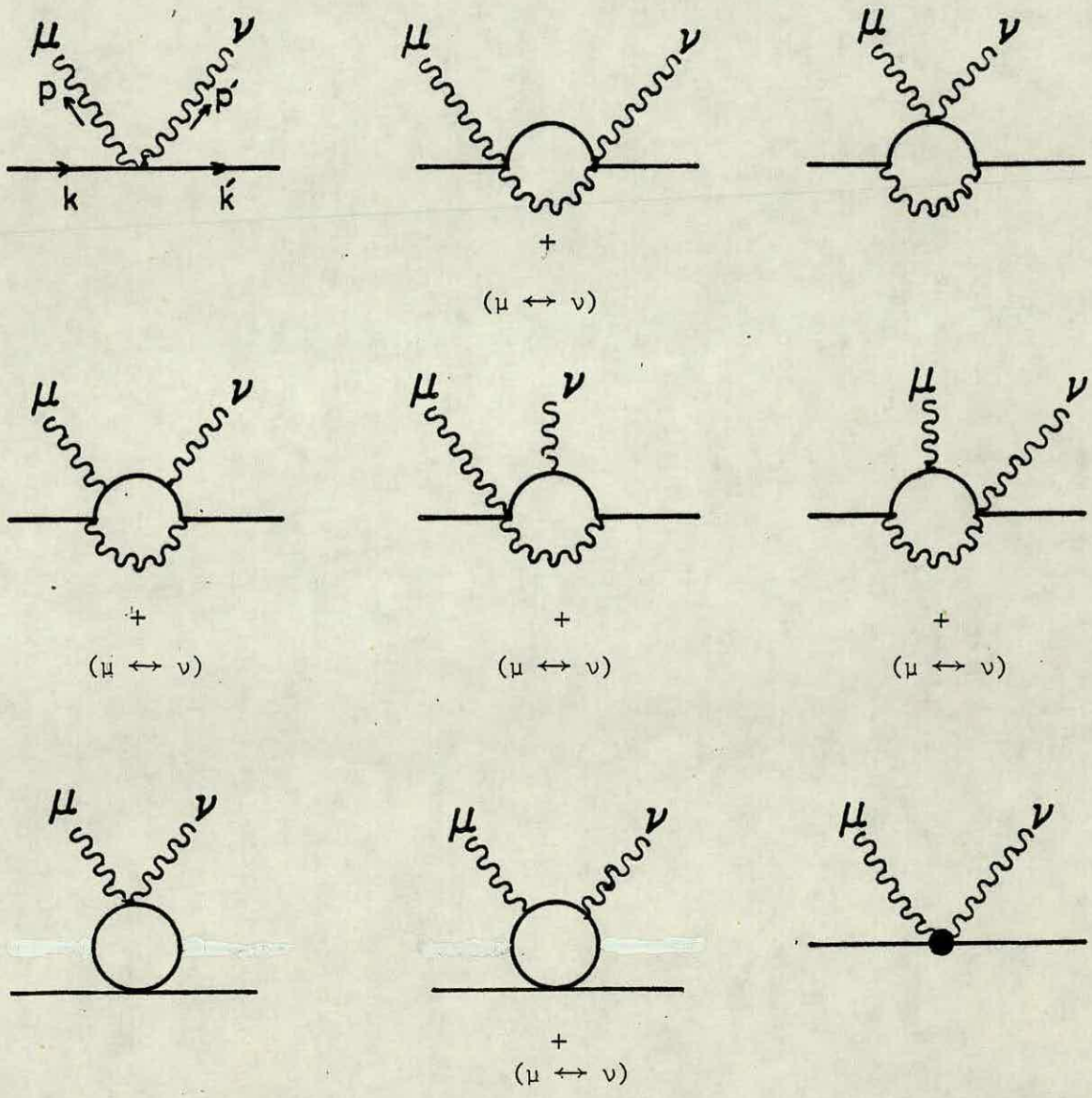

Fig. 2.6: One-loop diagrams contributing to $\Gamma^{\mu\nu(2,2)}$.

that

$$g_{\mu\nu}\,\Gamma^{\mu\nu(2,2)}_{(\underset{\rightarrow}{0})} = 2de^2 + 8ie^4(d-1)\int \frac{d^dq}{(2\pi)^d}\,\frac{1}{(q^2-m^2)(q^2-r^2)}$$

$$+\frac{(N+2)}{3}\,ge^2\left[id\int\frac{d^dq}{(2\pi)^d}\,\frac{1}{(q^2-m^2)^2} - 4i\int\frac{d^dq}{(2\pi)^d}\,\frac{q^2}{(q^2-m^2)^3}\right]$$

$$+ \quad 2Bd\,e^2 \quad + \quad \text{higher orders.} \qquad (2.20)$$

Evaluation of the integrals can be done after they are transformed into the Euclidean space through a Wick rotation. A list of the formulas useful to evaluate the integrals in the Euclidean space is given in the Appendix. Using (A-2) and (A-3) one can show that the two integrals in the bracket in eqn. (2.20) cancel. Imposing (2.14) and using (A-1) and (A-2) yields

$$B = \frac{8(d-1)}{d(d-2)}\,\frac{\Gamma(2-d/2)}{(4\pi)^{d/2}}\,\frac{(m^{d-2}-r^{d-2})}{(m^2-r^2)}\,e^2 \qquad (2.21)$$

$$+ \text{ higher orders.}$$

We shall also calculate B via eqn. (2.13). Considering the diagrams in Fig. 2.7, one can derive that

$$\Gamma^{\mu(2,1)}(k'=k,p=0) = -2ek^\mu + ie^3\int\frac{d^dq}{(2\pi)^d}\,\frac{2q^\mu(q+k)^\rho(q+k)^\sigma[g_{\sigma\rho}-\frac{(q-k)_\sigma(q-k)_\rho}{(q-k)^2}]}{[(q-k)^2-r^2](q^2-m^2)^2}$$

$$-4ie^3\int\frac{d^dq}{(2\pi)^d}\,\frac{(q+k)^\sigma\,g^{\mu\rho}[g_{\sigma\rho}-\frac{(q-k)_\sigma(q-k)_\rho}{(q-k)^2}]}{[(q-k)^2-r^2](q^2-m^2)} \qquad (2.22)$$

$$-i\frac{(N+2)}{6}\,ge\int\frac{d^dq}{(2\pi)^d}\,\frac{2q^\mu}{(q^2-m^2)^2} - 2e\,k^\mu B \quad + \quad \text{higher orders}$$

Hence one obtains

$$\frac{\partial}{\partial k^\mu}\,\Gamma^{\mu(2,1)}(k'=k,\ p=0)\Big|_{k=0} = -2de - 2deB$$

$$- 8(d-1)ie^3 \int \frac{d^dq}{(2\pi)^d}\,\frac{1}{(q^2-m^2)(q^2-r^2)}$$

$$+ \text{higher orders.} \qquad (2.23)$$

Then eqn. (2.13) implies that the solution to (2.23) gives the same B as in eqn. (2.21).

Finally, B can be obtained via eqn. (2.12) and Fig. 2.8; it is not difficult to show that it is the same result as in (2.21). Hence we have explicitly shown that the Ward identity is preserved in the presence of a photon mass, at least in the Landau gauge. However, there is more to discuss about this point, to which we will return after the calculation of the other renormalization constants.

Let us continue with the calculation of D. The contributing diagrams to $\Gamma^{\mu\nu(0,2)}$ are given in Fig. 2.9, from which one can get

$$g_{\mu\nu}\,\Gamma^{\mu\nu(0,2)}(p) = g_{\mu\nu}\Big[\underset{\mu}{\overset{\rightarrow p}{\sim\!\sim\!\sim}}\underset{\nu}{}\Big] - \frac{N}{2}\,ie^2 \int \frac{d^dq}{(2\pi)^d}\,\frac{(2q-p)^2}{(q^2-m^2)[(q-p)^2-m^2]}$$

$$+ iNde^2 \int \frac{d^dq}{(2\pi)^d}\,\frac{1}{(q^2-m^2)} + (d-1)p^2\,D - dr^2H$$

$$+ \text{higher orders.} \qquad (2.24)$$

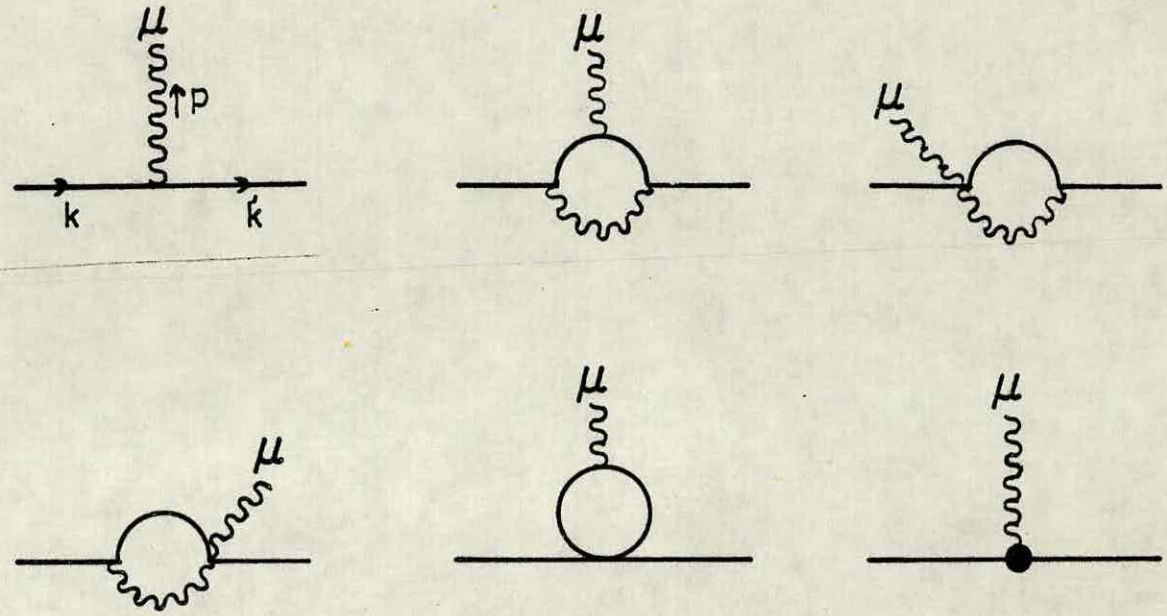

Fig. 2.7: One-loop diagrams contributing to $\Gamma^{\mu(2,1)}$.

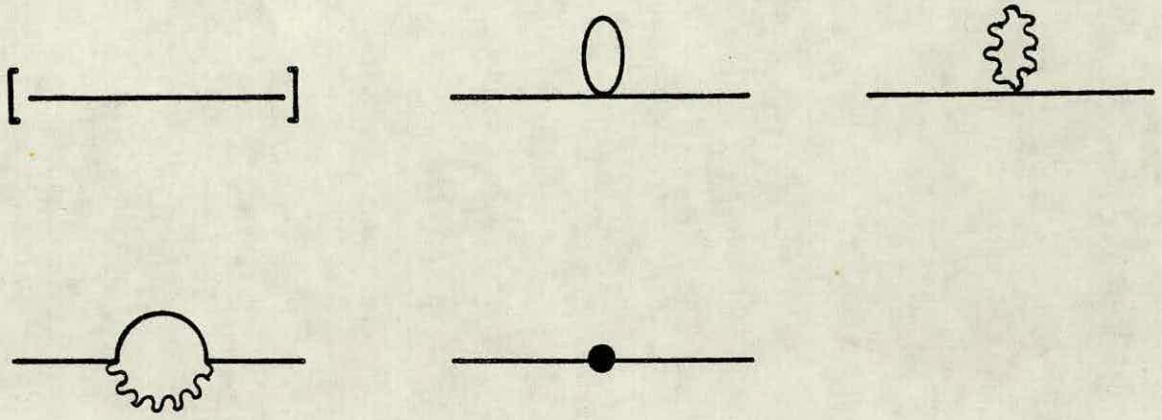

Fig. 2.8: One-loop diagrams contributing to $\Gamma^{(2,0)}$.

Transforming the integral to the Euclidean space after imposing eqn. (2.16) and using the Appendix yields

$$D = -\frac{N}{6}\,\frac{\Gamma(2-d/2)}{(4\pi)^{d/2}}\,(m^2)^{d/2-2}\,e^2 \qquad (2.25)$$

$$+ \text{ higher orders.}$$

To calculate E we use the diagrams given in Fig. 2.10. Three of the diagrams of Fig. 2.10 do not contribute to $\Gamma^{(4,0)}(\underset{\sim}{Q})$, hence one gets

$$\Gamma^{(4,0)}(\underset{\sim}{Q}) = -g - ig^2\,\frac{(N+8)}{6}\int \frac{d^dq}{(2\pi)^d}\,\frac{1}{(q^2-m^2)^2}$$

$$-6\,i\,e^4 g^{\mu\mu}g^{\nu\nu}\int \frac{d^dq}{(2\pi)^d}\,\frac{(g_{\mu\nu}-\frac{q_\mu q_\nu}{q^2})^2}{(q^2-r^2)^2} - gE$$

$$+ \text{ higher orders .} \qquad (2.26)$$

Eqn. (2.10) enables us to obtain

$$gE = \frac{\Gamma(2-d/2)}{(4\pi)^{d/2}}\left[\frac{(N+8)}{6}\,(m^2)^{d/2-2}\,g^2 + 6(d-1)(r^2)^{d/2-2}\,e^4\right]$$

$$+ \text{ higher orders .} \qquad (2.27)$$

Note that the renormalization constants should be dimensionless and that is the case in eqn. (2.21), (2.25) and (2.27) if g and e^2 have dimension $(\text{mass})^{4-d}$, which is of course the case, as can be be seen from dimensional analysis in the original lagrangian. The

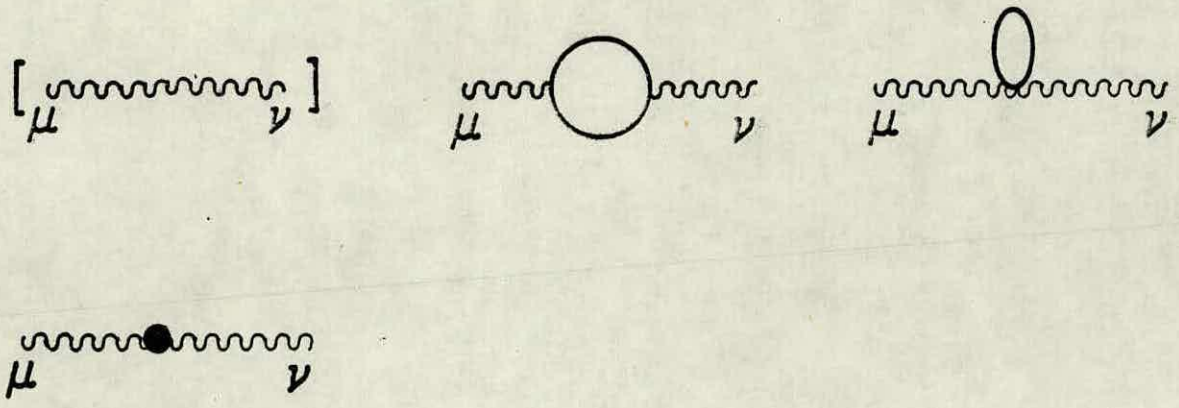

Fig. 2.9: One-loop diagrams contributing to $\Gamma^{\mu\nu(0,2)}$

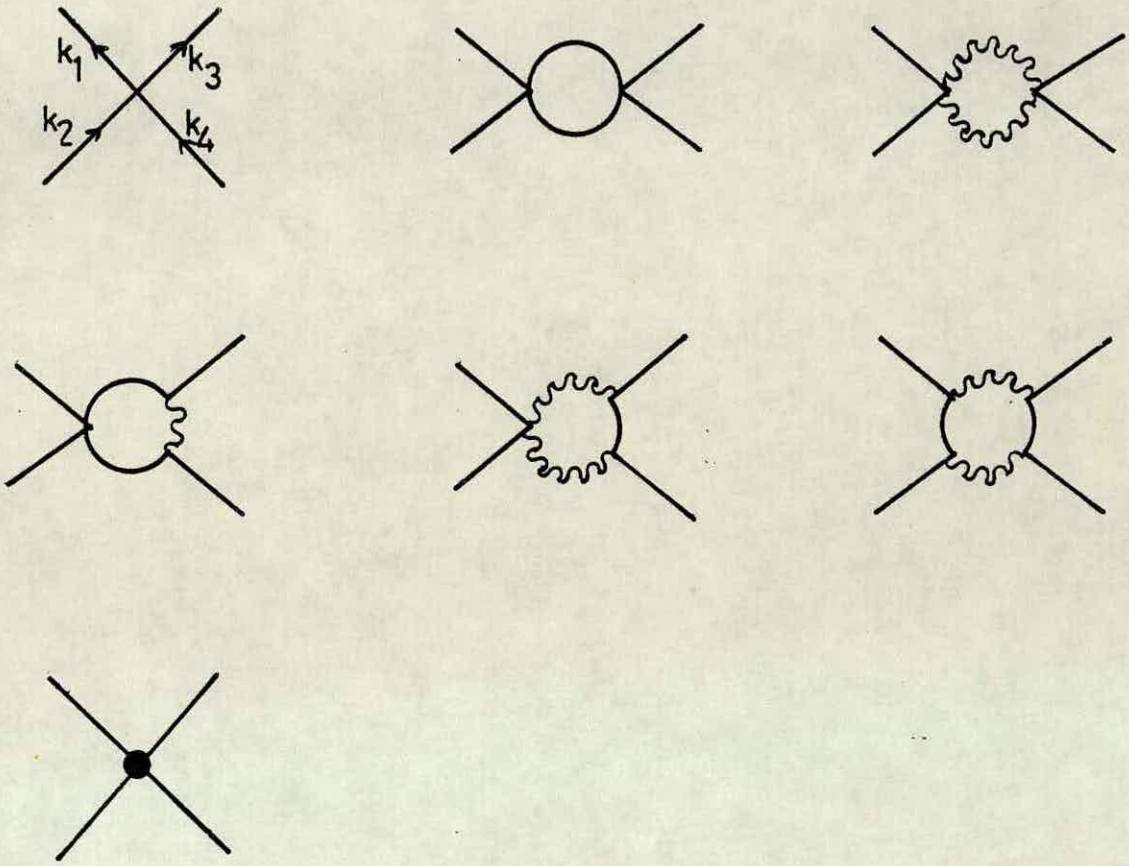

Fig. 2.10. One-loop diagrams contributing to $\Gamma^{(4,0)}$

other two renormalization constants C and H can also be calculated; however, they are not needed for our purposes.

Because we want to find the β-function and the fixed points of the theory, we need to write the bare couplings in terms of the renormalized ones. From eqns. (2.7) and (2.8) one can write that

$$e_B^2 = \frac{1}{1+D} e^2 = (1 - D + D^2 - D^3 + \ldots)e^2 \qquad (2.28)$$

$$\lambda = \frac{(1+E)}{(1+B)^2} g = (1+E)[1 - (2B + B^2) + \ldots]g \, . \qquad (2.29)$$

Substitution of the renormalization constants yields

$$e_B^2 = e^2 + \frac{N}{6} \frac{\Gamma(2 - d/2)}{(4\pi)^{d/2}} (m^2)^{d/2 - 2} e^4 + O(e^6, ge^4, g^2e^2, g^3) \qquad (2.30)$$

$$\lambda = g + \frac{(N+8)}{6} \frac{\Gamma(2-d/2)}{(4\pi)^{d/2}} (m^2)^{d/2 - 2} g^2$$

$$+ 6(d-1) \frac{\Gamma(2-d/2)}{(4\pi)^{d/2}} (r^2)^{d/2 - 2} e^4 \qquad (2.31)$$

$$- \frac{16(d-1)}{d(d-2)} \frac{\Gamma(2-d/2)}{(4\pi)^{d/2}} \frac{(m^{d-2} - r^{d-2})}{(m^2 - r^2)} ge^2 + O(g^3, g^2e^2, ge^4, e^6).$$

Eqn. (2.31) contains our arbitrary photon mass r and it is infrared divergent in the $r \to 0$ limit. One might think of keeping the photon mass non-zero but infinitesimally small, as can be done in many problems of

QED. However, careful thinking leads us to ask whether the Ward identity is satisfied in other gauges as well for arbitrary photon mass, or if the photon mass needs to be related to the scalar field mass somehow to preserve the Ward identity. As can be seen from the photon propagator the renormalization constants will be of the form $X + \alpha Y(\alpha)$ and we have shown that the different calculations for renormalization constant B yield the same result in the Landau gauge; that is to say, the X' part is the same for the three different calculations. Because $\alpha = 0$ in Landau gauge, our calculations do not tell us anything about the $Y(\alpha)$ parts of different B's. To investigate if different $Y(\alpha)$'s are equal, we have calculated B from $\Gamma^{\mu}(2,1)$ and $\Gamma^{\mu\nu}(2,2)$ respectively in Feynman gauge ($\alpha = 1$) as follows:

$$dB^{(2,1)} = e^2 \int_E \frac{d^d q}{(2\pi)^d} \frac{2dq^4 + 2(dr^2 - r^2 + d + 2)q^2 + 2dr^2}{(q^2 + 1)^2 (q^2 + r^2)^2} \quad (2.32)$$

$$+ \text{higher orders}$$

and

$$dB^{(2,2)} = e^2 \int_E \frac{d^d q}{(2\pi)^d} \frac{(3d-4)q^4 + (7d - 8)q^2 + 4d}{(q^2 + 1)^3 (q^2 + r^2)} \quad (2.33)$$

$$+ \text{higher orders}$$

where the integrals are in Euclidean space and we have chosen $m^2 = 1$ for simplicity. The difference of these two equations can be written as follows, by using the Appendix:

$$\frac{e^2\Gamma(2-d/2)}{2(4\pi)^{d/2}} \int_0^1 dx \left\{ \frac{d(d+2)}{4} \frac{[(4-7d)x^2 + 2(5d-4)x + (4-3d)]}{[1 + (r^2 - 1)x]^{2 - d/2}} \right.$$

$$+ \frac{d(4-d)}{4} \frac{[- \{4r^2(d-1)+11d\}x^2 + \{4r^2(d-1) + 2(9d-4)\}x - (7d-8)]}{[1 + (r^2 - 1)x]^{3-d/2}} \tag{2.34}$$

$$\left. + \frac{d(6-d)(4-d)}{[1 + (r^2 - 1)x]^{4 - d/2}} \{- (r^2+1)x^2 + (r^2 + 2)x - 1\} \right\}$$

$$+ \text{ higher orders.}$$

By giving different values for r^2 it can be seen that the equation vanishes only for $r^2 = 0$ and $r^2 = 1$. In other words the only non-zero value for r^2 which preserves the Ward identity is $r^2 = m^2$. One must note that the equality of the photon mass to the scalar field mass is a part of our renormalization scheme and without that equality our scheme would not be a consistent one. It is possible that in another scheme the relation of the masses might be a different one. One might think that the restriction on the photon mass is in contradiction with the argument of Section 2.1 that an arbitrary photon mass should not violate the Ward identity. However, as we have noted, the restriction is a part of our renormalization scheme and the argument in Section 2.1 allows us to choose a scheme with a non-zero photon mass.

In summary, eqn. (2.31) needs to be rewritten in the $r^2 \to m^2$ limit which reads

$$\lambda = g + \frac{(N+8)}{6}\frac{\Gamma(2-d/2)}{(4\pi)^{d/2}}(m^2)^{d/2-2}\,g^2 + 6(d-1)\frac{\Gamma(2-d/2)}{(4\pi)^{d/2}}(m^2)^{d/2-2}\,e^4 \tag{2.35}$$

$$- \frac{8(d-1)}{d}\frac{\Gamma(2-d/2)}{(4\pi)^{d/2}}(m^2)^{d/2-2}\,ge^2 + O(g^3, g^2e^2, ge^4, e^6) \quad .$$

2.5 Renormalization Group Analysis

Since a renormalization group equation includes derivatives of the dimensionless couplings with respect to a mass parameter, we define the dimensionless renormalized couplings $\bar{e}^2$ and $\bar{g}$ as

$$e^2 = m^{4-d}\,\bar{e}^2 = m^{\varepsilon}\,\bar{e}^2 \tag{2.36}$$

and

$$g = m^{4-d}\,\bar{g} = m^{\varepsilon}\,\bar{g} \tag{2.37}$$

respectively following Callan (1970) and Symanzik (1971). Hence eqn. (2.30) and eqn. (2.35) can be written respectively as follows, in terms of the dimensionless couplings:

$$e_B^2 = m^{\varepsilon}\left[\bar{e}^2 + \frac{N}{6}\frac{\Gamma(\varepsilon/2)}{(4\pi)^{2-\varepsilon/2}}\bar{e}^4\right] + O(\bar{e}^6, \bar{g}\bar{e}^4, \bar{g}^2\bar{e}^2, \bar{g}^3) \tag{2.38}$$

$$\lambda = m^{\varepsilon}\left[\bar{g} + \frac{(N+8)}{6}\frac{\Gamma(\varepsilon/2)}{(4\pi)^{2-\varepsilon/2}}\bar{g}^2 + 6(3-\varepsilon)\frac{\Gamma(\varepsilon/2)}{(4\pi)^{2-\varepsilon/2}}\bar{e}^4\right.$$

$$\left. - \frac{8(3-\varepsilon)}{(4-\varepsilon)}\frac{\Gamma(\varepsilon/2)}{(4\pi)^{2-\varepsilon/2}}\bar{g}\,\bar{e}^2\right] + O(\bar{g}^3, \bar{g}^2\bar{e}^2, \bar{g}\bar{e}^4, \bar{e}^6). \tag{2.39}$$

One must note that as one varies the mass parameter the dimensionless renormalized couplings should also very such that the bare couplings should be kept fixed, i.e.

$$\frac{de_B^2}{dm} = \frac{d\lambda}{dm} = 0 \ . \tag{2.40}$$

Hence the β-functions defined as

$$\beta(\bar{e}) = m \frac{d\bar{e}^2}{dm} \tag{2.41}$$

$$\beta(\bar{g}) = m \frac{d\bar{g}}{dm} \tag{2.42}$$

can be calculated as follows:

$$\beta(\bar{e}) = -\varepsilon \bar{e}^2 + \varepsilon \frac{N}{6} \frac{\Gamma(\varepsilon/2)}{(4\pi)^{2-\varepsilon/2}} \bar{e}^4 + O(\bar{e}^6, \bar{g}\,\bar{e}^4, \bar{g}^2\,\bar{e}^2, \bar{g}^3) \tag{2.43}$$

$$\beta(\bar{g}) = -\varepsilon \bar{g} + \varepsilon \frac{(N+8)}{6} \frac{\Gamma(\varepsilon/2)}{(4\pi)^{2-\varepsilon/2}} \bar{g}^2 - \varepsilon \frac{8(3-\varepsilon)}{(4-\varepsilon)} \frac{\Gamma(\varepsilon/2)}{(4\pi)^{2-\varepsilon/2}} \bar{g}\,\bar{e}^2 + 6\varepsilon(3-\varepsilon) \frac{\Gamma(\varepsilon/2)}{(4\pi)^{2-\varepsilon/2}} \bar{e}^4 + O(\bar{g}^3, \bar{g}^2\,\bar{e}^2, \bar{g}\,\bar{e}^4, \bar{e}^6) \ . \tag{2.44}$$

To make a comparison with the ε-expansion results in the literature [Halperin et al. (1974); Chen et al. (1978)] we shall take the ε-expansion of eqn. (2.43) and eqn. (2.44) by using $\Gamma(\varepsilon/2) = \frac{2}{\varepsilon}(1 + O(\varepsilon))$ which yields

$$\beta(\bar{e}) = -\varepsilon \bar{e}^2 + \frac{N}{3} \frac{1}{(4\pi)^{2-\varepsilon/2}} \bar{e}^4 + O(\bar{e}^6, \bar{g}\,\bar{e}^4, \bar{g}^2\,\bar{e}^2, \bar{g}^3) \tag{2.45}$$

and

$$\beta(\bar{g}) = -\varepsilon \bar{g} + \frac{(N+8)}{3} \frac{1}{(4\pi)^{2-\varepsilon/2}} \bar{g}^2 - \frac{12}{(4\pi)^{2-\varepsilon/2}} \bar{g}\,\bar{e}^2 + \frac{36}{(4\pi)^{2-\varepsilon/2}} \bar{e}^4 + O(\bar{g}^3, \bar{g}^2\,\bar{e}^2, \bar{g}\,\bar{e}^4, \bar{e}^6). \tag{2.46}$$

One can obtain the fixed points, i.e. solutions to $\beta(\bar{e}) = \beta(\bar{g}) = 0$ as:

i) Gaussian: $\bar{e}^2 = \bar{g} = 0$

ii) Heisenberg: $\bar{e}^2 = 0, \quad \bar{g} = \dfrac{3\varepsilon(4\pi)^{2-\varepsilon/2}}{(N+8)}$ (2.47)

iii) Superconductivity: $\bar{e}^2 = \dfrac{3\varepsilon(4\pi)^{2-\varepsilon/2}}{N}$ (2.48)

$$\bar{g} = \frac{3\varepsilon(4\pi)^{2-\varepsilon/2}}{2(N+8)} \left[(1 + \frac{36}{N}) \mp \frac{1}{N} \sqrt{N^2 - 360N - 2160} \right].$$

The square-root is imaginary for $N < N_o = 365.9$, hence the superconducting fixed points are not accessible for those values of N. The ε-expansion results we have got agree with the results of Halperin et al. (1974) and Chen et al. (1978), although our method is different.

As we have mentioned, our main interest is in three dimensions. Hence we put $\varepsilon = 1$ in eqn. (2.43) and eqn. (2.44) to obtain the β functions in three dimensions, which are

$$\beta(\bar{e}) = -\bar{e}^2 + \frac{1}{8\pi}\frac{N}{6}\bar{e}^4 + O(\bar{e}^6, \bar{g}\,\bar{e}^4, \bar{g}^2\,\bar{e}^2, \bar{g}^3) \qquad (2.49)$$

and

$$\beta(\bar{g}) = -\bar{g} + \frac{1}{8\pi}\frac{(N+8)}{6}\bar{g}^2 - \frac{1}{8\pi}\frac{16}{3}\bar{g}\,\bar{e}^2 + \frac{1}{8\pi}12\bar{e}^4 + O(\bar{g}^3, \bar{g}^2\,\bar{e}^2, \bar{g}\,\bar{e}^4, e^6). \qquad (2.50)$$

Hence the fixed points are as follows:

i) Gaussian : $\bar{e}^2 = \bar{g} = 0$

ii) Heisenberg : $\bar{e}^2 = 0, \quad \bar{g} = \frac{48\pi}{(N+8)}$ (2.51)

iii) Superconducting : $\bar{e}^2 = \frac{48\pi}{N}$

$$\bar{g} = \frac{24\pi}{(N+8)} \left[(1 + \frac{32}{N}) \pm \frac{1}{N} \sqrt{N^2 - 224N - 1280} \right]. \quad (2.52)$$

Of course higher order corrections will change these results, but let us proceed to analyse them. The first point to note is that the square root is imaginary for $N < N_o = 229.6$, which is a lower value than the N_o for the ε-expansion.

To specify the character of the phase transition one needs to draw the renormalization group flows for three different values of N, namely: $N < N_o$, $N = N_o$ and $N > N_o$. For an example, consider N = 16 and make identification

$$t = \log m \quad (2.53)$$

to rewrite eqn. (2.49) and eqn. (2.50) as

$$\beta(\bar{e}) = \frac{d\bar{e}^2}{dt} = -\bar{e}^2 + \frac{1}{3\pi} \bar{e}^4 \quad (2.54)$$

$$\beta(\bar{g}) = \frac{d\bar{g}}{dt} = -\bar{g} + \frac{1}{2\pi} \bar{g}^2 - \frac{2}{3\pi} \bar{g}\,\bar{e}^2 + \frac{3}{2\pi} \bar{e}^4 \quad (2.55)$$

respectively. Hence the stability matrix defined by

$$\begin{bmatrix} \frac{\partial\beta(\bar{e})}{\partial\bar{e}^2} & \frac{\partial\beta(\bar{e})}{\partial\bar{g}} \\ \frac{\partial\beta(\bar{g})}{\partial\bar{e}^2} & \frac{\partial\beta(\bar{g})}{\partial\bar{g}} \end{bmatrix} \tag{2.56}$$

reads

$$\begin{bmatrix} -1 + \frac{2}{3\pi}\bar{e}^2 & , & 0 \\ -\frac{2}{3\pi}\bar{g} + \frac{3}{\pi}\bar{e}^2 & , & -1 + \frac{1}{\pi}\bar{g} - \frac{2}{3\pi}\bar{e}^2 \end{bmatrix} \tag{2.57}$$

for our choice of N. One finds the eigenvalues and the eigenvectors of this matrix for the Gaussian and Heisenberg fixed points and can draw the renormalization group flows as shown in Fig. 2.11. If one compares our flow diagram in three dimensions with the one for the ε-expansion calculation, drawn by Chen et al. (1978), it can be seen that the two diagrams are qualitatively similar; both have a "runaway" at the Heisenberg fixed point, which was interpreted by Halperin and Lubensky (1974) to correspond to a first-order transition. The flow diagrams for $N = N_o$ and $N > N_o$ can be drawn in a similar fashion and it can be seen that they are too similar to the corresponding diagrams of the ε-expansion drawn by Chen et al. (1978).

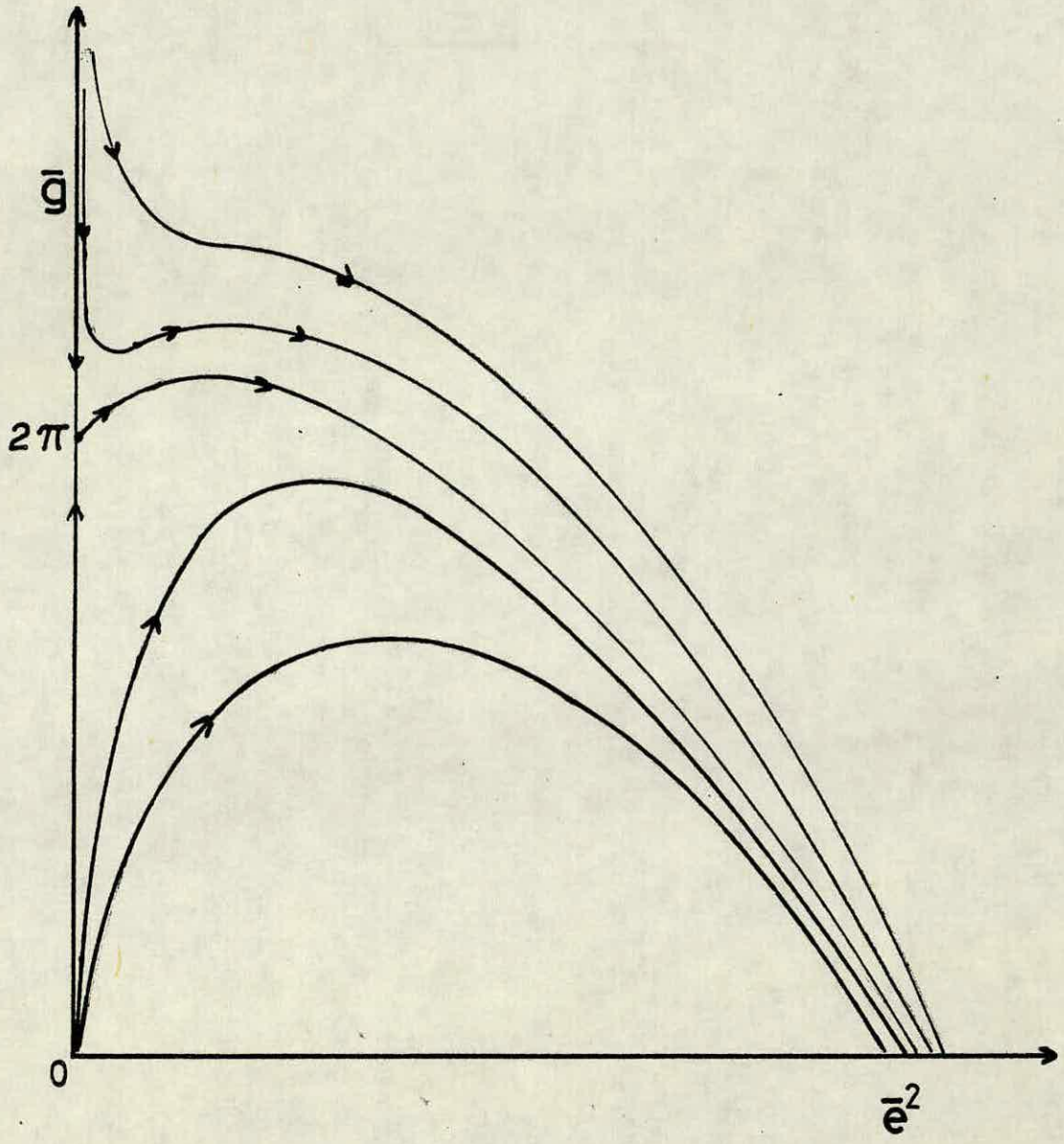

Fig. 2.11: Renormalization group flows for $N = 16$ in three dimensions as $t \to -\infty$.

2.6 Closing Remarks

As we have shown, the problem of infrared divergence in scalar electrodynamics can be controlled by assigning a photon mass. The assigned photon mass is not arbitrary and must be related to the scalar field mass as a part of the renormalization scheme†. We have also shown that in three dimensions the value of N_o, where the stability of the superconducting fixed point changes, is lower at one-loop than the N_o for the ε-expansion. However, it remains bigger than two. Our renormalization group flows in three dimensions have the same qualitative features as the ε-expansion ones, which indicates that the nature of the phase transition in three dimensions is the same as the nature of the transition in dimensions near to four, i.e. still a first-order phase transition. Hence we conclude that first-order character of the phase transition at three dimensions and near four dimensions, must be an aspect of low-order perturbation theory. Even though one can use our method to check if higher loop calculations make any difference to the character of the phase transition, deeper understanding of the subject requires a non-perturbative treatment. However, we will not discuss any non-perturbative calculations on scalar electrodynamics but concentrate on pure lattice gauge theories in the following chapters.

† The validity of this approach is not an obvious point; for example the fact that the Ward identity is satisfied to one loop does not guarantee that the critical behaviour is correct. However in the Callan-Symanzik approach adopted in this chapter, the critical behaviour is obtained by studying the regime in which the momenta are much larger than any masses; an artificial scalar boson mass might then be indeed irrelevant. The agreement of the ε-expansion results with the previous calculations support this conjecture.

CHAPTER 3

STRONG COUPLING PURE LATTICE GAUGE THEORIES

In this chapter we give a review of pure lattice gauge theories, introduce Münster's cluster expansion methods as a strong coupling expansion for the calculation of the string tension and the mass gap. An introduction to the group integral on the lattice is given and some integrals for SU(3) are explicitly calculated.

3.1 Review of Pure Lattice Gauge Theories

As was explained in the introduction, we are driven to the lattice mainly because we need a non-perturbative calculation to be able to understand confinement in non-abelian gauge theories. The lattice also represents a mathematical trick. It provides a cutoff, removing the ultraviolet infinities which exist in quantum field theory. As with any regulator, it must be removed after renormalization. Hence physics can only be extracted in the continuum limit, where the lattice spacing is taken to zero.

Formulation of gauge fields on a space-time lattice was originally introduced by Wilson (1974). The lattice chosen was hypercubic with an Euclidean metric (i.e. Imaginary time component). Consider the gauge group SU(n); we associate the matrix representation of an independent group element with each nearest-neighbour pair of lattice sites (i, j)

$$U_{ij} \quad \varepsilon \quad SU(n) \quad . \tag{3.1}$$

Note that U_{ij} itself is a matrix in the group. The indices i and j label the lattice sites at the ends of the link on which U_{ij} is defined. On reversing a link in the opposite direction, one should obtain the inverse element

$$U_{ji} = (U_{ij})^{-1} \quad . \tag{3.2}$$

U_{ij} is given as

$$U_{ij} = e^{\frac{1}{2}iag\, A_\mu} = e^{\frac{1}{2}iagA_\mu^\alpha \tau^\alpha} \quad . \tag{3.3}$$

Here a is the lattice spacing, A_μ is the vector potential and Lorentz index μ is the direction of a given link. g is the bare gauge coupling of the theory and τ^α (α=1,2,... n^2-1) are the generators of SU(n). We want to impose the local gauge invariance of the continuum theory to the action to be defined on the lattice. This is done by allowing an arbitrary rotation, G_i, at every site of the lattice. Namely,

$$U_{ij} \rightarrow G_i\, U_{ij}\, G_j^{-1} \quad . \tag{3.4}$$

Thus G_i defines the orientation of a local colour frame at the site i, while U_{ij} provides the transport from site i to site j.

The trace of the product of U variables around a closed path is invariant under eqn. (3.4). The simplest one of these closed paths is an elementary square called a plaquette. Hence the action over a plaquette p is

$$S_p = -\beta\, d_f^{-1}\, \mathrm{Re}\, X(p) = -\frac{\beta}{2}\, d_f^{-1}\, (X(p) + X^*(p)) \quad (3.5)$$

where

$$X(p) = \mathrm{Tr}(U_{ij}\, U_{jk}\, U_{k\ell}\, U_{\ell i}) \quad (3.6)$$

and $d_f = n$. Here the sites i, j, k and ℓ circulate about the plaquette in question. The normalization constant β will be defined in a moment.

The Wilson action over the lattice is

$$S = \sum_p S_p \quad (3.7)$$

where the sum is over all the plaquettes of the lattice.

One can Taylor expand U's in terms of A_μ's by using eqn. (3.3) to obtain

$$S_p = \frac{\beta g^2}{2n}\, a^4 \tfrac{1}{4}\mathrm{Tr}(F_{\mu\nu}\, F_{\mu\nu}) + O(a^6) \quad (3.8)$$

where $F_{\mu\nu}$ is the lattice version of the field strength tensor. It contains finite differences. However, as we take $a \to 0$, the finite differences are equal to the derivatives. Hence, $F_{\mu\nu}$ reduces to the usual field strength tensor of Yang-Mills theory. The term of order a^2 vanishes because generators of $SU(n)$ are traceless. Approximating the sum (3.7) with a space-time integral gives

$$S = \left(\frac{\beta g^2}{2n}\right) \int \tfrac{1}{4}\mathrm{Tr}(F_{\mu\nu}\, F_{\mu\nu})\, d^4x + O(a^6) \quad . \quad (3.9)$$

Thus we obtain the Euclidean action of classical Yang-Mills theory if we identify

$$\beta = \frac{2n}{g^2} \quad . \tag{3.10}$$

The terms with higher powers of the lattice spacing in (3.9) vanish in the classical continuum limit.

In a quantum theory, because of the uncertainty principle, we have a path integral formalism [Dirac (1933); Feynman (1948); Schwinger (1951)]. Hence to make our formulation a quantum theory, we define a partition function

$$Z = \int \prod_{\ell} dU(\ell)\, e^{-S} \tag{3.11}$$

where $dU(\ell)$ is the Haar measure for the link variable ℓ, which ensures that (3.11) is invariant under the gauge transformations. The integration is over all possible values of the gauge variables on each link in the lattice, hence path integration. In the next section we will discuss the group integral.

If Q is an operator composed of link variables, its expectation value is

$$\langle Q \rangle = \frac{1}{Z} \int \prod_{\ell} dU(\ell)\, Q e^{-S} \quad . \tag{3.12}$$

This equation is convenient for the calculation of $\langle Q \rangle$ in the strong coupling region as a series in powers of β. Thus, formulation of gauge theories on the lattice provides us with a strong

coupling expansion, which is our field of interest, hence enables us to do calculations beyond the standard perturbation theory. Having a strong coupling expansion as an infinite series raises the question of convergence. It was shown that the strong coupling expansions converge and have a finite radius of convergence, even for an infinite lattice [Osterwalder and Seiler (1978)]. Eqn. (3.12) can also be exploited by using the Monte Carlo computational techniques. However, we will not discuss these numerical simulations but refer the reader to some review articles [Cruetz et al. (1983); Cruetz (1983)] and give some other relevant references as we proceed.

Note that, since the gauge variables on the links are members of a compact group, the integrals over the links will be finite. Hence inclusion of a gauge-fixing term, which is necessary in a continuum gauge theory to control divergences arising from integration over all the group manifolds, is not necessary on the lattice. However, in the continuum limit such a gauge-fixing is essential.

To be able to remove the lattice spacing successfully, we must address the question of renormalization. Consider a physical observable q having dimension $-d$ in lattice units. If q is obtained from a lattice calculation, it will take the form

$$q = a^{-d} f(g) \tag{3.13}$$

where the dependence on the lattice spacing is trivial, and the physical content is incorporated in the function f of the dimensionless bare coupling constant g. We want the observable q to be a well-defined finite quantity after taking the $a \to 0$ limit.

Hence, to renormalize the theory, we require the physical quantity to be renormalization group invariant

$$\frac{dq}{da} = 0 \quad . \tag{3.14}$$

This equation implies that the coupling g and the lattice spacing a are no longer independent variables, therefore must be altered simultaneously. Note that as the lattice spacing becomes small, the bare coupling has to approach a fixed point, g_F, to keep q constant. The dependence of g on a is given by the renormalization group function defined as

$$\gamma(g) = a \frac{dg(a)}{da} \tag{3.15}$$

and satisfies

$$\gamma(g_F) = 0 \tag{3.16}$$

The continuum field theoretical analogy of eqn. (3.14) and eqn. (3.15) is the Zinn-Justin [Zinn-Justin (1973)] renormalization procedure, where the renormalized coupling is kept fixed and the bare coupling is changed with the cut-off.

Perturbative two-loop calculations [Cashwell (1974); Jones (1974)] have shown that, for pure $SU(n)$ gauge theory,

$$\gamma = \gamma_o g^3 + \gamma_1 g^5 + O(g^7) \tag{3.17}$$

where

$$\gamma_o = \frac{11}{3}\left(\frac{n}{16\pi^2}\right) \quad \text{and} \quad \gamma_1 = \frac{34}{3}\left(\frac{n}{16\pi^2}\right)^2. \tag{3.18}$$

Only the first two terms in eqn. (3.16) are universal. Higher order terms are regularization-dependent. Note that the sign of the first non-vanishing term, namely γ_o, is positive. Thus the origin (i.e. $g = 0$) is an ultraviolet attractive fixed point, which is a consequence of the asymptotic freedom of non-abelian gauge theories. Hence the fixed point at the origin can potentially give a continuum limit.

By using definition (3.15), eqn. (3.17) can be solved to yield

$$\begin{aligned} a &= \Lambda_L^{-1}\, h(g) \\ h(g) &= (g^2\gamma_o)^{\gamma_1/2\gamma_o^2}\, e^{-\frac{1}{2\gamma_o g^2}} \{1 + O(g^2)\} \end{aligned} \tag{3.19}$$

where Λ_L is a dimensionful constant of integration which sets the scale of the theory. Replacing (3.19) into (3.13) yields

$$q = \Lambda_L^d \frac{f(g)}{h^d(g)} \quad . \tag{3.20}$$

However, in the continuum limit we want q to be a constant. Hence in the continuum limit $f(g)$ must behave like $h^d(g)$, which gives

$$q = \text{const.}\ \Lambda_L^d \quad . \tag{3.21}$$

This equation is a scaling law. If behaviour consistent with eqn. (3.21) is found, then we may suggest that the lattice gauge theory provides us with a continuum quantum theory. A crucial point to be aware of is that even though restrictive methods can be used

to determine the form of scaling when $g = 0$, when we want to pin down a dimensionful physical quantity perturbation theory fails us. Thus, techniques which do not rely on perturbative expansions are required, and lattice gauge theory is one such which has proved remarkably successful.

The partition function defined by (3.11) is a path integral formalism in Euclidean space. Hence, we expect the lattice gauge theory to have an analogous statistical system. Indeed the lattice gauge theory can be expressed in the language of statistical spin systems [Kogut (1979)], the factor $\exp(-S/g^2)$ corresponds directly to the Boltzmann weight, $\exp(-E/kT)$. Hence the square of the coupling constant can be looked upon as representing the temperature of the system. Strong coupling becomes identified with high temperature and weak coupling with low temperature.

The U_{ij} are much like spins located on the bonds of the crystal. These variables then interact through the four-spin coupling in the Wilson action. Thus our gauge theory on the lattice might reveal critical points, hence phase transitions. Spontaneous magnetisation $\langle\sigma\rangle$ in the spin systems is an order parameter to distinguish various phases. Thus we might look for phases of the lattice gauge theory where $\langle U_{ij}\rangle \neq 0$. If this were to occur, however, it would break local gauge invariance and we invoke Elitzur's theorem [Elitzur (1975)], which shows that any non-gauge invariant quantity on the lattice must have zero expectation value. Hence $\langle U_{ij}\rangle$ cannot be used as an order parameter. We should look for a gauge-invariant order parameter. The simplest such object is

the trace of the product of four links around a plaquette. Its expectation value represents the internal energy of the corresponding thermodynamic system and is given by

$$\langle 1 - \frac{1}{n} X(p) \rangle = \frac{1}{6} \frac{\partial}{\partial \beta} \log Z. \tag{3.22}$$

The factor $1/6$ is the ratio of the number of sites to the number of plaquettes on a four-dimensional lattice. However, this object lacks the useful property of a magnetisation in that it never vanishes except exactly at zero temperature. Wilson has generalised this local object to a non-local one, known as the Wilson loop. Again, it is the trace of a product of link variables around a closed path but now the path may be of any size. It is denoted by

$$W(C) = \langle X(\prod_{i,j \in C} U_{ij}) \rangle \tag{3.23}$$

Here C denotes the loop in question and the group elements are ordered as encountered in circumnavigation of the contour. The Wilson loop has deep significance concerning the confinement of quarks. Assume a quark were to pass around the contour C, its wave function would pick up an internal symmetry rotation given by the product of the link variables encountered. The Wilson loop essentially measures the response of the gauge fields to an external quarklike source passing around its perimeter. For a timelike loop, this represents the production of a quark-antiquark pair at the earliest time, moving them along the world lines dictated by the sides of the loop, and then annihilating at the

latest time. In the continuum, the Euclidean amplitude for this process is the matrix element of the evolution operator between the initial and final states, namely $\langle i|e^{-Ht}|f\rangle$. Here $|i\rangle$ and $|f\rangle$ represent a quark-antiquark pair a distance R apart and H is the Hamiltonian of the SU(n) gauge theory. Since we are formulating the problem in Euclidean space, the evolution operator is a decaying exponential in time and does not oscillate. Since $|i\rangle$ and $|f\rangle$ are identical and since the process is static

$$\langle i|e^{-Ht}|f\rangle = e^{-V(R)t} \langle \mathrm{Tr}\ \mathbb{1} \rangle \tag{3.24}$$

where $V(R)$ is the heavy-quark potential, given by

$$V(R) = - \lim_{t\to\infty} \frac{1}{t} \log \langle \mathrm{Tr}\ P \exp[ig\oint A_\mu^\alpha \tau^\alpha dx_\mu]\rangle \times \langle \mathrm{tr}\,\mathbb{1}\rangle^{-1} \tag{3.25}$$

where P represents path ordering. Note that, on the lattice, $\langle \mathrm{Tr}\ P \exp[ig \oint A_\mu^\alpha \tau^\alpha dx_\mu]$ becomes the Wilson loop. Hence

$$W(C) \sim e^{-V(R)t} \tag{3.26}$$

for large t. Since the Wilson operator consists of link variables, the strong coupling expansion for it converges, hence, the Wilson loop gives an area low in the strong coupling region [Osterwalder and Seiler (1978)]

$$W(C) \sim e^{-KRt} \quad . \tag{3.27}$$

where K is called the string tension. Note that area Rt has dimensions of a^2, hence K must have dimension of $\frac{1}{a^2}$. Also note that in order to stay in the strong coupling region we have to choose large Wilson loops. Hence eqn. (3.27) is correct only for large loops. Combining eqns. (3.26) and (3.27) we get

$$V(R) \underset{R\to\infty}{\to} KR \quad . \tag{3.28}$$

This equation tells us that an infinite amount of energy would be required to separate the quarks by an infinite distance. Confinement is thus shown to be a natural consequence of the physics in the strong coupling region. Thus dimensionless string tension Ka^2 is a good order parameter, it vanishes identically in unconfined phases, while remaining non-zero whenever quark sources experience a linear long-range potential. Note that the area law criterion for confinement loses its value when quarks are introduced as dynamical variables. In this situation widely separated sources will reduce their energy by creating a pair of quarks from the vacuum fluctuations and screening their long range gauge fields. Effectively, a large Wilson loop measures the potential between two mesons rather than simple bare quarks.

In a confined theory, in contrast to an unconfined theory, we expect to have a spectrum of massive particle-like colourless excitations, which are called glueballs. The lowest mass in the glueball spectrum is the mass gap of the gluon field. It is a non-perturbative quantity and perturbation theory says nothing about glueballs. In statistical mechanics language, the mass gap

is the inverse of the correlation length. A correlation function defined as

$$G(r) = \langle Q_1(0) \; Q_2(r) \rangle_{\text{conn.}} \tag{3.29}$$

behaves like

$$G(r) \underset{r \to \infty}{\sim} A_1(r)\, e^{-m_1(\hat{r})r} + A_2(r) e^{-m_2(\hat{r})r} + \ldots \tag{3.30}$$

for large distances, with several mass gaps $m_1(\hat{r}) < m_2(\hat{r}) < \ldots$ depending on the direction of observation $\hat{r}$. In a lattice gauge theory, the simplest choice for Q_1 and Q_2 is to take two distant plaquettes in various relative orientations

$$G(r) = \langle X(p_1(0)) X(p_2(r)) \rangle_{\text{conn.}} \tag{3.31}$$

Only the smallest mass contributes to the leading asymptotic behaviour, but it may be that these masses are degenerate in the strong coupling limit; then the identification of the different masses m_1, m_2, ... on the strong coupling expansion may be problematical. This is a well-known problem in the context of spin models. For example, the first two orders of the connected correlation function of the two-dimensional Ising model at high temperature do not sum up as a single exponential.

In such a case, where one looks at the asymptotic behaviour along an axis of the lattice, one may use the transfer matrix formalism [Wilson and Kogut (1974); Lüscher (1977); Osterwalder and Seiler (1978)]; e^{-m_1}, e^{-m_2} in (3.30) correspond to various eigenvalues of the transfer matrix, and, to disentangle them, it is

suggested to project the correlation functions on eigenstates of the transfer matrix. As the latter commutes with spatial discrete translations and rotations (in the (d-1)-space orthogonal to the time axis), one may consider linear combinations of definite spatial momentum, $\underline{p}$, and which transform under an irreducible representation of the (d-1)-cubic group [Kogut et al. (1976); Berg and Billoire (1983a)]. Moreover, in gauge groups with complex character, like SU(3), a plaquette can also be tiled with the conjugate representation. Hence, there is a discrete C-symmetry under $X(p) \to X^*(p)$, and states may be classified according to charge conjugation even or odd. For example, the rotation invariant (under the cubic group) charge conjugation even state, which should give the lowest mass in the glueball spectrum of four-dimensional lattice gauge theory, reads

$$G(\underline{p},t) = \sum_{\substack{\underline{x} \\ 6 \text{ spatial} \\ \text{directions} \\ \text{of } p_1 \text{ and } p_2}} \sum e^{-i\underline{p}\cdot\underline{x}} \langle X(p_1(\underline{0},0))\, X(p_2(\underline{x},t)) \rangle_{\text{conn.}} \tag{3.32}$$

Here the sum is over the six plaquettes forming the cube centred at $\underline{0}$ (resp. at $\underline{x}$), over $\underline{x}$, and over the conjugate representation as well as the representation itself of the plaquettes p_1 and p_2, with a fixed time separation. At large t, one has simple exponential damping

$$G(\underline{p},t) \underset{t \to \infty}{\sim} e^{-E_o(\underline{p})t} \,. \tag{3.33}$$

Hence the mass gap is given by

$$G(\underline{0},t) \underset{t \to \infty}{\sim} e^{-mt} \quad . \tag{3.34}$$

Since eqn. (3.32) represents correlations along a lattice axis, the mass gap in (3.34) is called on-axis mass gap. Note that, because correlation function (3.32) is invariant under the cubic group, the mass gap is a scalar (singlet). Similarly, by construction other than linear combinations of on-axis correlation functions, one can get an axial vector (triplet) and a tensor (doublet) [Kogut et al. (1976)]. In the continuum limit, these multiplets are expected to become minimal multiplets with definite angular momentum which include them. Then the singlet, the doublet, and the triplet should become, respectively, states of $J^{PC} = 0^{++}$, 2^{++}, and 1^{+-}.

In lattice gauge theories Lorentz (rotational) invariance is explicitly broken. However, the Lorentz invariance is restored in the continuum limit. One possible method of investigating the recovery of the Lorentz invariance is to study the directional dependence of the glueball masses. In other words, one looks at the exponential decay of correlations in directions which differ from the lattice axes, hence calculates off-axis glueball masses.

The dimensionless mass gap ma is another order parameter on the lattice, like the dimensionless string tension Ka^2 it is non-zero in a confining phase but identically vanishes in a non-confining phase.

In the next section we will discuss the calculation of the dimensionless string tension and glueball mass as a strong coupling expansion. However, as was mentioned before, to get physics we have to take the continuum limit. But to take the $g^2 \to 0$ limit

of a strong coupling expansion is not possible. Similarly, to do a Monte Carlo calculation for small values of the coupling is, practically, not possible; that is because one gets overwhelming finite size effects. Hence such a computational calculation requires much bigger and faster computers than the present time ones. However, all is not lost. Usually, as soon as we leave the strong coupling region we see (asymptotic) scaling that is a physical observable obeys eqn. (3.21) or ratios like $\frac{\sqrt{K}}{m}$, $\frac{m_{o^{++}}}{m_{2^{++}}}$ are constants. Hence, Monte Carlo calculation results in this intermediate cross-over region (i.e. the region between the strong coupling and the weak coupling regions) are "continuum" results with very subjective error bars. Present time computers (like ICL Distributed Array Processor) are powerful enough to perform a computation in the cross-over region. As far as the strong coupling expansions are concerned, one can extrapolate the result to the scaling region by using various approximation methods (like Padé approximation).

Calculations in the cross-over region are reliable, assuming that the region has no singularities in it or in its neighbourhood. However, in a confining theory, we expect no phase transitions, hence no singularities. Indeed the numerical work for SU(2) and SU(3), using the Wilson action, has found no phase transitions preventing the extrapolation of confinement through to $g = 0$ [Cruetz (1979); Lautrup and Nauenberg (1980b): Cruetz (1980b)], and analytic work [Tomboulis (1983)] for SU(2) has provided a preliminary argument to support this conclusion. However, the Wilson action is

not the only possible action one can choose on the lattice. Any gauge-invariant lattice action which reduces to the continuum Yang-Mills action in the $a \to 0$ limit, is equally acceptable; that is referred to as universality. Group theory states that all functions invariant under gauge transformation (3.4) are linear combinations of the group characters in various representations:

$$S_p = - \sum_r \frac{\beta_r}{d_r} \mathrm{Re}(X_r(p)) \quad . \tag{3.35}$$

Here $X_r(p)$ is the character over the plaquette p in the representation r, d_r is the dimension of that representation. The coefficient β_r is related to $\frac{1}{g^2}$ such that the continuum limit gives the Yang-Mills action. The sum is over the irreducible representations of the group. By picking up any particular representation, or any particular combination of different representations one can obtain very large numbers of different actions. The Wilson action, as being the choice of the fundamental representations, is the simplest one. Thus, to be sure that the cross-over region is far from any singularity, we have to make sure that none of these multi-parameter actions have critical points close to the region in the multi-parameter plane. Different "geometric" actions have also been constructed [Villain (1975); Drouffe (1978); Manton (1980); Menotti and Onofri (1981)] which we are not going to discuss.

It is known that Z_2 and SO(3) lattice gauge theories display first-order phase transitions in 4-dimensions [Balian et al. (1975); Halliday and Schwimmer (1981)]. This suggests that, considering

$SO(3) \overset{\sim}{\sim} SU(2)/Z(2)$, the SU(2) mixed action with fundamental and adjoint parts from (3.35), must have non-trivial phase structure, with two first order lines entering the phase diagram in the fundamental-adjoint plane.

The interesting thing came from the simulations of the SU(2) mixed action [Bhanot and Cruetz (1981)]. It was found that the Z(2) and SO(3) transitions are stable and meet at a triple point. However, a third first-order line extends from the triple point and aims toward the cross-over region on the Wilson axis, but terminates before reaching it at a critical endpoint. These authors also found that Monte Carlo calculations near the critical endpoint and far from it, give different results. That means near the critical endpoint important additional physics is affecting the Monte Carlo results. However, the cross-over region on the Wilson axis was found, by the same authors, to be far enough from the critical endpoint so that the results there are reasonably reliable. The same phase structure was also found by using the Migdal-Kadanoff renormalization group techniques [Bitar et al. (1982)]. Bhanot (1982) has studied the phase structure for the SU(3) fundamental-adjoint mixed action; he finds qualitatively the same structure as in SU(2). However, it appears that, in contrast to SU(2), the critical endpoint is close enough to the cross-over region to distract the reliability of any result on the Wilson axis. Indeed, as we will discuss in Chapter 4, Monte Carlo calculations for the Wilson SU(3) are even not able to see scaling properly. Hence, one is forced to work below the Wilson axis by using the mixed

action or else working in the weak coupling region of the Wilson action.

In Chapter 4, we will discuss an investigation of the features related to the phase line by using the strong coupling expansions of the two SU(3) mixed action order parameters (the string tension and the mass gap), which we will also calculate in the same chapter. Higher groups SU(4), SU(5) and SU(6) display first-order phase transitions even for the Wilson action [Cruetz (1981); Moriarty (1981); Cruetz and Moriarty (1982a)]. One begins to worry that we are losing the confinement. However, because one can avoid the phase line by moving below the Wilson axis, the transition is not deconfining and is simply an artifact of the lattice action. Thus the fundamental-adjoint mixed action well deserves attention, and, because the region below the Wilson axis is a strong coupling region, the importance of the strong coupling calculations is emphasized once more.

One can also include matter fields in the lattice action [Kogut and Susskind (1975); Wilson (1977); Kawamoto and Smit (1981)]. Even though there is doubling problem with fermions [Karsten and Smit (1981)], various encouraging hadron mass calculations have been done [Hamber and Parisi (1981); Marinari et al. (1981); Weingarten (1982); Bowler et al. (1984)]. We shall not discuss these and other features of the lattice, but rather point to their exposure in the literature [Kogut (1983)].

3.2 Group Integration

A strong coupling expansion calculation requires evaluation of integrals over the gauge group. In this section we shall give a brief review of the group integration for SU(3). Integration results we will present, some of which have not been calculated before, will be needed in Chapter 4.

A group integral can be performed explicitly by setting up a generalised Euler angle representation for SU(3) unitary matrices and determining explicitly the form of the group integral in terms of the eight generalised Euler angles. The parametrisation of the group measure is given in Beg and Ruegg (1965). Since we have a compact group, the measure can be normalised such that

$$\int dU = 1 \ . \tag{3.36}$$

This measure is unique. We must also have the basic properties of any integral

$$\int dU(af(U) + bh(U)) = a\int dUf(U) + b\int dUh(U) \tag{3.37}$$

$$\int dUf(U) > 0 \quad \text{whenever} \quad f(U) > 0 \quad \text{for all} \quad U. \tag{3.38}$$

Here f and h are arbitrary functions over the group and a and b are arbitrary complex numbers. We impose the additional constraint that the measure be invariant

$$\int dUf(U) = \int dUf(UV) = \int dUf(VU) \tag{3.39}$$

where V is an arbitrary fixed element of the group. We also note

that

$$\int dU f(U^{+}) \quad = \quad \int dU \; f(U) \quad . \tag{3.40}$$

However, for many purposes an explicit form for the measure is unnecessary. Many integrals can be done using symmetry arguments. For example, if r and s are non-trivial irreducible matrix representations

$$\int dU \; X_r(U) \quad = \int dU \; X_r^{*}(U) \quad = \quad 0 \tag{3.41}$$

and the orthogonality of characters

$$\int dU \; X_r(U) \; X_s^{*}(U) \quad = \quad \delta_{r,s} . \tag{3.42}$$

A set of graphical rules for the evaluation of such integrals is given in Cruetz (1978). A useful formula is

$$\int dU \; X_3^{*\,3q}(U) \quad = \quad \int dU \; X_3^{3q}(U) \quad = \quad (3q)! \prod_{i=0}^{2} \frac{i!}{(i+q)!} \tag{3.43}$$

where X_3 is the character in the fundamental representation, and q is an integer. We also need solution to integrals of the form $\int X_3^{p} \; X_3^{*q}$ and $\int X_3^{p} \; X_3^{*q} \; X_r^{*}$; unlike the integral in (3.43) these integrals do not have a generic solution. However, these integrals can be solved for a given p,q and representation r by using the Young tableau. Consider a Young tableau as in Fig. 3.1 and Let $X_{m,n}$ represent the character of that tableau. The conjugate representation $X_{n,m}$ will satisfy

$$X_{n,m} \quad = \quad X_{m,n}^{*} \quad . \tag{3.44}$$

A particularly useful decomposition rule presented by Fig. 3.2 is

$$X_{m,n} = X_{1,0} X_{m-1,n} - X_{m-1,n-1} - X_{m-2,n+1} \tag{3.45}$$

where $X_{0,0} = 1$ and $X_{-|m|,n} = X_{m,-|n|} = X_{-|m|,-|n|} = 0$.

As an example, one can write

$$X_{1,1} = X^*_{1,1} = X_{1,0} X^*_{1,0} - 1 \ . \tag{3.46}$$

If X_N labels the character in $N \times N$ matrix representation, the correspondence with the young tableau notation will be

$$X_3 = X_{1,0}, \quad X_6 = X_{2,0}, \quad X_8 = X_{1,1}, \quad X_{10} = X_{3,0}, \quad X_{15^a} = X_{2,1}$$
$$X_{15^b} = X_{4,0}, \quad X_{21} = X_{5,0}, \quad X_{24} = X_{3,1}, \quad X_{27} = X_{2,2} \tag{3.47}$$

and so on. The orthogonality relation (3.42) can be written, in the Young tableau notation as

$$\int dU \, X_{i,j}(U) \, X^*_{k,\ell}(U) = \delta_{i,k} \, \delta_{j,\ell} \tag{3.48}$$

The integral $\int dU \, X_3^k(U) \, X_3^{*\ell}(U) \, X_r^*(U)$ can be reduced to $I_{p,q} \equiv \int dU \, X_3^p(U) \, X_3^{*q}(U)$ by using (3.45) and (3.48), which can be evaluated by using the same equations. We have evaluated $I_{p,q}$ for various values of p and q, the results are given in Table 3.1. Note that $I_{p,q} = I_{q,p}$ and $I_{p,q} = 0$ if $2q+p$ is not a multiple of 3. If either p or q is 0 we use the generic formula (3.43).

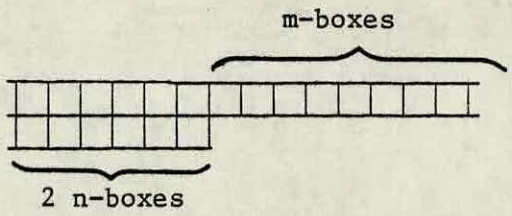

Fig. 3.1: Young tableau corresponding to $X_{m,n}$.

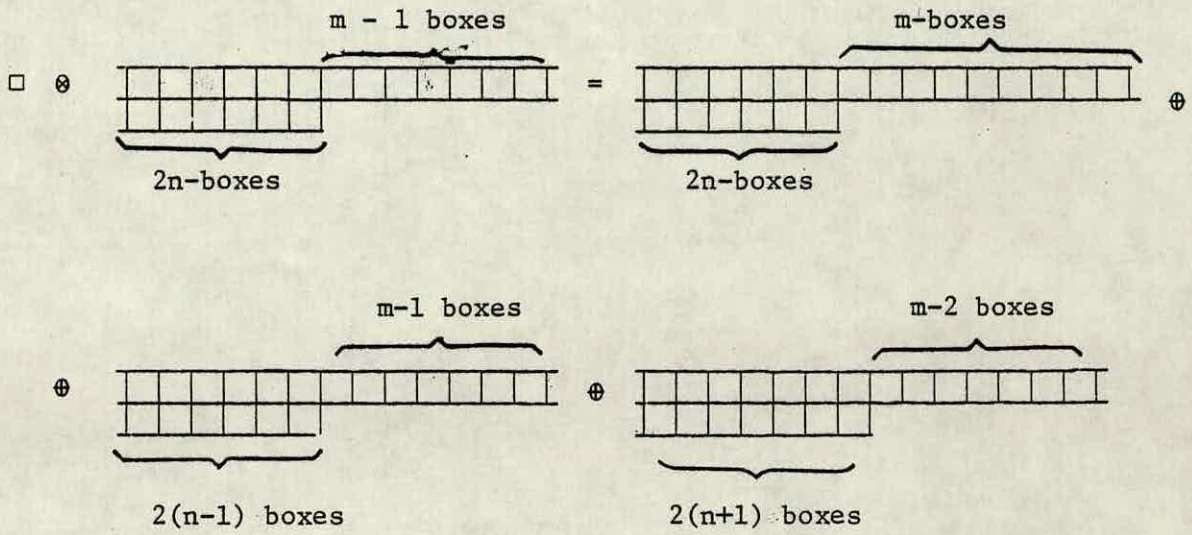

Fig. 3.2: Derivation of eqn. (3.45) by using the Young tableau.

p	q	$I_{p,q}$
1	1	1
2	2	2
3	3	6
4	1	3
4	4	23
5	2	11
5	5	121
6	3	50
6	6	745
7	1	22
7	4	297
8	2	110

Table 3.1: Some non-zero results for $I_{p,q} = \int dU\ X_3^p(U)\ X_3^{*q}(U)$.

3.3 Strong Coupling Expansions

Calculation of integrals (3.11) and (3.12) as a strong coupling expansion is not straightforward; one needs a systematic approach. We refer the reader to Drouffe and Zuber (1983) for a discussion of the subject where essential references are also given. We will follow a cluster expansion method in our calculations developed by Münster (1981a). The method applies to gauge group SU(n) as well as Z_n. Even though it was developed for the Wilson action, it can be generalised to the mixed actions. We will use that approach for our mixed action calculations in Chapter 4. However, for the moment we shall take the Wilson action and give an introduction of the method.

Consider the action given by eqn. (3.5). One can write the Fourier expansion of $\exp(-S_p)$ as

$$e^{-S_p} = \tilde{b}_o \left[1 + \sum_r d_r b_r X_r(p)\right] . \qquad (3.49)$$

Here the sum extends over all non-trivial, inequivalent irreducible representations of the group. b_r's are functions of β and called character expansion coefficients. Since our action is real, conjugate representations r and r^*, which both appear in the sum if they are inequivalent, contribute equally

$$b_r = b_{r^*} . \qquad (3.50)$$

With the help of the orthogonality relation (3.42) one can write

$$\tilde{b}_o = \int dU\, e^{-S(U)} \qquad (3.51)$$

$$b_r = \frac{1}{d_r \tilde{b}_o} \int dU \, X_r^*(U) \, e^{-S(U)} \quad . \tag{3.52}$$

Let Λ label our lattice, $|\Lambda|$ its volume and M the number of plaquettes it has. Also let an integer be assigned to each plaquette between 1 and M such that no two different plaquettes have the same number assigned to them. However, at the end we will take our lattice to be infinite. For simplicity, we shall choose the lattice spacing to be 1. Exp(-S) on this lattice can be written in terms of the character expansion coefficients as

$$\begin{aligned} e^{-S} = 1 + \sum_{i=1}^{M} \sum_r d_r b_r X_r(p_i) + \sum_{\substack{i;j=1 \\ i>j}}^{M} \sum_{r,s} d_r d_s b_r b_s X_r(p_i) X_s(p_j) + \ldots \\ \ldots + \sum_{\substack{i_1;i_2;\ldots;i_{M-1}=1 \\ i_1>i_2>\ldots>i_{M-1}}}^{M} \sum_{r,s,\ldots\alpha} d_r d_s \ldots d_\alpha \, b_r b_s \ldots b_\alpha \\ \times X_r(p_{i_1}) X_s(p_{i_2}) \ldots X_\alpha(p_{i_{M-1}}) \\ + \sum_{r,s,\ldots\alpha} d_r d_s \ldots d_\alpha b_r b_s \ldots b_\alpha \, X_r(p_1) X_s(p_2) \ldots X_\alpha(p_M) \end{aligned} \tag{3.53}$$

Note that we dropped out the normalisation $\tilde{b}_o$ because, in expectation values, it will cancel.

Let us introduce some definitions. One defines plaquettes as connected if they share a link. A link is called free if it belongs to one plaquette only. A connected set of plaquettes which have no free links or whose free links are contained in the boundary $\partial\Lambda$ of Λ is called a polymer and labelled by P. If a polymer consists of plaquettes $p_{i_1}, p_{i_2}, \ldots, p_{i_N}$ we define its activity

$\Phi(P)$ as

$$\Phi(P) = \sum_{r,s,\ldots,\alpha} d_r d_s \ldots d_\alpha b_r b_s \ldots b_\alpha \int \prod_{\ell} dU(\ell) X_r(p_{i_1}) X_s(p_{i_2}) \ldots X_\alpha(p_{i_N}) \tag{3.54}$$

The partition function can be written in terms of the activities

$$Z = 1 + \sum_{n=1}^{\max(n)} \sum_{\{P_1, P_2, \ldots, P_n\}} \langle P_1, P_2, \ldots, P_n \rangle \Phi(P_1)\Phi(P_2), \ldots, \Phi(P_n) \tag{3.55}$$

where $\max(n)$ is the maximum number of polymers one can define on Λ. The bracket $\{P_1, P_2, \ldots, P_n\}$ represents a combination of n polymers and the sum is over all of these sets. The second bracket is defined as

$$\langle P_1, P_2, \ldots, P_n \rangle = \begin{cases} 1, & \text{if every pair } P_i, P_j \text{ is disconnected} \\ 0, & \text{otherwise.} \end{cases} \tag{3.56}$$

Note that we did not include plaquettes with free links in (3.55). The reason is that the integration over a free link vanishes. We are interested in $\log Z$ rather than Z itself. After taking the logarithm of (3.55) one uses the Taylor expansion of $\log(1 + x)$ to get

$$\log Z = \sum_{n=1}^{\max(n)} \sum_{\{P_1, P_2, \ldots, P_n\}} \left(\prod_i n_i! \right)^{-1} [P_1, P_2, \ldots, P_n] \times \Phi(P_1)\Phi(P_2), \ldots, \Phi(P_n) \tag{3.57}$$

where n_i is the multiplicity of P_i. It can be proven by induction that

$$[\alpha,\ldots,\rho] = \sum_{\text{(permutations)}} (-1)^{k-1}(k-1)! \underbrace{\langle\alpha,\ldots,\beta\rangle\langle\gamma,\ldots,\delta\rangle\ldots\ldots\langle\mu,\ldots,\nu\rangle}_{k \text{ factors}} \tag{3.58}$$

and $[P_1, P_2, \ldots, P_n] = 0$ unless $P_1UP_2U,\ldots, UP_n$ is connected.

A connected set of different polymers P_i, $i = 1,\ldots, k$ with multiplicities n_i will be called a cluster and denoted by

$$C = (P_1^{n_1}, P_2^{n_2}, \ldots, P_k^{n_k}) . \tag{3.59}$$

If one defines

$$a(C) = (\prod_i n_i!)^{-1} \underbrace{[X_1,\ldots,X_1}_{n_1}, \underbrace{X_2,\ldots,X_2}_{n_2}, \ldots, \underbrace{X_k,\ldots,X_k]}_{n_k} \tag{3.60}$$

eqn. (3.57) can be written as a cluster expansion

$$\log Z = \sum_C a(C) \prod_{P_i \in C} \Phi(P_i)^{n_i} . \tag{3.61}$$

There is a simplification of the cluster expansion. If a polymer P can be decomposed into two polymers P_1 and P_2, which are connected only through a single link, the activity factorizes as

$$\Phi(P) = \Phi(P_1)\,\Phi(P_2) . \tag{3.62}$$

In the expansion of $\log Z$ the contribution of such a polymer P

appears twice. First P is counted as a cluster consisting of a single polymer. Besides that, one has a cluster consisting of the polymers P_1 and P_2. Both contributions cancel against each other. Thus one does not consider clusters of this type.

If one wants to evaluate the free energy $F = (\beta|\Lambda|)^{-1} \log Z$, one may use the translation invariance for a simpler calculation. Free energy has been calculated for the Wilson action for various groups (see Drouffe and Zuber (1983) for references) as well as the SU(2) mixed action [Dashen et al. (1983)]. However, for the calculation of the string tension and the mass gap, one is not allowed to use the translational invariance. One reason for this is the fact that the graphs under consideration cover a whole cross-section of the lattice and their occurrence factors are not proportional to $|\Lambda|$. Thus we should use the cluster expansion.

Münster (1981a) applies the cluster expansion method to the calculation of the free energy of certain gauge field configurations called vortices. He shows that the vortex free energy satisfies exponentially decreasing area law and the coefficient for an infinite lattice is the same as the string tension of the Wilson loop. The vortex free energy $f_\Lambda(U)$ is defined through the change of $\log Z$ as one changes the boundary conditions. Fix the boundary conditions $U = \{U(b), b \in \partial\Lambda\}$, and denote the partition function $Z_\Lambda(U)$. Now change the vorticity with a gauge transformation $U \to U_\gamma$ of the boundary conditions by an element γ of the group centre,

$$U(b) \to \begin{cases} U(b), & b \notin T \\ U(b)\gamma, & b \in T \end{cases}, \quad b \in \partial\Lambda \tag{3.63}$$

Here T is a set of links defined by Mack and Petkova (1980). If the vortex container has a length t in the time direction, one can consider T as the set of links on the boundary with time coordinate t. Then the vortex free energy $f_\Lambda(U)$ is given by

$$f_\Lambda(U) = - L^{-1}[\log Z_\Lambda(U_\gamma) - \log Z_\Lambda(U)] \tag{3.64}$$

where $L = d_1$ in three dimensions and $L = d_1 d_2$ in four dimensions. For a detailed discussion we refer the reader to Münster (1980). We insert the cluster expansion for log Z into eqn. (3.64) to get

$$f_\Lambda(U) = - L^{-1} \sum_C a(C) \{ \prod_{P_i \varepsilon C} \Phi_\gamma (P_i)^{n_i} - \prod_{P_i \varepsilon C} \Phi(P_i)^{n_i} \}. \tag{3.65}$$

If the intersection of a polymer P with $\partial\Lambda$ is completely contained in a simply connected part of $\partial\Lambda$, the activities $\Phi(P)$ and $\Phi_\gamma(P)$ are equal. That is because U_γ differs from U by a gauge transformation on every simply connected part of $\partial\Lambda$. The minimal clusters which contribute to $f_\Lambda(U)$ are planes Ξ_o: $x_1 = \text{const.}$ in three dimensions and planes Ξ_o: $x_1 = \text{const.}$, $x_2 = \text{const.}$ in four dimensions. Thus the leading term in the expansion of $f_\Lambda(U)$ comes from these minimal surfaces and with reference to Münster (1981a) one writes

$$f_\Lambda(U) = \text{const.}\ e^{-\alpha_o |\Xi_o|} \tag{3.66}$$

$$\alpha_o = - \log(b_f(\beta)) \tag{3.67}$$

where $|\Xi_o|$ is the area of Ξ_o and b_f is the character expansion coefficient for the fundamental representation. Note that the plane Ξ_o is the equivalent of the Wilson loop, and α_o is the dimensionless string tension in the limit $|\Lambda| \to \infty$. Higher order contributions to the string tension are obtained by decorating the leading polymer Ξ_o with additional polymers. One cuts out a hole of Ξ_o by removing a connected set of plaquettes and then takes a rigid configuration of plaquettes as decoration and fits it into the hole and continues decorating up to a desired order. Eqn. (3.54) with the orthogonality relation enables us to calculate the activity of each configuration. Note that we have also to take into consideration the "occurrence factor" of each diagram. For instance, the cube in Fig. 4.1 can occur at $4|\Xi_o|$ different positions in four dimensions, hence its occurrance factor is 4. The string tension for the Wilson action has been calculated to 14th order [Duncan and Vaidya (1979); Kimura (1980); Münster (1981a)] for Z_2 and SU(2), and to 12th order [see Drouffe and Zuber (1983)] for SU(3). Note that these results are in powers of b_f rather than β. The mixed action SU(2) string tension has also been calculated as a function of the character expansion coefficients [Arroyo et al. (1982)]. We will calculate the string tension for the mixed SU(3) action in Chapter 4.

The cluster expansion can also be applied to the calculation of the on-axis glueball masses. Consider two parallel space-like plaquettes p_1 and p_2 carrying the fundamental representation, which are located at the same space coordinates but separated in Euclidean time by a distance t. The correlation function of these

two plaquettes is

$$\rho(t) = \langle X(p_1)X(p_2)\rangle - \langle X(p_1)\rangle\langle X(p_2)\rangle. \tag{3.68}$$

In order to study the correlation by using the cluster expansion, we consider the partition function of a model where the coupling β_i on plaquettes p_i, $i = 1,2$, and β elsewhere. We get the correlation function by

$$\rho(t) = d_f^2 \frac{\partial^2}{\partial\beta_1\partial\beta_2} \log Z(\beta, \beta_1, \beta_2)\Big|_{\beta_i=\beta} \tag{3.69}$$

and use the cluster expansion (3.61) for $\log Z$. Every cluster contributing to $\rho(t)$ must contain both plaquettes p_1 and p_2. The minimal cluster consists of a single polymer, namely a long tube connecting p_1 and p_2. Because of the orthogonality of characters the minimal tube is tiled with the fundamental representation. Hence the correlation function for the minimal tube is

$$\rho(t) = \text{const. } b_f^{4t} = e^{-mt} \tag{3.70}$$

where m is the mass with leading term

$$m = -4 \log b_f. \tag{3.71}$$

Further contributions come from all other possible clusters. However one must be careful. As was mentioned in Section 3.1 and expressed by eqn. (3.32), we have to sum over all space-like orientations of p_1 and p_2 to get a simple exponential damping,

and to get a charge conjugate even state, p_1 and p_2 must carry the conjugate representation as well as the fundamental representation itself. Taking these modifications into consideration, one proceeds to calculate the expansion of m by selecting the terms linear in t in the cluster expansion of $\log \rho(t)$. Note that each diagram contributing to $\rho(t)$ has an occurrence factor which depends on t. We refer the reader to Münster (1981b) for the Wilson mass gap calculations for gauge groups Z_2, Z_3, SU(2) and SU(3). See also Münster (1982a,b) for a correction to the SU(3) result.

Masses of the other glueballs have also been calculated for the on-axis case [Seo (1982); Münster (1983)] as well as the off-axis case [Seo and Ukawa (1982); Seo (1982); Kawai and Nakayama (1982)] for the Wilson action. However, there is no mixed action glueball mass calculation in the literature. We will calculate the mixed action mass gap for SU(3) in Chapter 4.

We shall pinpoint some important features of the strong coupling expansions. As we have already mentioned, a strong coupling series has a finite radius of convergence and, as a consequence of this convergence, we have exponential clustering of correlation functions and area law of the Wilson loop in the strong coupling region. One of the important features of the strong coupling expansions is that they seem to be capable of making some predictions relevant to the phase structure and critical points. Consider the Z_2 gauge theory, as an example. As we mentioned, in 4 dimensions this model reveals a first-order phase transition. It was seen that the strong coupling expansions for the string

tension [Münster (1981a)] and the mass gap [Münster (1981b)] give non-vanishing values for $\beta > \beta_c$ (critical coupling), which is consistent with the first-order character of the transition. On the other hand, the Z_2 model undergoes a second-order phase transition in 3-dimensions [Sykes et al. (1972)]. Therefore, one expects both the string tension and the mass gap to vanish at the critical β. As expected the mass gap vanishes at $\beta = \beta_c$ in Münster's calculation. However, the string tension already vanishes at some value $\beta < \beta_c$, a phenomenon known as roughening. The string tension, which, loosely speaking, is an observable related to a two dimensional surface, is sensitive to the roughening transition of that surface. By duality [Balian et al. (1975); Wegner (1971)] the three-dimensional Z_2 gauge theory can be transformed into the three-dimensional Ising model. The string tension at inverse temperature β in the gauge model is by duality equal to the surface tension of the Ising model at inverse temperature $\beta^* = -\frac{1}{2} \log \tanh \beta$ [Bricmont et al. (1979)]. The inverse roughening temperature $\beta_R \tilde{\simeq} \beta_c$ in 4-dimensions and $\beta_R > \beta_c$ in 5-dimensions for the Z_2 theory. Even in a gauge theory like SU(3), where no phase transition exists, the roughening transition occurs in the string tension [Hasenfratz and Hasenfratz (1981); Itzykson et al. (1980); Lüscher et al. (1981)]. The roughening effect is a special one, which only occurs if one chooses to compute the planar string tension. If one takes a twisted Wilson loop instead of the conventional planar one, it takes place in the strong coupling limit $\beta = 0$. Therefore such an off-axis string tension should have better analyticity properties than the planar

one. This phenomenon has been exposed particularly clearly in the Hamiltonian formalism [Kogut et al. (1981); Kogut and Sinclair (1981)]. However, a method known as Exact Linked Cluster Expansion has been developed to get good results beyond the roughening transition for the planar string tension in the Hamiltonian formalism [Irving and Hamer (1984a,b)].

Bulk properties of the system, such as the specific heat or the mass gap, do not appear to be affected by the roughening which makes the mass gap calculations more favourable than the string tension ones.

CHAPTER 4

THE STRING TENSION AND THE MASS GAP FOR SU(3) IN THE FUNDAMENTAL-ADJOINT PLANE

In this chapter we calculate the string tension and the mass of the lowest glueball 0^{++} (on-axis case) for the SU(3) fundamental-adjoint mixed action by using Münster's cluster expansion method. To improve the results we use Padé approximation. We also study the ratio $m/\sqrt{K}$ along various lines in the fundamental-adjoint plane. Our results are expressed explicitly in terms of the two coupling parameters β and β_A of the fundamental-adjoint action. Some of the character expansion coefficients are also calculated as explicit functions of β and β_A, which we present first.

4.1 The Character Expansion Coefficients

The fundamental-adjoint mixed action for SU(3) over a plaquette p is given by

$$S_p = -\frac{\beta}{6}(X_3(p) + X_3^*(p)) - \frac{\beta_A}{8} X_8(p) \qquad (4.1)$$

where the choice of normalisation for β and β_A is conventional. The constraint, that the continuum limit of the action should give the Yang-Mills theory, yields

$$\frac{1}{g^2} = \frac{\beta}{6} + \frac{3}{8}\beta_A \qquad (4.2)$$

for our choice of convention.

Therefore a strong coupling expansion will be in powers of β and β_A. Consider a term like $\beta^m \beta_A^n$ in the expansion. The order

of this term should be considered to be $m+n$ and will be denoted by $O(m+n)$. Note that when $\beta_A = 0$ we recover the Wilson action.

The character expansion (3.49) still applies, but the b_r's are functions of β_A as well as β. To calculate the b_r's we Taylor expand the exponential in eqn. (3.52) and use the binomial expansion for each term and eq. (3.46) to get

$$b_r = \frac{1}{d_r \tilde{b}_o} \sum_{n=0}^{\infty} \sum_{m=0}^{n} \sum_{k=0}^{n-m} \sum_{j=0}^{m} \frac{(-1)^j}{j!k!(m-j)!(n-m-k)!} \left(\frac{\beta}{6}\right)^{n-m} \left(\frac{\beta_A}{8}\right)^{m} \times \int dU\, X_r^*(U)\, X_3^{n-k-j}(U)\, X_3^{*\,k+m-j}(U) \qquad (4.3)$$

where we replace X_r^* in terms of X_3 and X_3^* and use our results in Chapter 3 to get the given solution to the integral. $\tilde{b}_o$ can be written in powers of β and β_A then $\frac{1}{\tilde{b}_o}$ can be expanded. We choose $\bar{\beta} \equiv \beta/6$ and $\bar{\beta}_A \equiv \bar{\beta}_{A/8}$ for simplicity. Some of the results we have obtained are as follows:

$$u \equiv b_3 = \frac{1}{3}\bar{\beta} + \frac{1}{6}\bar{\beta}^2 + \frac{1}{3}\bar{\beta}\,\bar{\beta}_A + \frac{1}{3}\bar{\beta}^2\,\bar{\beta}_A + \frac{1}{3}\bar{\beta}\,\bar{\beta}_A^2 - \frac{5}{72}\bar{\beta}^4 + \frac{5}{12}\bar{\beta}^2\,\bar{\beta}_A^2$$
$$+ \frac{5}{18}\bar{\beta}\,\bar{\beta}_A^3 + \frac{17}{72}\bar{\beta}^5 + \frac{1}{18}\bar{\beta}^4\,\bar{\beta}_A - \frac{1}{12}\bar{\beta}^3\,\bar{\beta}_A^2 + \frac{17}{36}\bar{\beta}^2\,\bar{\beta}_A^3 + \frac{5}{12}\bar{\beta}\,\bar{\beta}_A^4$$
$$+ \frac{7}{720}\bar{\beta}^6 - \frac{13}{360}\bar{\beta}^5\,\bar{\beta}_A - \frac{2}{9}\bar{\beta}^4\,\bar{\beta}_A^2 + \frac{2}{9}\bar{\beta}^3\,\bar{\beta}_A^3 + \frac{49}{72}\bar{\beta}^2\,\bar{\beta}_A^4$$
$$+ \frac{139}{360}\bar{\beta}\,\bar{\beta}_A^5 + O(7) \qquad (4.4)$$

$$v \equiv b_6 = \frac{1}{6}\left[\frac{1}{2}\bar{\beta}^2 + \frac{1}{2}\bar{\beta}^3 + \bar{\beta}^2\,\bar{\beta}_A + \frac{3}{2}\bar{\beta}\,\bar{\beta}_A^2\right] + O(4) \qquad (4.5)$$

$$w \equiv b_8 = \frac{1}{8}\left[\bar{\beta}_A + \bar{\beta}^2 + \bar{\beta}_A^2 + \frac{2}{3}\bar{\beta}^3 + 2\bar{\beta}^2\bar{\beta}_A + \frac{5}{6}\bar{\beta}_A^3\right] + O(4) \qquad (4.6)$$

$$y \equiv b_{15a} = \frac{1}{15}\bar{\beta}\bar{\beta}_A + O(3) \quad . \qquad (4.7)$$

Note that the order of the lowest order terms in these coefficients is not necessarily the same as the order for the Wilson action case (i.e. $\beta_A = 0$). For our mixed action b_3 and b_8 are O(1), b_6, b_{10}, b_{15a} and b_{27} are O(2), the others are either O(3) or higher.

4.2 The String Tension

As we mentioned in Chapter 3 the string tension can be calculated by using Münster's cluster expansion method. Our choice of the Wilson loop is the conventional planar one. The leading polymer Ξ_o is tiled with the lowest character expansion coefficient, namely b_3, as in the Wilson action case. However note that it is different from the Wilson b_3 and given by eqn. (4.4). To calculate the higher order contributions we decorate the leading polymer exactly as in the Wilson action case. The diagrams which one decorates to the leading polymer to get the higher order contributions will be exactly as the Wilson ones. That is because the geometry of the character expansion does not depend on the choice of the action, only the coefficients are dependent to the form of the action. However, because the order of our character expansion coefficients can be different from the order for the Wilson action case, diagrams which contribute to a given order are not necessarily the same ones as the Wilson case. Our

calculation is up to 8th order (inclusively). The diagrams up to that order and their contributions to $-Ka^2$ are listed in Fig. 4.1. For the "occurrence factor" of each diagram in 4-dimensions see Münster (1981a). Note that the minus sign for the unattached cube is due to $a(C) = -1$ for a cluster of two polymers. The notation $N_{3r \ldots t} \equiv \int dU X_3(U) X_r(U) \ldots X_t(U)$ is introduced in Fig. 4.1 which will be also used in the mass gap calculation. $N_{3r \ldots t}$ can be calculated for a given $r \ldots t$ by using the group integral techniques introduced in Chapter 3. One obtains the string tension as follows:

$$\begin{aligned} Ka^2 = & -\log u - 4u^4 - 12u^5 - 24u^4 v - 32u^4 w - 32w^5 - 64\frac{w^5 v}{u} \\ & - 160\frac{w^5 y}{u} + 64u^6 + 256w^6 - 128u^8 - 160u^6 w^2 - 128u^4 w^4 \\ & - 64w^8 + O(9) . \end{aligned} \tag{4.8}$$

To compare this result in the $\bar{\beta}_A \to 0$ limit with the Wilson action calculations, we replace the order of the character expansion coefficients in eqn. (4.8) with the order after $\bar{\beta}_A \to 0$ limit is taken from eqns. (4.4-7). That reproduces the Wilson action results up to O(8).

Eqn. (4.8) can be rewritten as an explicit function of $\bar{\beta}$ and $\bar{\beta}_A$ by using the explicit expressions for u, v, w and y. However we will consider the string tension as a function of $\bar{\beta}$ and $\bar{\beta}_A$ only up to O(3), which reads

$$\begin{aligned} Ka^2 = & -\log(\bar{\beta}/3) - \frac{1}{2}\bar{\beta} - \bar{\beta}_A + \frac{1}{8}\bar{\beta}^2 - \frac{1}{2}\bar{\beta}\bar{\beta}_A - \frac{1}{2}\bar{\beta}_A^2 + \frac{1}{6}\bar{\beta}^3 \\ & + \frac{1}{4}\bar{\beta}^2\bar{\beta}_A - \frac{1}{4}\bar{\beta}\bar{\beta}_A^2 - \frac{1}{6}\bar{\beta}_A^3 + O(4) . \end{aligned} \tag{4.9}$$

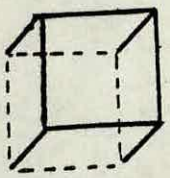

$4u^4$

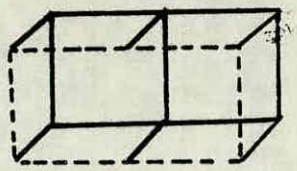

$8u^6$

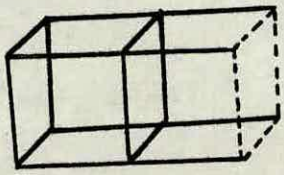

$4u^8$

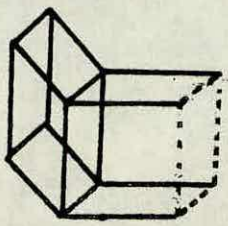

$8u^8$

Fig. 4.1 : (see over): Diagrams and their contributions to $-Ka^2$ up to 8th order. $N_{3rs} \equiv \int dU\ X_3(U)\ X_r(U)\ X_s(U)$. The sums are over all the non trivial, inequivalent, irreducible representations such that the order of the sums does not exceed eight. The dashed lines indicate where the decorations are fitted to the leading polymer. Lines which are not parallel are meant to be orthogonal. The last diagram is not attached to the leading polymer.

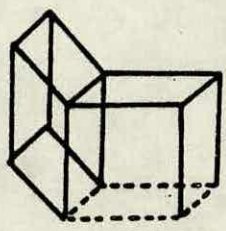

$32u^8$

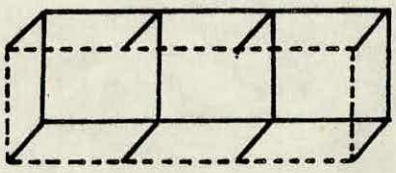

$8u^8$

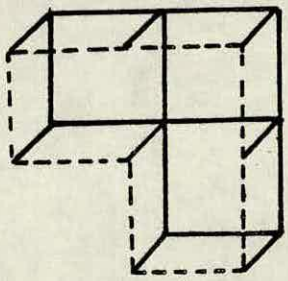

$16u^8$

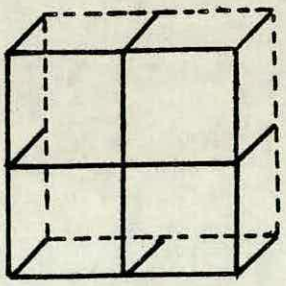

$4u^8$

Fig. 4.1 (see over)

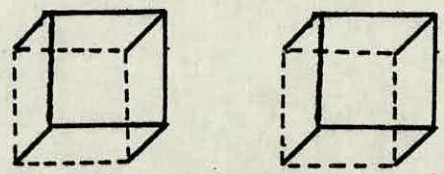

$$- 16u^8$$

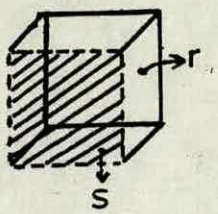

$$4 \sum_{r,s} N_{3rs} \frac{d_r d_s}{d_3} \frac{b_r^5 b_s}{u}$$

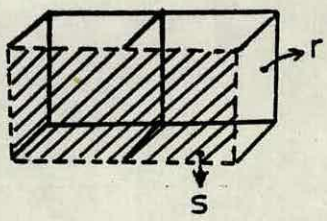

$$8 \sum_{r,s} N_{3rs} \frac{d_r d_s}{d_3} \frac{b_r^8 b_s^2}{u^2}$$

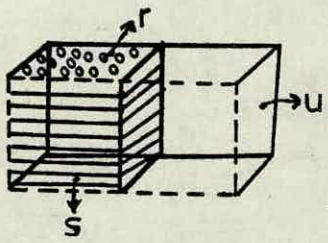

$$16 \sum_{r,s} N_{3rs} \frac{d_r d_s}{d_3} b_r^4 b_s^2 \; u^2$$

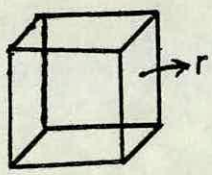

$$-4 \sum_{r} d_r^2 \, b_r^6$$

Fig. 4.1

There are various reasons for us not to consider the higher order contributions. As we will see in the following section, our mass gap calculation is up to O(3) inclusively; we prefer to keep both the string tension and the mass gap at the same order to decide $m/\sqrt{K}$. We will apply the same kind of Padé approximation to both calculations, which we also prefer at the same order. Because we have the constant string tension lines in the fundamental-adjoint plane (i.e. $\beta - \beta_A$ plane) already obtained by some method other than the strong coupling expansions in the literature [Bowler et al. (1984); Jurkiewicz et al. (1984); Grossman and Samuel (1983)], we can compare our O(3) string tension calculation and the Padé approximated calculation at O(3) with these results, to decide if our O(3) string tension is a good one, and to see how much better is the Padé approximated version of it. Then, one can naively argue that if the string tension at O(3) and its Pade approximated version are good results, so is the mass gap at this order and its Padé approximated version of the same kind. Note that there are no references available in the literature for the constant mass gap lines in the fundamental-adjoint plane.

The constant string tension lines in the fundamental-adjoint plane which we show from order one to three in Fig. 4.3a, b, c tell us how the physics changes for different ratios $\overline{\beta}_A/\overline{\beta}$. We have also shown the first-order phase lines of the theory in Fig. 4.2, as investigated by Bhanot (1982).

In Fig. 4.3a we have almost straight lines which is contrary to the O(1) string tension of SU(2) where these lines are very much curved [Bhanot and Dashen (1982)]. That is because, for SU(3), we have a β term, as seen in eqn. (4.9), due to the fact that the integral $\int dU\, X_3^3(U)$ is a non-vanishing one; the β term added

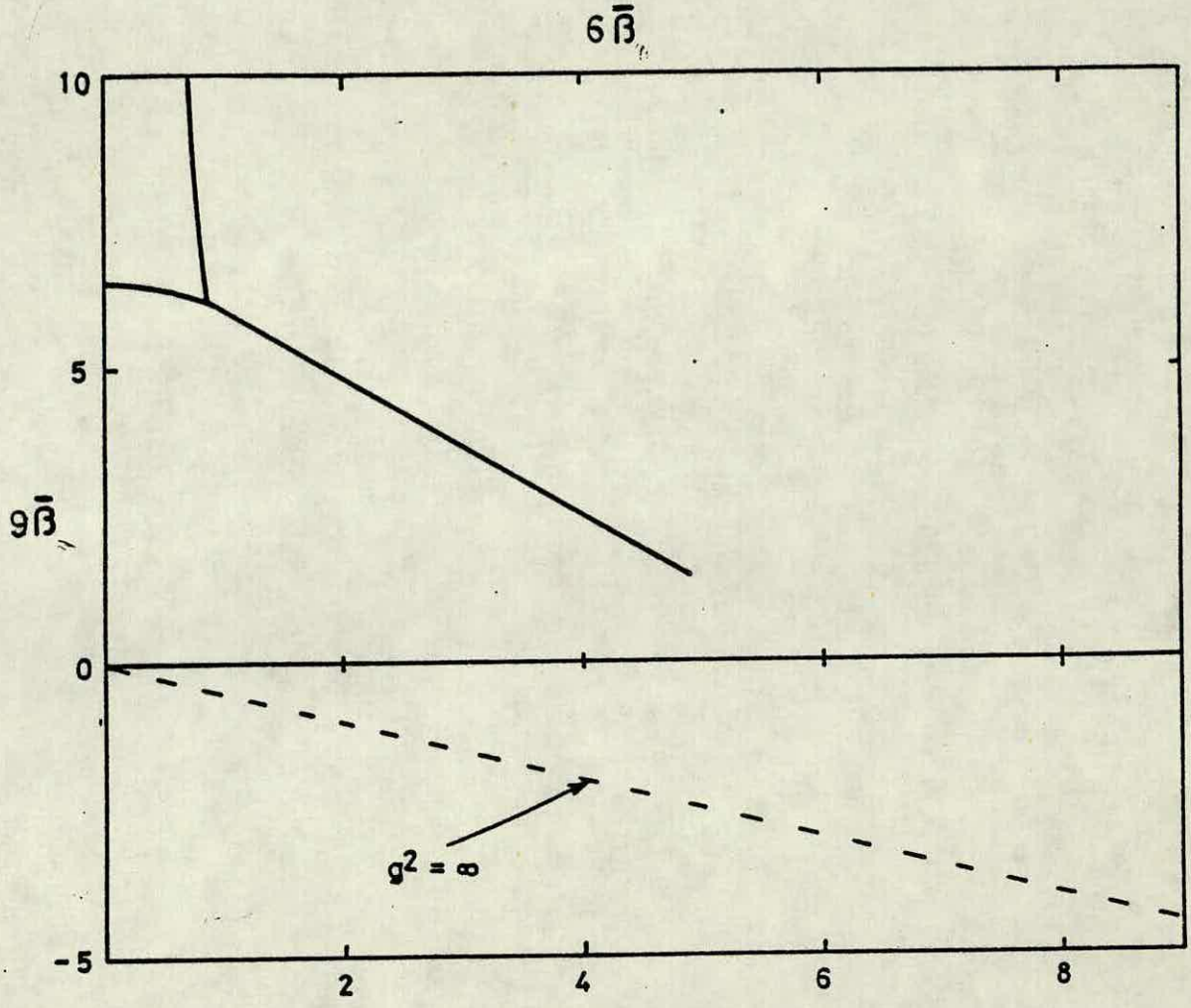

Fig. 4.2: Phase diagram of the SU(3) gauge theory in the fundamental-adjoint plane from Bhanot (1982). The lines represent first-order phase transitions.

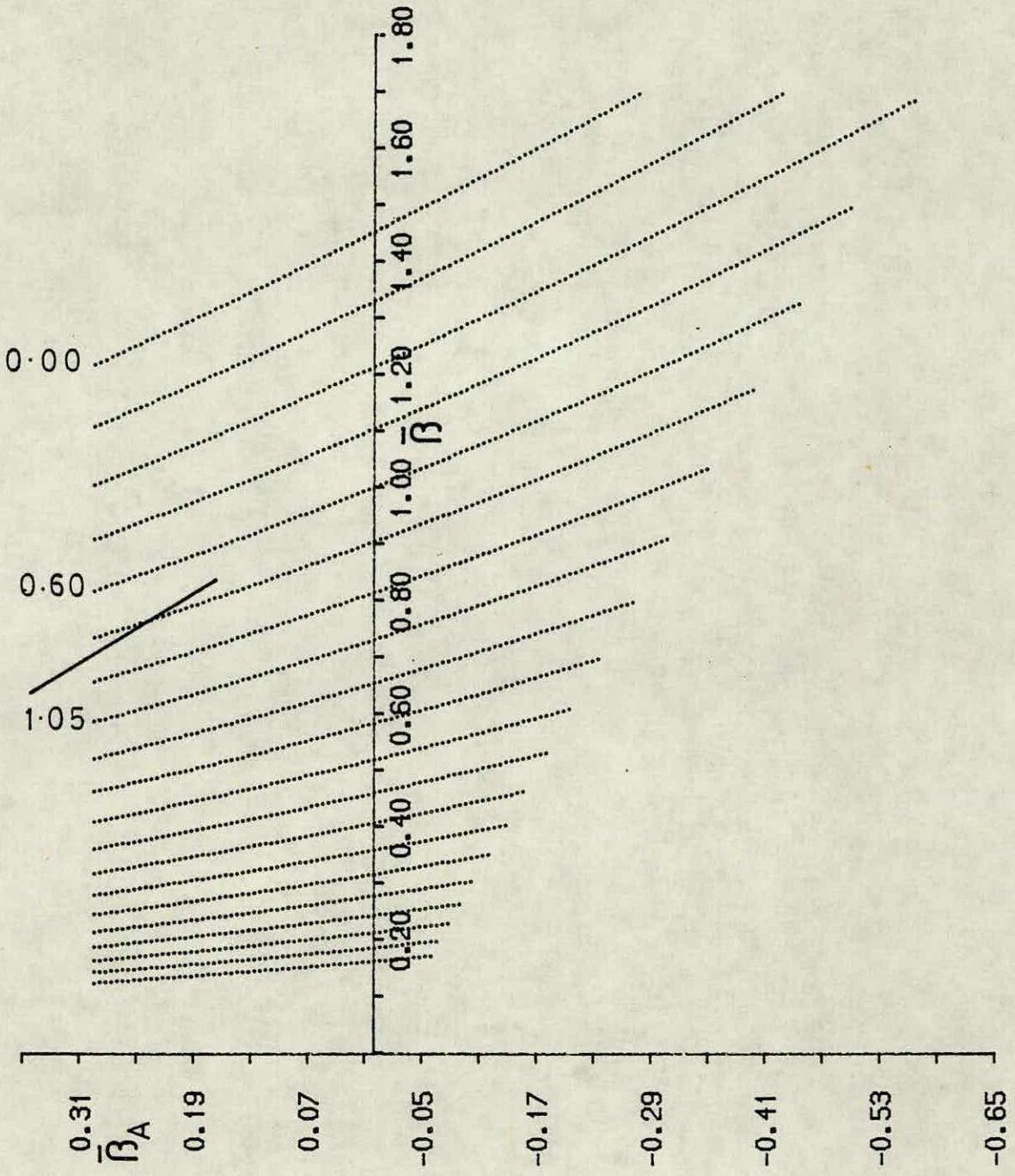

Fig. 4.3a: Lines of constant string tension (Ka^2) at O(1) from eqn. (4.9). The values of the string tension at some lines are indicated. The values of two successive lines differ by 0.15. The continuous line is a part of the phase line from Fig. 4.2.

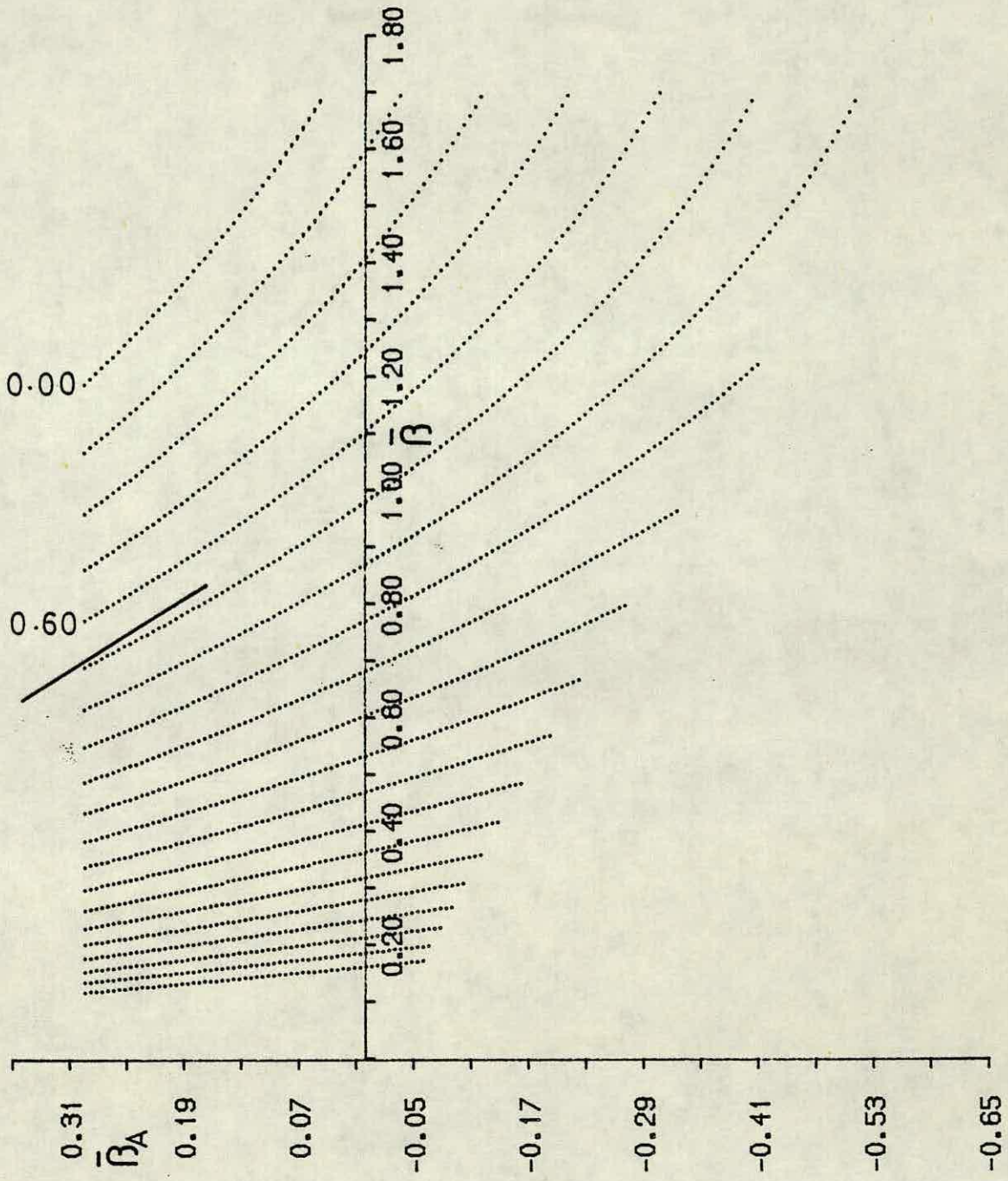

Fig. 4.3b: As Fig. 4.3a, but for O(2).

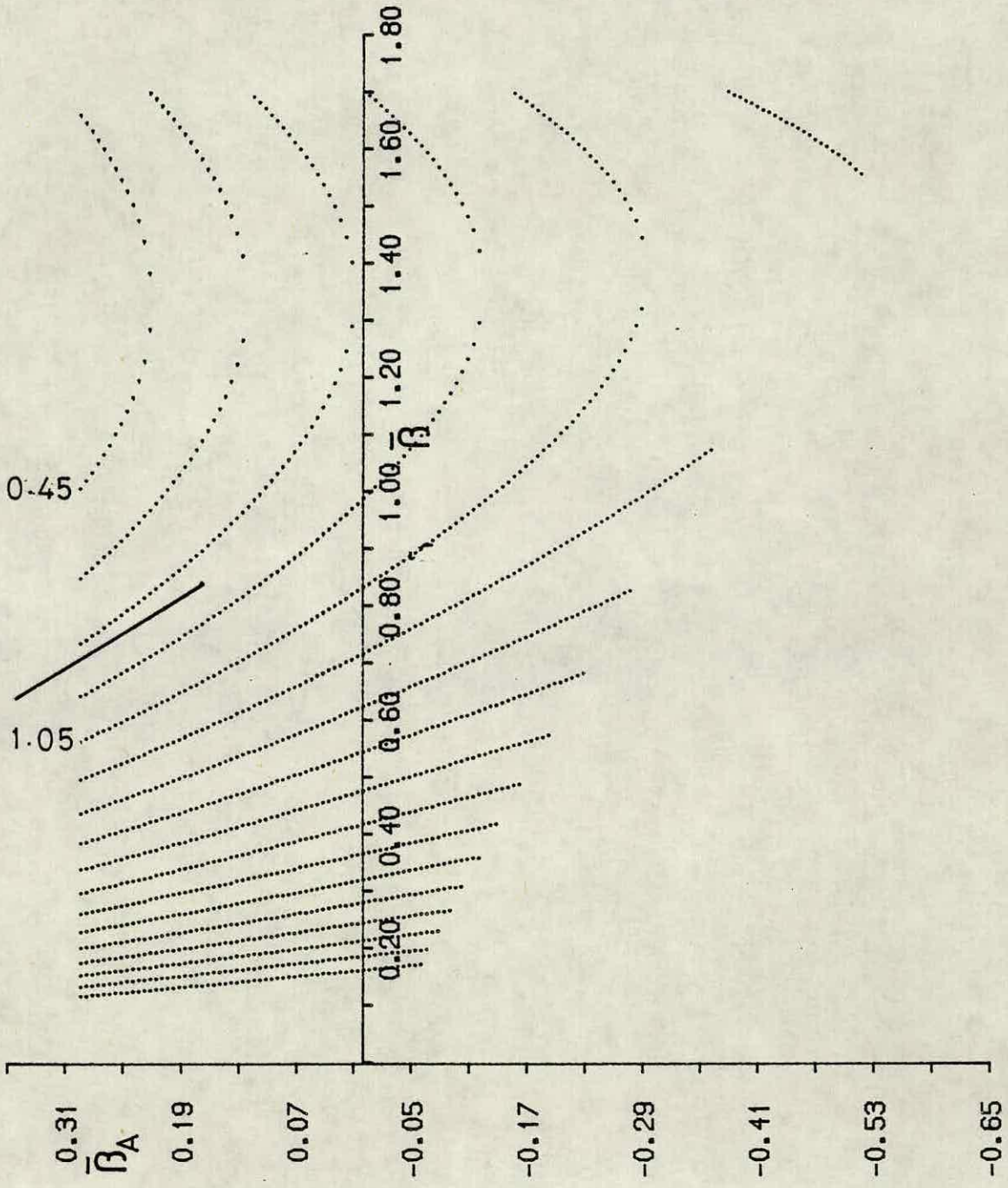

Fig. 4.3c: As Fig. 4.3a, but for O(3).

to the logarithmic term gives a line close to a straight line for $\bar{\beta} < 3$. On the other hand, for SU(2), if X_2 is the character in the fundamental representation, the integral $\int dU\, X_2^3(U)$ vanishes, meaning that there is no β term in the string tension at this order apart from the logarithmic term; hence a curved line.

The O(3) lines in Fig. 4.3c show a quick "turn up" at about $\bar{\beta} = 1.3$; we interpret this as meaning that our strong coupling expansion series for the string tension at O(3) is not applicable for $\bar{\beta} \gtrsim 1.2$. Considering scaling for the string tension sets in at about $\bar{\beta} \gtrsim 1.1$ on the Wilson axis [Hasenfratz and Hasenfratz (1984); Bowler et al. (1985); Kennedy et al. (1985)], our strong coupling string tension result should be a useful one, particularly below the Wilson axis (i.e β_A negative).

We shall try to extend the applicability region of these lines further through a Padé approximation. When one attempts to Padé approximate a truncated series expansion like the one in eqn. (4.9), one has to make a choice. This is because, in general, there are more than one possible ways to approximate the given truncated series. We will not try to give a full account of the Padé approximations but pinpoint the main concept in it. The idea is to approximate the truncated series as a ratio of two polynomials where the coefficients of these polynomials are decided by the coefficients of the truncated series. As a simple example, consider the series $1 + x + 2x^2 + O(x^3)$. There are two possible ways of writing this series as a ratio of the two polynomials, i.e. two different Padé approximations of it; $(1 - x)/(1 - 2x)$ and $1/(1 - x - x^2)$. Both of these approximations satisfy the original series up to $O(x^3)$ and both of them are equally

acceptable. For a full discussion of the subject we refer the reader to a book on approximation theories.

Of the many possibilities we choose to study in detail the "diagonal" two-variable approximant to the string tension in (4.9) is as follows:

$$Ka^2 = -\log(\bar{\beta}/3) + \frac{-\frac{1}{2}\bar{\beta} - \bar{\beta}_A + \frac{1}{4}\bar{\beta}^2}{1 - \frac{1}{4}\bar{\beta} - \frac{1}{2}\bar{\beta}_A + \frac{13}{48}\bar{\beta}^2 + \frac{1}{12}\bar{\beta}\,\bar{\beta}_A + \frac{1}{12}\bar{\beta}_A^2} \qquad (4.10)$$

We have shown the constant string tension lines from this equation in Fig. 4.4. The first point to note about these lines is that, unlike the O(3) lines in Fig. 4.3c, they do not show a turn up and they are straight lines; it looks like the Padé approximation enabled us to extend the validity of our string tension calculations further, and it is very likely that the Padé approximated lines are closer to the true string tension lines in the intermediate region.

We have mentioned that we have the chance of comparing our lines with the ones already available in the literature. Our lines are in close agreement with the ones obtained via a Monte Carlo calculation by Bowler et al. (1984). One can also extract these lines from the large N calculation of Grossman and Samuel (1983) as well as from the two-loop calculations of Jurkiewicz et al. (1984). The lines from these two calculations are slightly different from the Bowler et al. lines. Our lines are closer to the Bowler et al. ones.

In Fig. 4.3c and Fig. 4.4, the lines appear to be more or less parallel to the phase line around it. However, there is a "splay out" of the lines as one moves towards the smaller values of $\bar{\beta}_A$

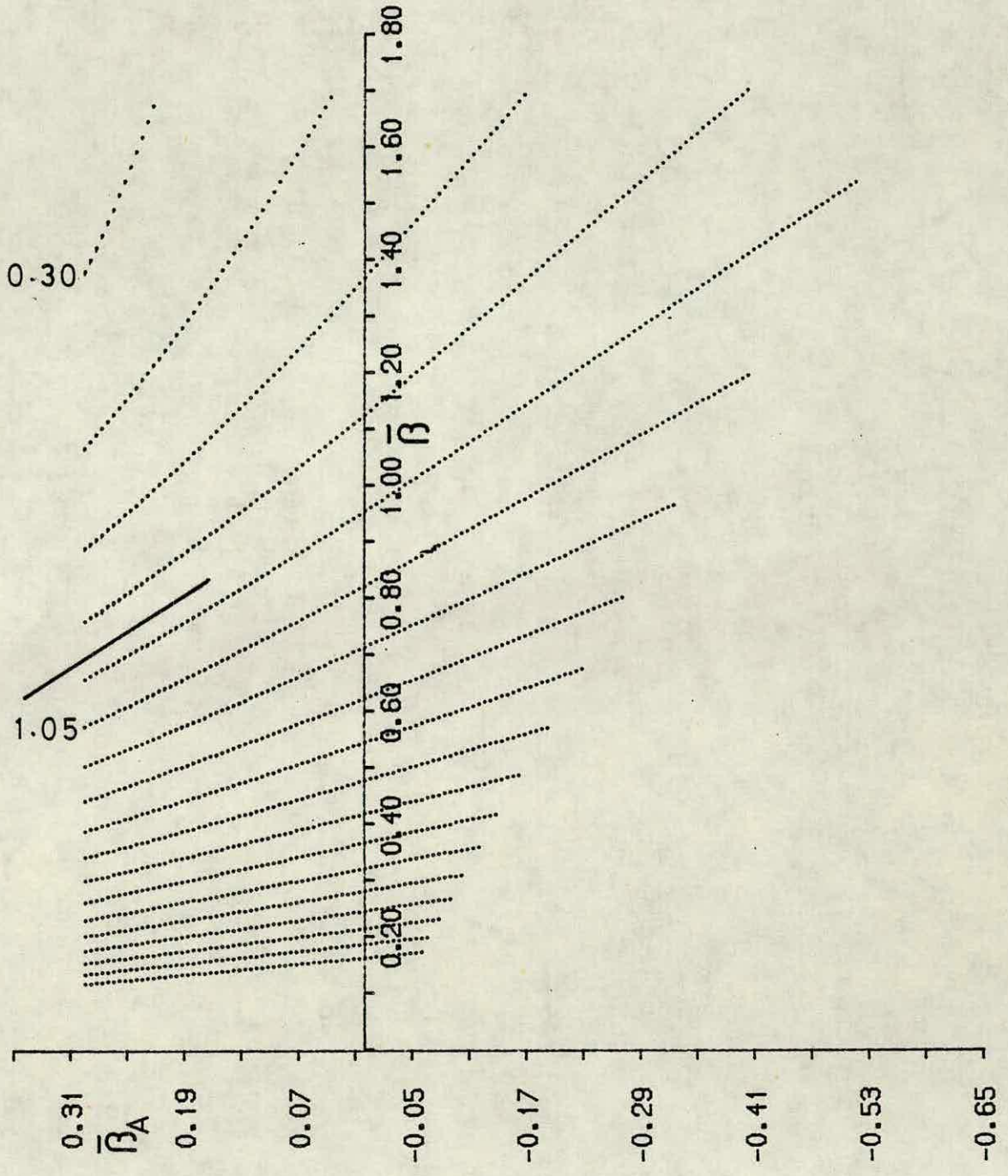

Fig. 4.4: As Fig. 4.3a but for Padé approximated eqn. (4.10).

in the direction of the phase line. The splay out is particularly clear for the Padé approximated lines in Fig. 4.4. As a consequence of the splay out there is a fast change in the value of string tension for positive β_A contrary to negative β_A where the change is more gradual. The value of the string tension over the phase line and the critical endpoint is roughly 0.8 (i.e. it does not vanish), which is consistent with the first-order character of the phase line. Those features of the lines can also be observed from the other calculations in the literature we have mentioned in the previous paragraph. The same features have also been observed for the SU(2) mixed action string tension lines by various authors; via large N expansions [Grossman and Samuel (1983)], via Monte Carlo calculations [Bhanot and Dashen 1982] and via strong coupling expansions [Arroyo et al. (1982)].

4.3 The Mass Gap

The glueball mass calculations for different groups in the literature, which we have listed in Chapter 3, are all for the Wilson action; there are no mixed action results available, and a mixed action calculation is not straightforward from the results for the Wilson action. Consider the fundamental-adjoint mixed action SU(3) theory. The order of w in eqn. (4.6) is 1 instead of 2, which is the case for the Wilson action. That is the main reason for one's inability to generate the mixed action glueball masses from the Wilson action calculations in a straightforward fashion. This point will become clear as we proceed in

the calculation of the mass of 0^{++}. Our calculation is for the on-axis case.

As in Chapter 3, we consider two parallel space-like plaquettes p_1 and p_2 which are located at the same space coordinates but separated in Euclidean time by a distance t. The contribution to the correlation function $\rho(t)$ due to the minimal tube which connects p_1 and p_2 is u^{4t} as before. However, u is given by eqn. (4.4) instead of the u of the Wilson action.

We will consider the diagrams contributing to the correlation function up to O(3) inclusively. The diagrams and their contributions are given in Fig. 4.5. Fig. 4.5a represents a partition inserted into the minimal tube. The $N_{33}{}^*{}_r$ term in E arises because we made a substitution

$$X_3(U) \rightarrow \frac{1}{\sqrt{2}} (X_3(U) + X_3{}^*(U)) \tag{4.11}$$

for all the plaquettes of the minimal tube, including p_1 and p_2. That is because the glueball 0^{++} is a charge conjugate even state, and the substitution (4.11) is equivalent to summing over p_1 and p_2 in the conjugate representation as well as in the fundamental representation itself. The $N_{3r}\, N_3{}^*{}_s$ term in F, the $N_{3rs}\, N_3{}^*{}_\alpha$ term in B_n, the $N_{3rs}\, N_3{}^*{}_{r\ell}$ term in A_n and the $N_{3\alpha s}\, N_3{}^*{}_{\gamma\ell}\, N_{\alpha\gamma r}$ term in A_{mn} also arise for the same reason. Fig. 4.5d represents the minimal tube with length $t+1$ but four mutually perpendicular plaquettes removed from it and the loose ends are covered with two plaquettes in representations r and s. Note that, even though that tube has a length of $t+1$, it still contributes to $\rho(t)$

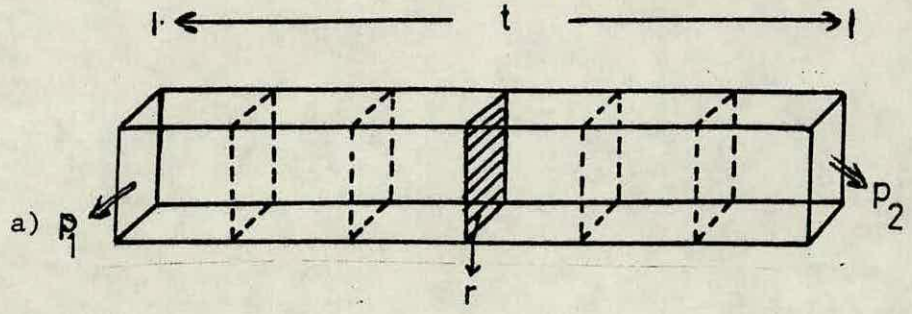

$$E = \sum_r d_r(N_{33r} + N_{33^*r})b_r$$

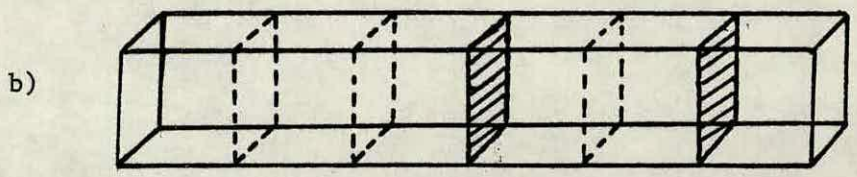

E^2

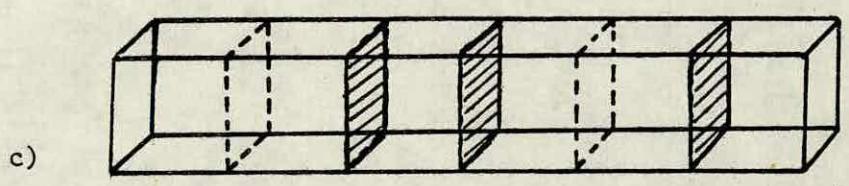

E^3

Fig. 4.5 (see over): Diagrams and their values, labelled as E, F, A_n, A_{mn}, and B_n, which contribute to $\rho(t)$ up to $O(3)$ inclusively. The sums are over all the non-trivial, inequivalent, irreducible representations such that the order of the sums does not exceed three. The values do not include the occurrence factors.

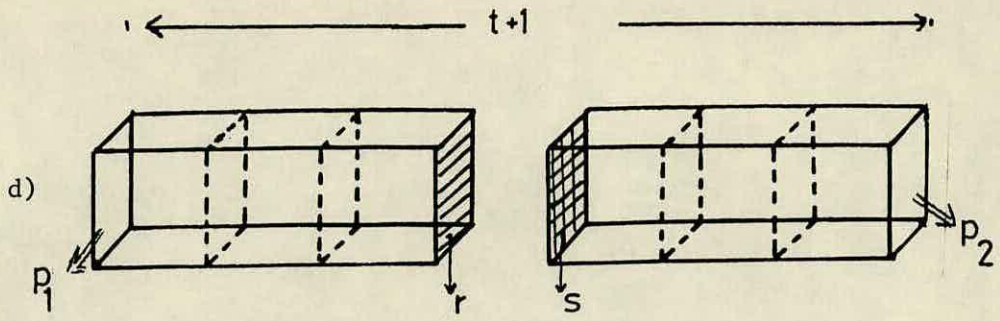

$$F = - \sum_{r,s} d_r d_s (N_{3r} N_{3s} + N_{3r} N_{3}{}^{*}{}_{s}) b_r b_s$$

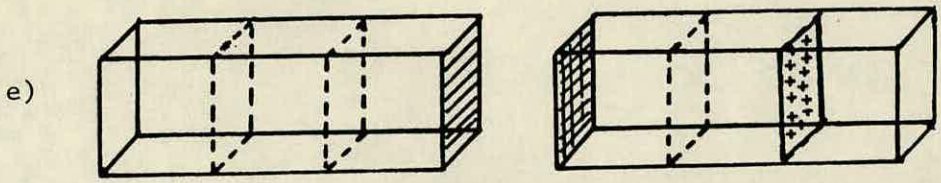

FE

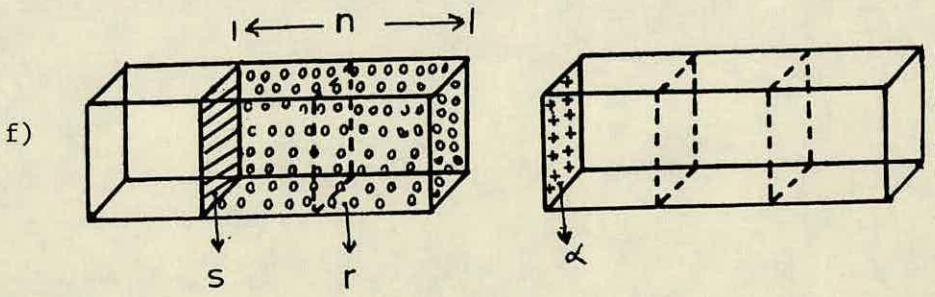

$$B_n = - \sum_{\substack{r,s,\alpha \\ r \neq 3,3^*}} d_r d_s d_\alpha (N_{3rs} N_{3\alpha} + N_{3rs} N_{3}{}^{*}{}_{\alpha}) \frac{b_r^{4n+1} b_s b_\alpha}{u^{4n}}$$

$$(n = 1,2, \ldots, t-2)$$

Fig. 4.5 (see over).

g)

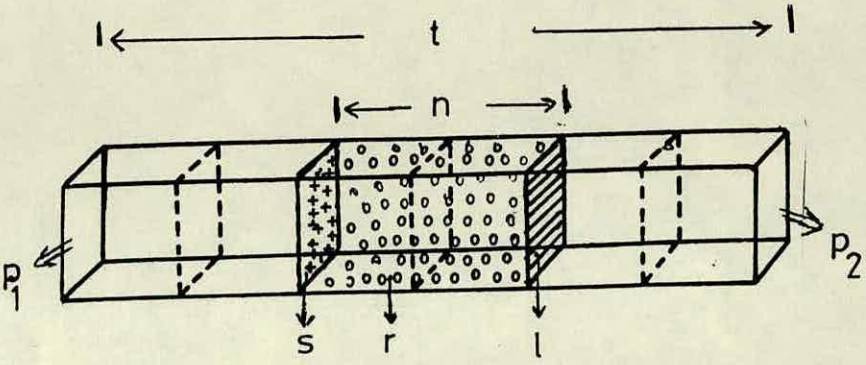

$$A_n = \sum_{\substack{r,s,\ell \\ r\neq 3,3^*}} d_s d_\ell (N_{3rs}\, N_{3r\ell} + N_{3rs}\, N_{3^*r\ell}) \frac{b_r^{4n}\, b_s b_\ell}{u^{4n}}$$

$(n = 1,2, \ldots, t-2).$

h)

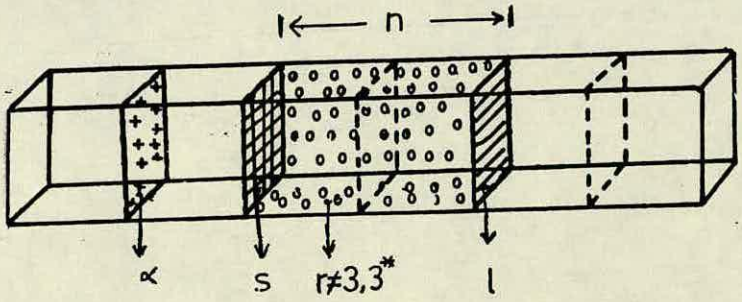

$A_n E$

$(n = 1,2, \ldots, t-3).$

Fig. 4.5 (see over).

i)

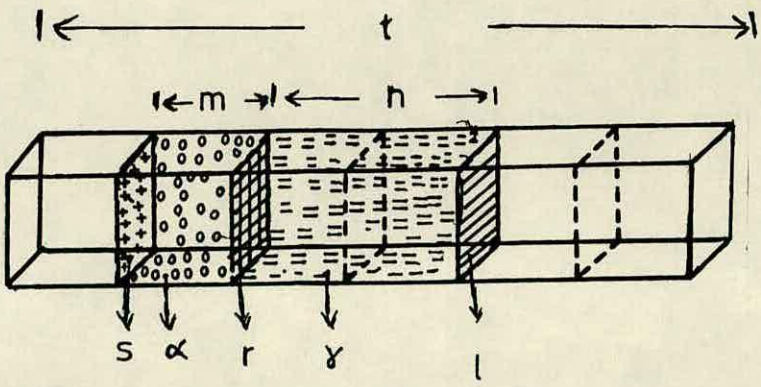

$$A_{mn} = \sum_{\substack{\alpha,\gamma,r,s,\ell \\ \alpha \neq 3,3^* \\ \gamma \neq 3,3^*}} d_s\, d_\ell\, d_r (N_{3\alpha s}\, N_{3\gamma\ell}\, N_{\alpha\gamma r} + N_{3\alpha s}\, N_{3^*\gamma\ell}\, N_{\alpha\gamma r}) \times \frac{b_\alpha^{4m}\, b_\gamma^{4n}\, b_s\, b_\ell\, b_r}{u^{4m+4n}}$$

$$(m+n = 2,3, \ldots t-2).$$

Fig. 4.5

rather than $\rho(t+1)$, that is because we have four plaquettes removed from it. The same also applies to Fig. 4.5e and Fig. 4.5f. To get Fig. 4.5f, one inserts a partition with representation s into Fig. 4.5d, at a distance n from the loose end, and tiles the $4n$ plaquettes between the partition and the loose end with a representation r different from the fundamental representation or its conjugate. The minus signs for F and B_n arise because Fig. 4.5d and Fig. 4.5f consist of two disconnected polymers. Fig. 4.5g represents two partitions with representations s and ℓ inserted into the minimal tube at a distance n from each other such that the $4n$ plaquettes between the partitions are tiled with a representation r different from the fundamental representation or its conjugate. Finally, Fig. 4.5i can be obtained from Fig. 4.5g by inserting another partition to it such that the plaquettes of the minimal tube between the two partitions are tiled with a representation other than the fundamental representation or its conjugate.

The group integration formulas of Chapter 3 enable us to calculate the summations in Fig. 4.5 as follows:

$$E = 3u + 6v + 8w \tag{4.12}$$

$$F = -18u^2 \tag{4.13}$$

$$A_n = \left(\frac{w}{u}\right)^{4n}(18u + 72uv + 180uy) + O(4) \tag{4.14}$$

$$A_{mn} = 288\left(\frac{w}{u}\right)^{4m+4n-2} w^3 + O(4) \tag{4.15}$$

$$B_n = -144\left(\frac{w}{u}\right)^{4n-2} w^3 + O(4) \quad . \tag{4.16}$$

It is important to note that $\frac{w}{u}$ is $O(0)$ for the mixed action and $O(1)$ for the Wilson action.

The final ingredient one needs for the calculation of the correlation function $\rho(t)$ is the occurrence factor of each diagram in Fig. 4.5. For instance the occurrence factor of Fig. 4.5a is $t-1$, that is to say, one can put the partition at $t-1$ different positions. Considering the occurrence factors of the other diagrams in the same way, one obtains:

$$\rho(t) = u^{4t}\Big[1 + (t-1)E + \frac{(t-1)(t-2)}{2!}E^2 + \frac{(t-1)(t-2)(t-3)}{3!}E^3 + (t-1)F + (t-1)(t-2)FE + \sum_{n=1}^{t-2}(t-n-1)A_n + \sum_{n=1}^{t-3} n(t-n-2)A_{1n} + 2\sum_{n=1}^{t-2}(t-n-1)B_n + \sum_{n=1}^{t-3}(t-n-1)(t-n-2)A_nE\Big] + O(4) \quad (4.17)$$

where we used $A_{mn} = A_{m'n'}$ if $m' + n' = m + n$ from eqn. (4.15). The factor of 2 in front of the third sum arises due to the symmetry in Fig. 4.4f. Note that the result is true for any dimension. That is because up to the given order all the diagrams consist of partitions inserted into the minimal tube. The dimension dependence starts at $O(4)$ as one attaches a cube to the minimal tube. Also note that we did not consider different space-like orientations of p_1 and p_2. That is because, in our diagrams, changing the orientation of p_1 or p_2 does not make any difference in the value of a diagram or its occurrence factor.

To evaluate the mass gap, we take the logarithm of both sides in eqn. (4.17) and keep only the linear terms in t. At the end

we take $t \to \infty$ limit for a large distance correlation. The result is as follows:

$$ma = -4\,\log u - \log(1+E+F) - \sum_{n=1}^{\infty} A_n - \sum_{n=1}^{\infty} n\,A_{1n} - 2\sum_{n=1}^{\infty} B_n + \sum_{n=1}^{\infty} (n+1)A_n E + O(4) \quad . \tag{4.18}$$

Here m is in physical units. Note that the infinite sums, which do not appear for the Wilson case, will survive because the order of the sums does not rise with n due to w/u being $O(0)$ for the mixed action. Eqns. (4.12-16) enable us to write this expression in terms of the character expansion coefficients:

$$ma = -4\,\log u - \log(1+3u+6v+8w-18u^2) + \frac{(w/u)^4}{[1-(w/u)^4]}\,(-18u^2 - 72uv - 180uy + 432u^2w + 54u^3) + \frac{(w/u)^4}{[1-(w/u)^4]^2}\,(54u^3 + 144u^2w - 288\,\frac{w^5}{u^2}) + O(4) \tag{4.19}$$

where we used $\sum_{n=1}^{\infty} x^n = \frac{1}{1-x} - 1$ and $\sum_{n=1}^{\infty} (n+1)x^n = \frac{1}{(1-x)^2} - 1$ to replace the infinite sums. Note that the infinite sums in eqn. (4.18) will diverge for $\left|\frac{w}{u}\right| \geq 1$, therefore the mass gap expressed by eqn. (4.19) is applicable only for $\left|\frac{w}{u}\right| < 1$. However, that region of divergence is a narrow one near the origin in the $\beta - \beta_A$ plane, that is to say, it is a region of very strong

coupling. Hence, such a divergence is not a total surprise. The analogy of that for the Wilson case is the divergence of the mass gap at $\beta = 0$.

One can take the $\bar{\beta}_A \to 0$ limit of our mass gap result in eqn. (4.19) in the same way as we did for the string tension. Comparison of our result in that limit with the 8th order Wilson action mass gap calculation by Seo (1982) shows that all the terms up to $O(3)$ are in agreement except two; we have an extra $\frac{w^9}{u^6}$ term in our result and a $\frac{w^4 v^2}{u^4}$ term missing from it. That is because the extra term is $O(12)$ for the Wilson action and the missing term is $O(4)$ for the mixed action.

The explicit expression for the mass gap reads

$$
\begin{aligned}
ma = & -4\log(\bar{\beta}/3) - 3\bar{\beta} - 5\bar{\beta}_A + \bar{\beta}^2 - 2\bar{\beta}\bar{\beta}_A - \frac{5}{2}\bar{\beta}_A^2 + \frac{7}{6}\bar{\beta}^3 + \bar{\beta}^2\bar{\beta}_A \\
& - \frac{5}{2}\bar{\beta}\bar{\beta}_A^2 - \frac{5}{6}\bar{\beta}_A^3 - \frac{(\frac{3}{8})^4 (\frac{\bar{\beta}_A}{\bar{\beta}})^4}{1 - (\frac{3}{8})^4 (\frac{\bar{\beta}_A}{\bar{\beta}})^4} (2\bar{\beta}^2 + 2\bar{\beta}^3 + 2\bar{\beta}^2\bar{\beta}_A) \qquad (4.20) \\
& + \frac{(\frac{3}{8})^4}{[1 - (\frac{3}{8})^4 (\frac{\bar{\beta}_A}{\bar{\beta}})^4]^2} \left(6\frac{\bar{\beta}_A^4}{\bar{\beta}} + 2\frac{\bar{\beta}_A^5}{\bar{\beta}^2} - 8\bar{\beta}_A^3 - \frac{81}{1024}\frac{\bar{\beta}_A^9}{\bar{\beta}^6} \right) + O(4) .
\end{aligned}
$$

We have shown the constant mass gap lines from order one to three in Fig. 4.6a, b, c. The lines behave very much the same as the string tension ones; there is a parallelism to the phase line along with the splay out and a non-vanishing mass gap over the phase. However, the value of $\bar{\beta}$ where the turn up of the lines in Fig. 4.6c occurs is slightly smaller than the value of $\bar{\beta}$ for the string tension. However, it is known that [De Forcrand et al. (1985a)]

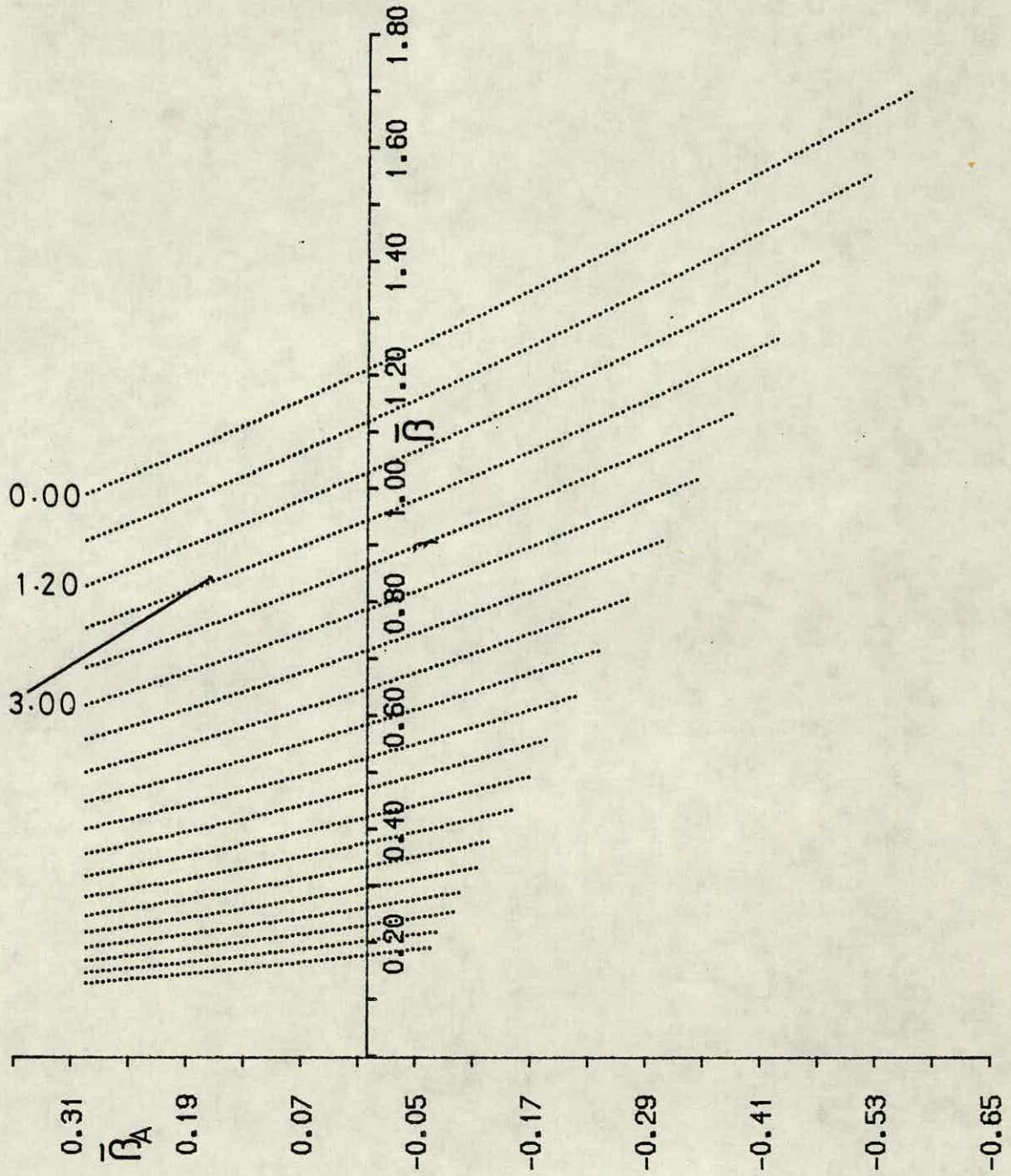

Fig. 4.6a: Lines of constant mass gap (ma) at O(1) from eqn. (4.20). The values of the mass gap at some lines are indicated. The values of two successive lines differ by 0.6. The continuous line is a part of the phase line from Figure 4.2.

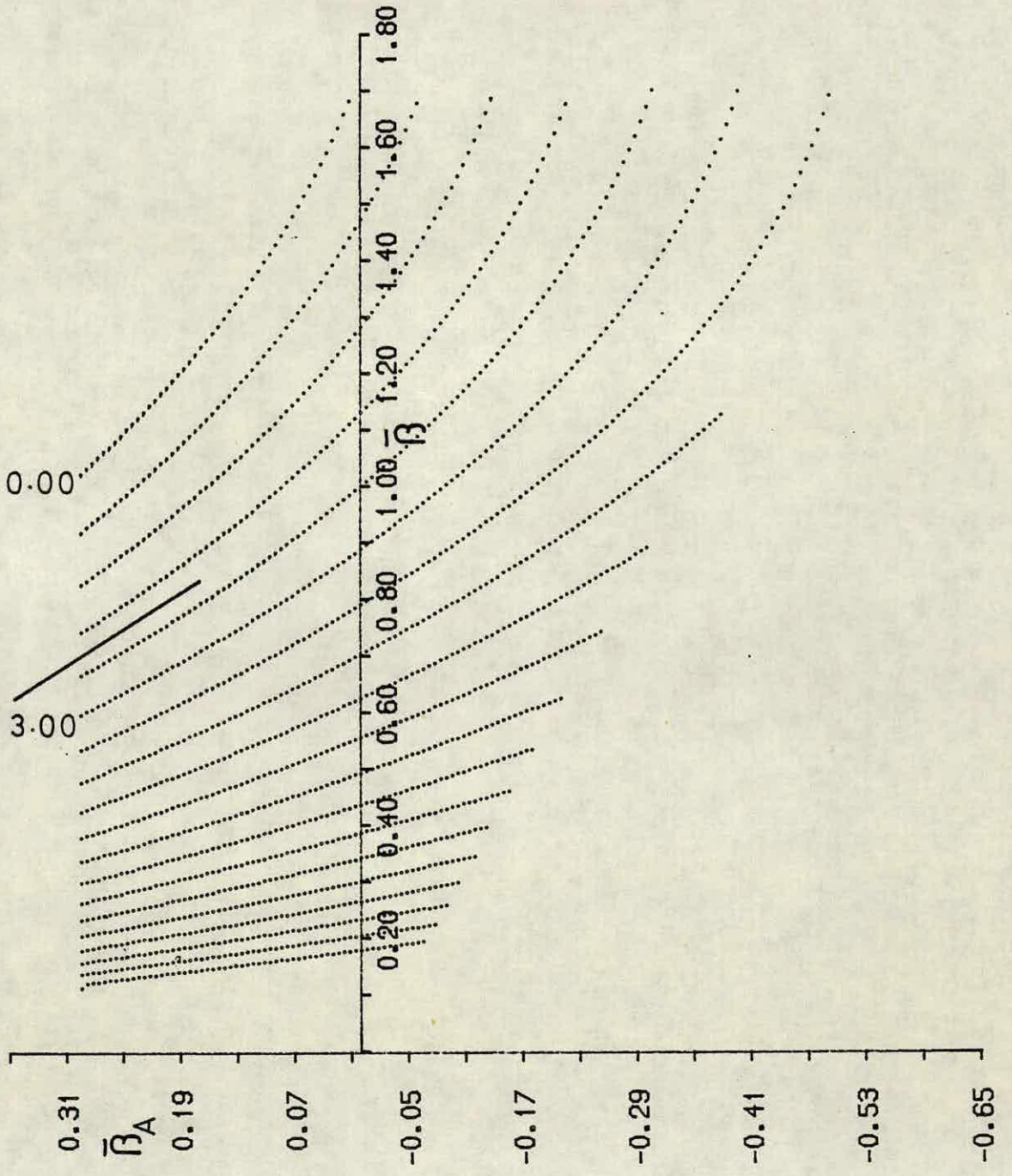

Fig. 4.6b.: As Fig. 4.6a but for O(2).

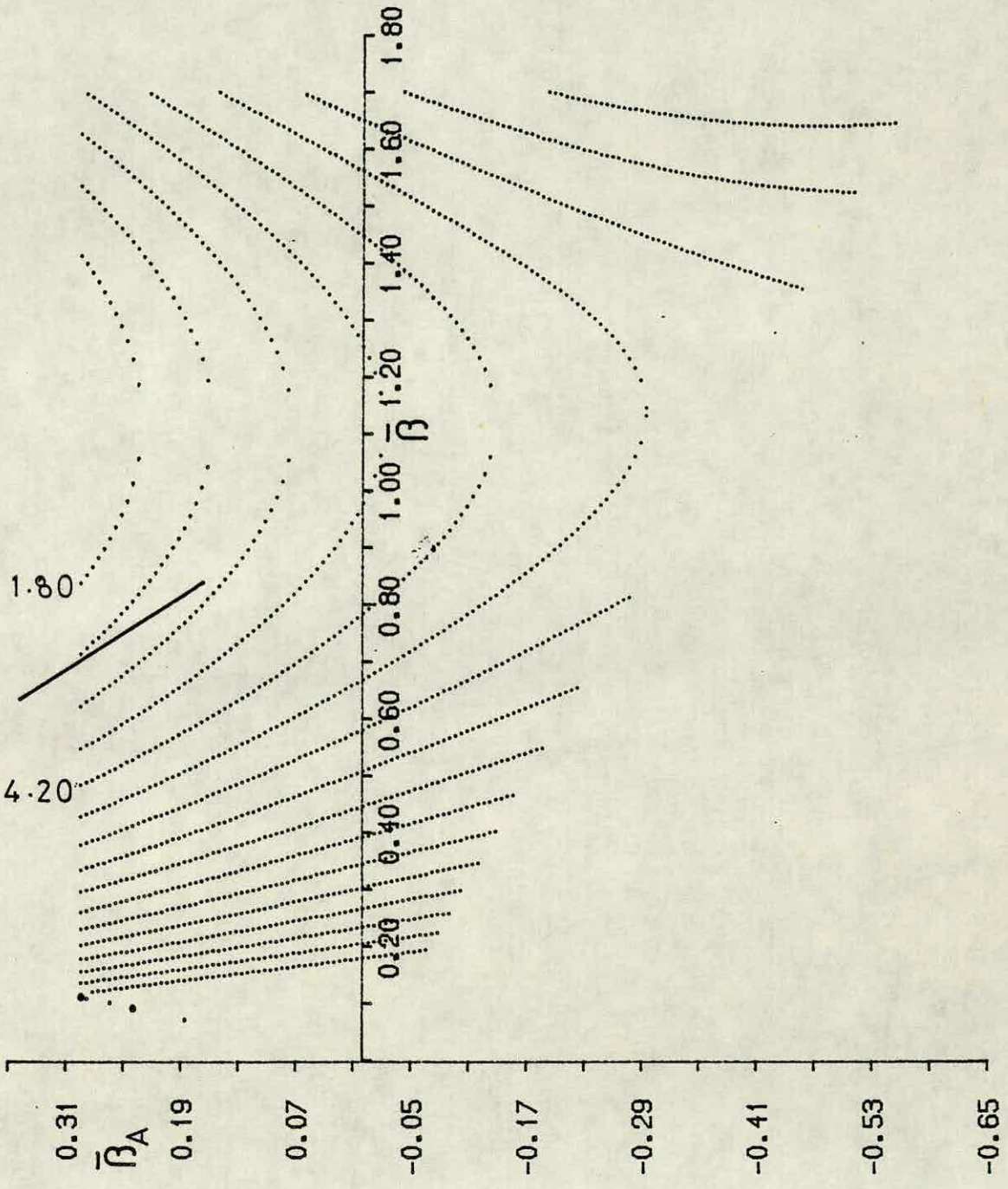

Fig. 4.6c: As Fig. 4.6a but for O(3).

scaling for the mass gap sets in a little earlier than it does for the string tension, at about $\bar{\beta} \approx 0.9$. Therefore, our strong coupling mass gap result is still a useful one for the investigation of scaling.

The type of Padé approximation we apply to the mass gap is the same as we did for the string tension and reads

$$ma = -4 \log(\bar{\beta}/3) + \frac{S_1 \bar{\beta} + S_2 \bar{\beta}_A + S_3 \bar{\beta}^2 + S_4 \bar{\beta} \bar{\beta}_A}{1 + T_1 \bar{\beta} + T_2 \bar{\beta}_A + T_3 \bar{\beta}^2 + T_4 \bar{\beta} \bar{\beta}_A + T_5 \bar{\beta}_A^2} \tag{4.21}$$

where the coefficients are given as

$$S_1 = -3, \qquad S_2 = -5, \qquad T_2 = -\frac{1}{2} \tag{4.22}$$

$$T_5 = -\frac{81}{5120} \frac{R}{W^2} \left(\frac{\bar{\beta}_A}{\bar{\beta}} \right)^2 + \frac{1}{12} \tag{4.23}$$

$$S_4 = \frac{\frac{40}{3} \frac{1}{W^2} \left(\frac{3}{8}\right)^4 \left(\frac{\bar{\beta}_A}{\bar{\beta}}\right)^3 - \frac{729}{25600} \frac{R}{W^2} \left(\frac{\bar{\beta}_A}{\bar{\beta}}\right)^2 - 8 \frac{R}{W^2} + 2 \frac{R}{W} - \frac{8}{45}}{\frac{2}{3} \frac{R}{W} - \frac{13}{30}} \tag{4.24}$$

$$T_1 = -\frac{1}{5} S_4 - \frac{1}{10} \tag{4.25}$$

$$S_3 = -3T_1 - 2 \frac{R}{W} + 1 \tag{4.26}$$

$$T_3 = \frac{1}{3}\left(1 - 2 \frac{R}{W}\right) T_1 + \frac{7}{18} - \frac{2}{3} \frac{R}{W} + 2 \frac{R}{W^2} - \frac{\left(\frac{3}{8}\right)^3}{W^2} \left(\frac{\bar{\beta}_A}{\bar{\beta}}\right)^3 \tag{4.27}$$

$$T_4 = -\frac{5}{3} T_3 - \frac{1}{6} \left(1 - 2 \frac{R}{W}\right) - \frac{2}{3} T_1 + \frac{1}{3} - \frac{2}{3} \frac{R}{W} + \frac{2}{3} \frac{R}{W^2} \tag{4.28}$$

where

$$R \equiv \left(\frac{3}{8}\right)^4 \left(\frac{\overline{\beta}_A}{\overline{\beta}}\right)^4 \quad \text{and} \quad W = 1 - R \,.$$

The constant Padé approximated mass gap lines are shown in Fig. 4.7. There is no turn up and they are straight lines in the intermediate region like the Padé approximated string tension lines. It is also of interest to study the other Padé approximations for a comparison.

4.4 Scaling, universality and the Monte Carlo simulations - An Investigation using the ratio $m/\sqrt{K}$.

Having calculated Ka^2 and ma we would like to see a plot for $m/\sqrt{K}$ versus $\overline{\beta}$ along various lines in the fundamental-adjoint plane. There are various reasons for that; the obvious one being that we want to know the value for $\dot{m}/\sqrt{K}$. The second reason follows from the fact that $m/\sqrt{K}$ must stay constant in a scaling region; hence it is a good parameter to test scaling. It is also a good parameter to test universality. In other words, $m/\sqrt{K}$ must give the same plot along different lines in the fundamental-adjoint plane when one is close enough to the continuum limit so that scaling has set in. However, having a phase line approaching to the Wilson axis but terminating at a critical endpoint can potentially violate scaling and universality. Such a violation will mean that that the critical endpoint is not the true continuum limit and any prediction for a physical observable by a calculation which has been performed close to the phase line, such that universality and scaling do not

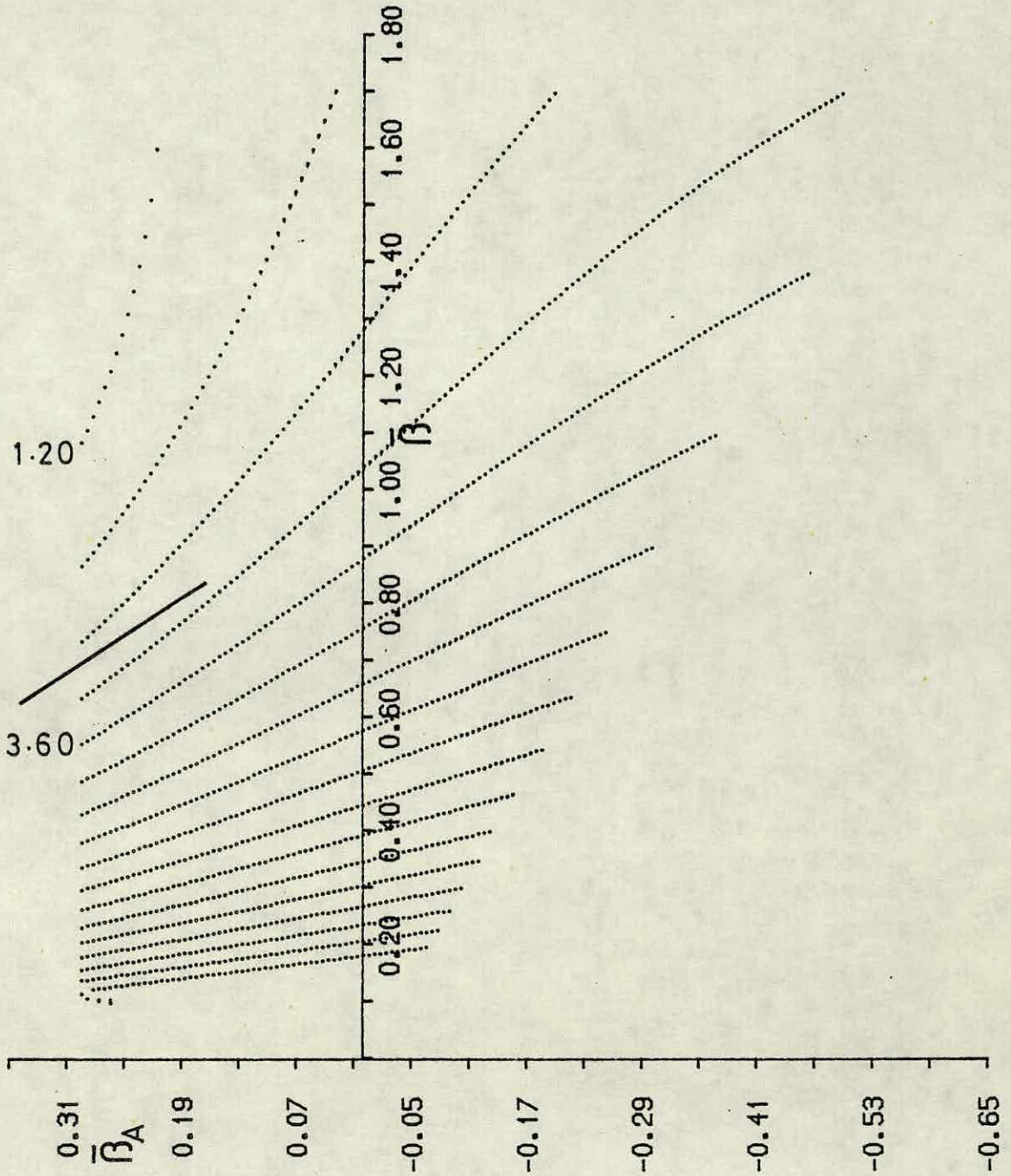

Fig. 4.7: As Fig. 4.6c but for Padé approximated eqn. (4.21).

hold, is not reliable. In particular, we want to investigate whether the intermediate region on the Wilson axis is a region where scaling and universality hold. The importance of that region follows from the fact that it is believed to be the region close enough to the continuum limit so that weak coupling scaling law holds. Therefore, the Monte Carlo simulations measuring the Wilson loops and correlation functions have been done on that region. Hence, before we draw the plots for $m/\sqrt{K}$ and discuss the implications, we shall mention some of these numerical calculations relevant to the subject, their predictions and their situation at present.

In a Monte Carlo simulation, to measure string tension one considers ratios of Wilson loops [Cruetz (1980b)] such as

$$f_2 = \frac{W(i_1,i_2)}{W(i_3,i_4)}$$

$$f_4 = \frac{W(i_1,i_2)W(i_3,i_4)}{W(i_5,i_6)Wi_7,i_8)} \qquad (4.29)$$

where $W(i_1,i_2)$ denotes the expectation of a rectangular Wilson loop of the lattice dimensions i_1 by i_2. Because the loops are finite, in addition to the area law, there should be perimeter dependence from the self energies of the quark sources and yet further corrections from perturbative gluon exchange across the loops. To cancel out this distraction, one imposes constraints

$$i_1 + i_2 = i_3 + i_4$$

and (4.30)

$$i_1 + i_2 + i_3 + i_4 = i_5 + i_6 + i_7 + i_8$$

for f_2 and f_4 respectively. Both f_2 and f_4 directly measure exponential of the string tension Ka^2 provided the loops in consideration are large or else the coupling constant is large.

Present time computers are not powerful enough to perform a calculation for couplings smaller than the couplings in the intermediate region, hence the Monte Carlo simulation results so far have been for $\beta \lesssim 6.2$. That is to say, they have been performed in a narrow region on the Wilson axis very close to the critical endpoint of the fundamental-adjoint plane. That also applies to the mass gap measurements where one simulates the correlation of two Wilson loops at a given distance.

Measurements of the dimensionful string tension K and mass gap m follow from the scaling law (3.21). One seeks scaling consistent with the weak coupling behaviour, hence Monte Carlo results are the results for $\frac{\sqrt{K}}{\Lambda_L}$ and $\frac{m}{\Lambda_L}$ where Λ_L is given by eqn. (3.19). There are various simulation results available in the literature for $\frac{\sqrt{K}}{\Lambda_L}$ [Cruetz and Moriarty (1982b); Gutbrod et al. (1983); Gutbrod and Montvay (1983); Parisi et al. (1983); De Forcrand et al. (1985b)] and for $\frac{m}{\Lambda_L}$ [Hamber and Parisi (1981); Berg and Billoire (1982a,b); Ishikawa et al. (1982); Ishikawa et al. (1983); Michael and Teasdale (1983); Berg and Billoire (1983a, b); De Forcrand et al. (1985a)]. The ratio $m/\sqrt{K}$ from these results is not consistent and it varies from 1.6 to 2.8, depending on which calculation one chooses. That is not the only ambiguity these results show. There are problems related to scaling of the string tension and the ratio $m/\sqrt{K}$. Even the latest simulations [De Forcrand et al. (1985a, b)], which measure both the string tension and the mass gap by using the same method, give a result for $m/\sqrt{K}$ which varies even with a small change

in the coupling. It was also found that the string tension drops faster than the asymptotic freedom formulas [Gutbrod et al. (1983); Barkai et al. (1984)]. Only in a narrow coupling constant range has asymptotic freedom been seen which constrasts with the SU(2) case where scaling sets in as soon as the data breaks away from the strong coupling expansion. On the other hand, simulations with SU(5) have found the drop in the string tension even faster than the SU(3) case [Barkai et al. (1983)], which is what one would expect due to the fact that SU(5) undergoes a first-order phase transition on the Wilson axis.

A semi-perturbative improvement of the asymptotic freedom formula was developed [Martin et al. (1985)] and a wider region, over which one may extrapolate Monte Carlo results to their continuum limit, was found. This suggests that the fast drop in the string tension might be due to some sizeable contributions from non-perturbative phenomena, and the two-loop perturbative result has been naively used so far to observe scaling, even though the simulations have been done at $g \gtrsim 1$.

The γ-function (usually referred to as the β-function in the literature) defined by eqn. (3.15) has been calculated along the Wilson axis [Hasenfratz et al. (1984); Bowler et al. (1985); Gupta et al. (1985)], using the non-perturbative numerical techniques known as the Monte Carlo renormalization group method. First the ratios, as in eqn. (4.29), are taken and then compared with ratios formed from loops whose edges are twice as long. They satisfy the renormalization group equation

$$f_2(2i_1, 2i_2, \ldots; \beta; L) = f_2(i_1, i_2, \ldots; \beta'; L/2). \quad (4.31)$$

Any linear combination of the functions f_2, f_4, ... defined in eqn. (4.29) satisfies eqn. (4.31) also. Thus $\Delta\beta(\beta) \equiv \beta - \beta'$ is the change of the coupling constant required to decrease the lattice spacing by a factor of 2. The function $\Delta\beta(\beta)$ is directly related to the integral of the inverse of the γ-function and contains the same information:

$$\int_{\beta}^{\beta-\Delta\beta} \frac{dx}{x^{3/2}\,\gamma_{\text{funct.}}\sqrt{6/x}} = \frac{2}{\sqrt{6}} \int_{a}^{a/2} \frac{da}{a} = -\frac{2\log 2}{\sqrt{6}} \quad (4.32)$$

In Fig. 4.8 we show $\Delta\beta$ as a function of β as obtained by Hasenfratz et al. (1984), using the improved ratio method. In this method, the mixing coefficients are determined by the requirement of cancelling the lattice artifact corrections to eqn. (4.31) systematically, order by order, in perturbation theory. We have also shown the predictions for $\Delta\beta$ obtained from the string tension [Gutbrod et al. (1983); Barkai et al. (1984)] and the critical temperature T_c [Celik et al. (1983); Karsch and Petronzio (1983)] on the same graph. We observe that the string tension and deconfinement temperature scale in agreement with the non-perturbative γ-function. However, it appears [De Forcrand et al. (1985a)] that the mass gap has a qualitatively different behaviour and is consistent with asymptotic scaling in the intermediate region. As a consequence of the difference of scaling between the string tension and the mass gap the ratio $m/\sqrt{K}$ does not show scaling. The inconsistencies exhibited by the Monte Carlo simulations still survive.

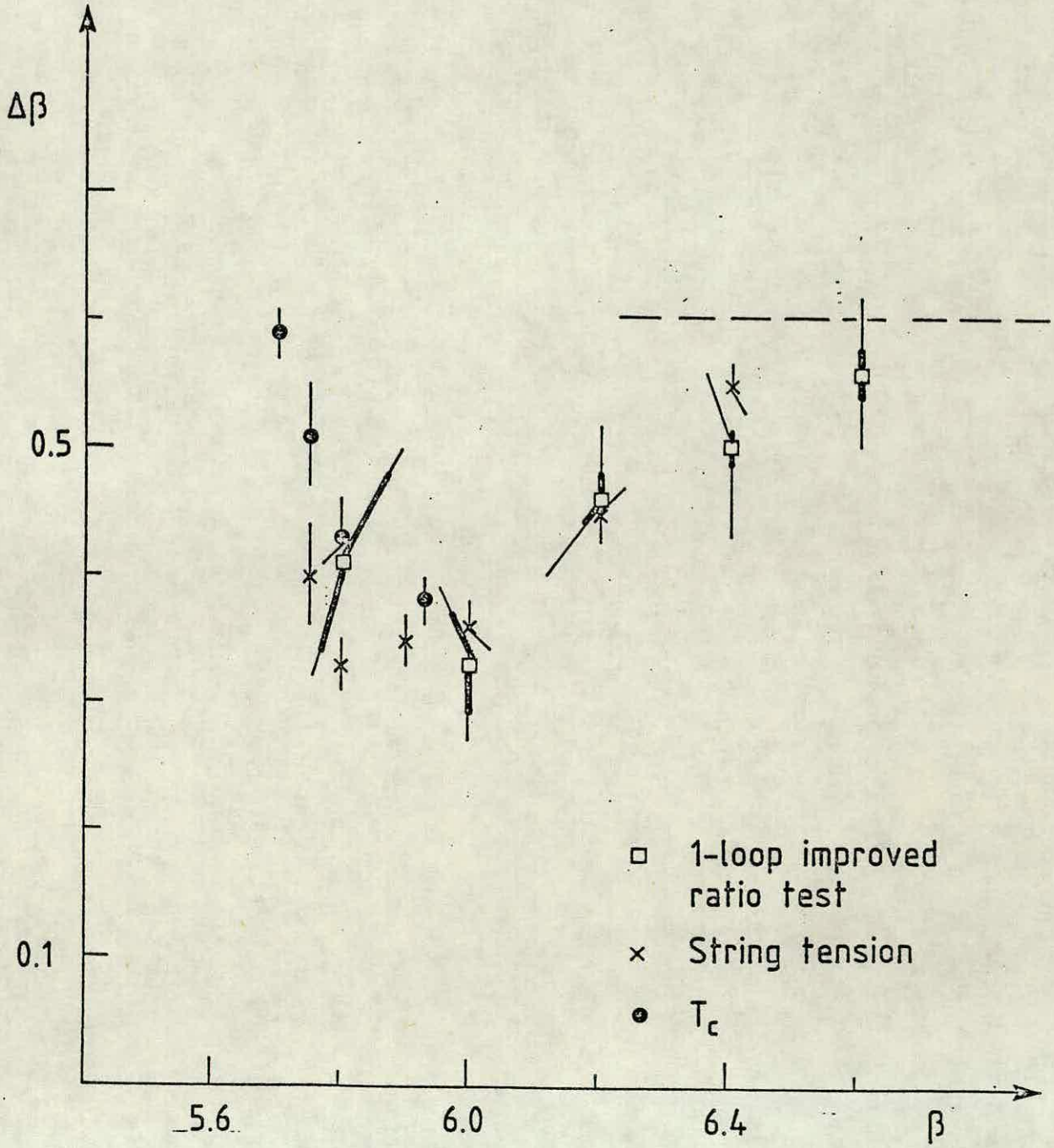

Fig. 4.8: The shift $\Delta\beta$ as obtained by Hasenfratz et al. (1984) using the improved ratio test. The predictions from the string tension and the critical temperature are also shown. The dashed line corresponds to the two-loop perturbative result

We now return to our calculations and plot $\frac{m}{\sqrt{K}}$ against $\bar{\beta}$ along various lines in the fundamental-adjoint plane, using the results in the previous two sections. We have chosen six different lines, namely $\frac{\bar{\beta}_A}{\bar{\beta}} = \frac{1}{4}, \frac{1}{6}, 0, -\frac{1}{6}, -\frac{1}{4}, -\frac{1}{3}$, to study the behaviour of $\frac{m}{\sqrt{K}}$. Note that $\frac{\bar{\beta}_A}{\bar{\beta}} = -\frac{1}{4}$ line is naively the line on which we should approach the continuum limit more quickly than on any other line. This is because, as shown by Barkai et al. (1984), in a perturbative expansion of the action, terms of $O((ga^2)^4)$ vanish. We have shown the plot along those lines in Fig. 4.9a, b, c where both ma and Ka^2 are $O(1)$, $O(2)$ and $O(3)$ respectively. We have also shown the same plot using the Padé approximated ma and Ka^2 in Fig. 4.10.

In Fig. 4.9a, we observe neither universality nor scaling and $m/\sqrt{K}$ falls rapidly along the six lines. This is because the order of the strong coupling series used in this graph is too low.

In Fig. 4.9b, we still do not observe universality. However, we see a sign of scaling along the lines with negative $\bar{\beta}_A$, but not along the Wilson axis or above it.

In Fig. 4.9c, we observe a behaviour clearly consistent with universality in the negative $\bar{\beta}_A$ region; in fact, $m/\sqrt{K}$ behaves almost identically along the three lines in that region. However, there is no universality for $\bar{\beta}_A \gtrsim 0$; we do not observe any less directional dependence in the behaviour of $m/\sqrt{K}$ in that region than in the same region in Fig. 4.9a, b. We also observe that universality and scaling go together; there is no scaling in the positive $\bar{\beta}_A$ region, contrary to the negative $\bar{\beta}_A$ region where we

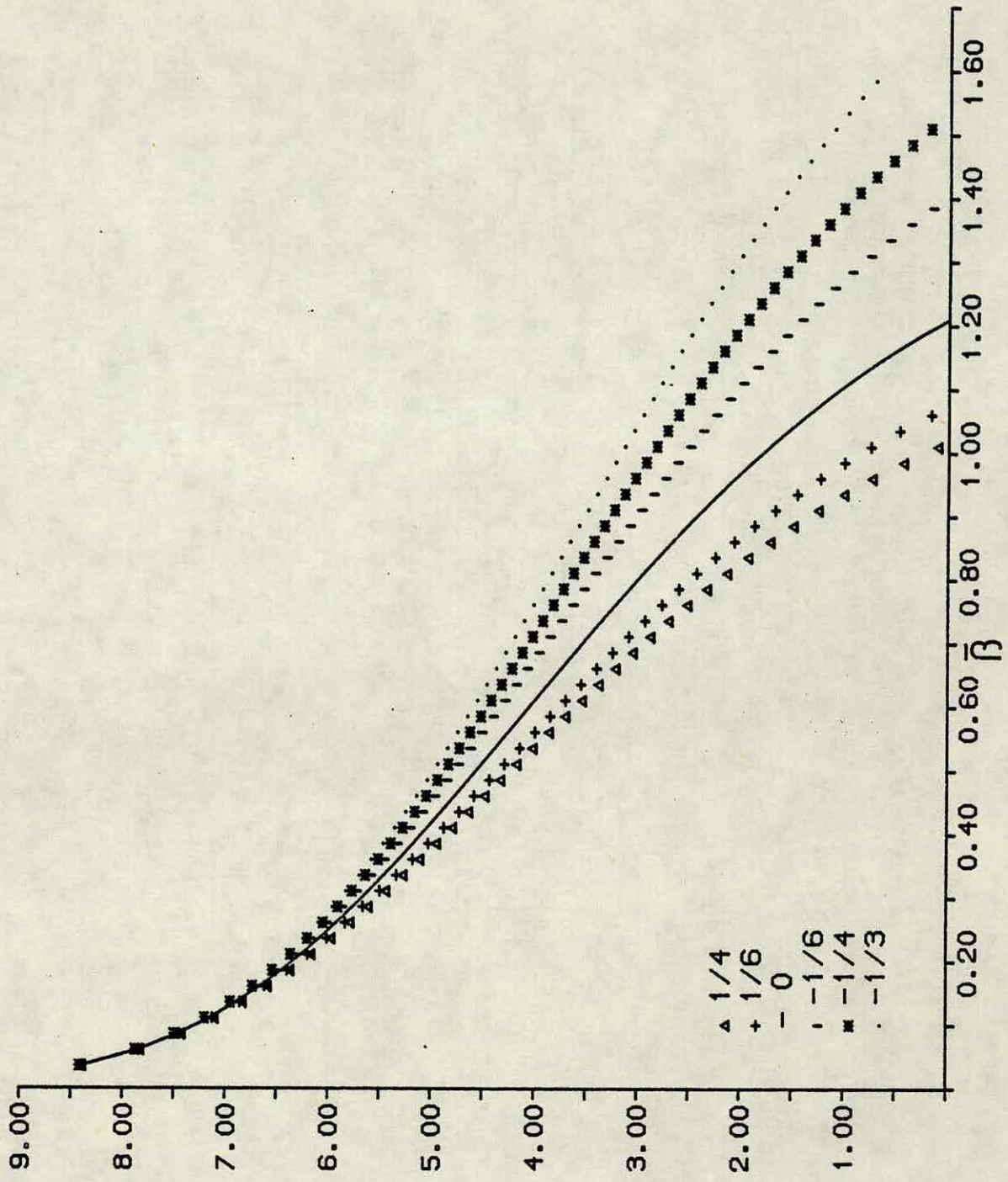

Fig. 4.9a: The behaviour of $\frac{m}{\sqrt{K}}$ along $\frac{\bar{\beta}_A}{\bar{\beta}} = \frac{1}{4}, \frac{1}{6}, 0, -\frac{1}{6}, -\frac{1}{4}, -\frac{1}{3}$ lines in the fundamental-adjoint plane, where both ma and Ka^2 are $O(1)$ from eqns. (4.20) and (4.9) respectively.

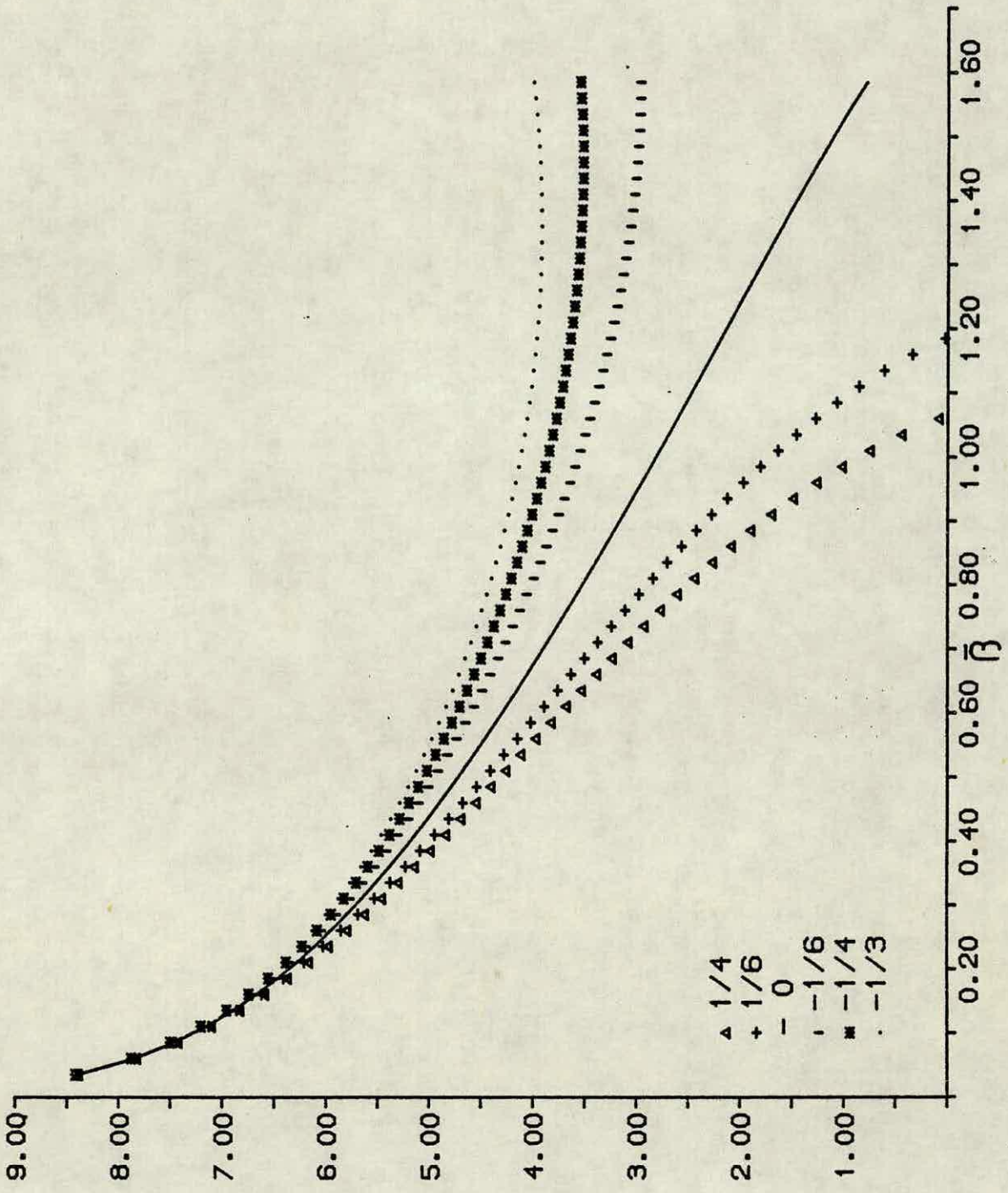

Fig. 4.9b: As Fig. 4.9a but for the O(2) ma and Ka^2.

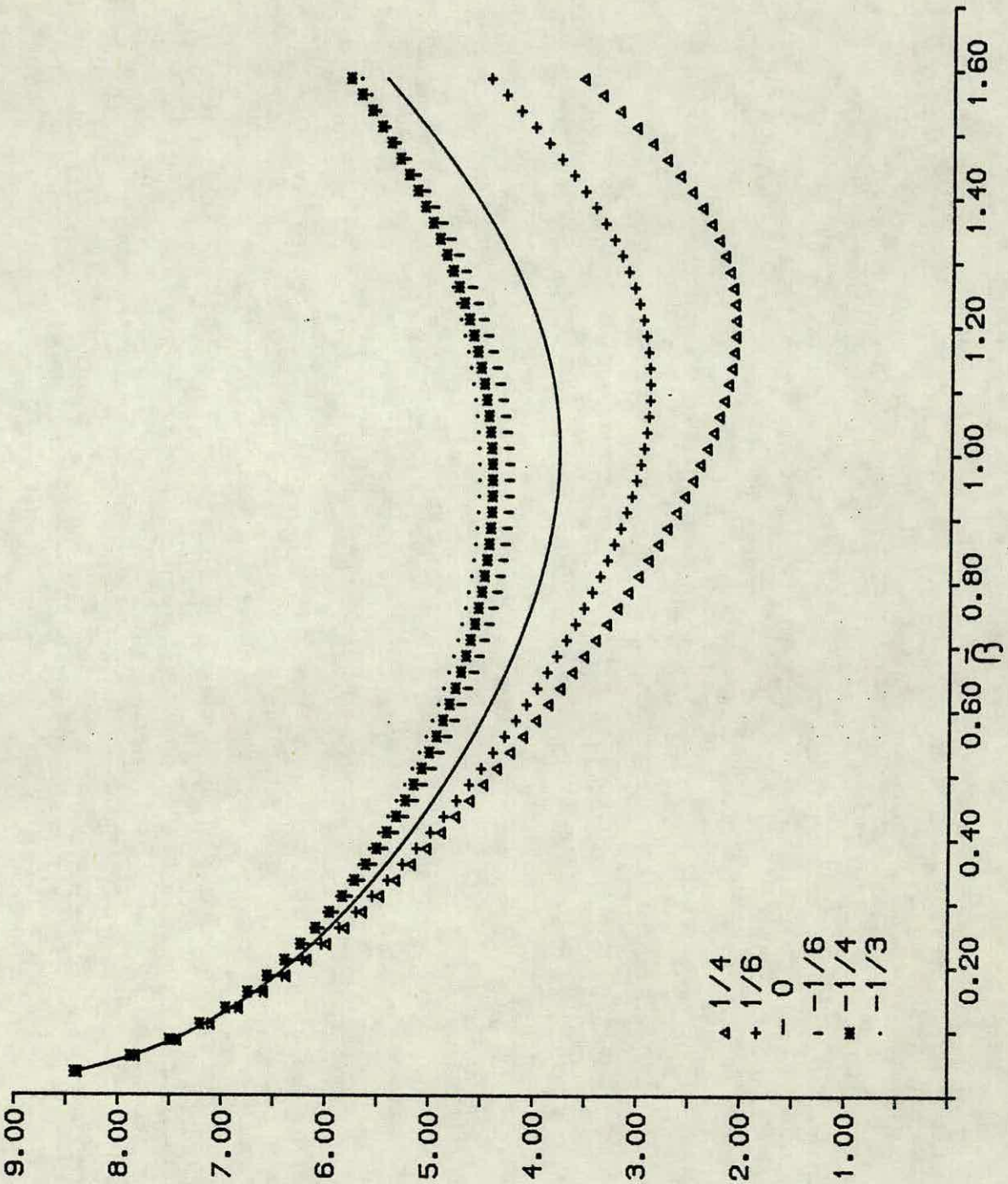

Fig. 4.9c: As Fig. 4.9a but for the O(3) ma and Ka^2.

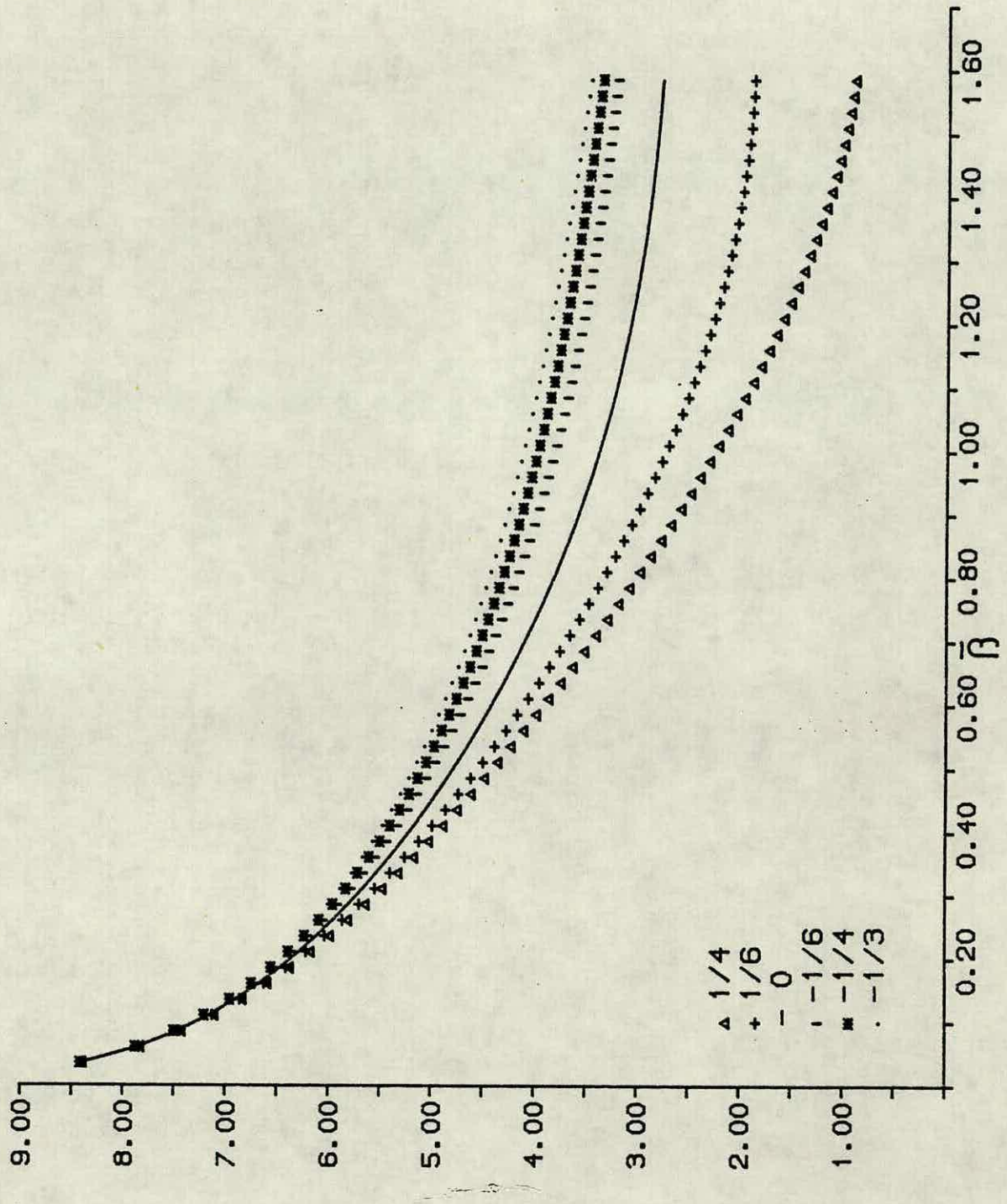

Fig. 4.10: As Fig. 4.9 but for the Padé approximated ma and Ka^2 from eqns. (4.21) and (4.10) respectively.

see a good sign of scaling as we reach the intermediate values of $\overline{\beta}$. Even though there is a narrow region on the Wilson axis, where there might be an indication of scaling before our strong coupling series break down, $m/\sqrt{K}$ shows a smoother behaviour along the lines in the negative $\overline{\beta}_A$ region and scaling sets in earlier than it does on the Wilson axis.

One might suggest that the higher order terms in the strong coupling series may change the situation in the $\overline{\beta}_A \geq 0$ region such that universality holds everywhere in the fundamental-adjoint plane. However, in Fig. 4.9c, we observe that even for small values of $\overline{\beta}$, where the strong coupling series are reliable even at low orders, the ratio lines for $\overline{\beta}_A \geq 0$ start to spread out. Hence, such an effect from the higher order terms is very unlikely. Besides, the Padé approximated ratio lines in Fig. 4.10 do not display any better universality in that region.

Another significant observation we make is that, because of the lack of universality in the $\overline{\beta}_A \geq 0$ region, the value for $m/\sqrt{K}$ gets bigger as we move from the positive $\overline{\beta}_A$ region towards the negative $\overline{\beta}_A$ region where it becomes stable. The higher order terms in the strong coupling calculation can change the value of $m/\sqrt{K}$ along the Wilson axis as well as in the negative $\overline{\beta}_A$ region. However, as was argued in the previous paragraph, it is very unlikely that the Wilson axis will be included in the universality region under the effect of the higher order contributions. Hence, the value for $m/\sqrt{K}$ on the Wilson axis will still be lower than the value in the universality region.

Our observations so far have been qualitative rather than

quantitative. Even though one can estimate the value for $m/\sqrt{K}$ from Fig. 4.9c and Fig. 4.10, it would not be a precise one, partially because our series expansions are at relatively low orders and partially because, in general, strong coupling expansions are not capable of giving precise quantitative answers in the intermediate region, even at high orders. However, we can still make a rough estimate. Consider the Wilson line in Fig. 4.9c. The value we observe on this line is higher than the high order strong coupling series estimates in the literature. However, we expect the value in Fig. 4.9c to get smaller as the higher order contributions are included in our calculations. The Padé approximated calculation indeed gives a lower value, as seen in Fig. 4.10. We estimate that $m/\sqrt{K}$ is about 3.0 on the Wilson axis and about 3.5 in the negative $\bar{\beta}_A$ region.

As we have pointed out, measurement of a physical observable using the lattice formulation must be done in a region where both scaling and universality hold. Our observations tell us that this condition is satisfied only in the negative $\bar{\beta}_A$ region below the Wilson axis as long as we are not in the deep weak coupling region. Therefore, the Monte Carlo simulations which have been performed in the intermediate region on the Wilson axis should be looked upon with suspicion, even if they show some form of scaling. Reliable simulation results should be obtained by working below the Wilson axis by means of the fundamental-adjoint mixed action. Such a simulation should give $m/\sqrt{K}$ higher than the simulation results on the Wilson axis, probably as high as 4.

We also observe, in Fig. 4.9c and Fig. 4.10, that as we approach the critical endpoint we see more and more "unnatural" behaviour; scaling is totally lost for the positive values of $\overline{\beta}_A$ and universality gets worse. This suggests that the loss of scaling and universality for the non-negative values of $\overline{\beta}_A$ is caused by the presence of the phase line and the critical endpoint in the upper half of the fundamental-adjoint coupling constant plane. That confirms our original assumption that the presence of a phase structure affects the physics in its neighbourhood, hence such a neighbourhood should be avoided. This observation also shows that the critical endpoint is not the true continuum limit.

The specific heat defined by

$$C = \frac{\partial}{\partial \beta} \langle \mathrm{Re}\ X(p) \rangle \qquad (4.33)$$

has been studied numerically [Bowler et al. (1984)] along various lines in the fundamental-adjoint plane. That study has found that the specific heat shows a peak on the Wilson axis. However, the peak disappears as one moves down into the negative adjoint plane. This is parallel to our observations from the behaviour of $m/\sqrt{K}$. Bowler et al. (1984) have also found that the hadron masses calculated in the negative adjoint plane are in better agreement with experimental values.

4.5 Renormalization Group Analysis

Numerical Wilson action studies of the non-perturbative γ-function have found a "dip" at about $\beta = 6$ as was shown in Fig. 4.8. The dip might be because of the contributions from the higher order terms in the perturbation theory. It might also be because of the presence of the critical endpoint in the fundamental-adjoint plane. However, a high order perturbative calculation [Ellis and Martinelli (1984)] finds no indication of such a dip. Since, for the positive values of $\overline{\beta}_A$, the coupling constant is smaller, it is very unlikely that the higher order terms in the perturbation theory are responsible for the dip. One can only attribute the dip to the line of first-order transition close by. That was the suggestion made by Bowler et al. (1985). They claim that, for large β, the renormalization group flow away from the critical endpoint is expected to impede the flow in from $\beta = \infty$. However, for β sufficiently small, the flows will reinforce each other and increase the flow towards the fixed point $\beta = \beta_A = 0$, hence the "dip".

The renormalization group function defined by

$$\gamma(C) = -a \frac{d\overline{\beta}}{da} \tag{4.34}$$

along various lines in the fundamental-adjoint plane can be studied using the mixed action string tension and mass gap results to investigate the behaviour near the critical endpoint and far from it. C in eqn. (4.34) corresponds to $\overline{\beta}_A / \overline{\beta}$ for a given line. One obtains $\gamma(C)$ from Ka^2 by keeping K fixed as well as from ma by keeping m fixed. Note that by fixing two different physical

quantities we are picking two different renormalization schemes. Thus, it is not expected that the $\gamma(C)$ obtained from string tension will be equal to the $\gamma(C)$ obtained from mass gap. Nevertheless, both of the γ-functions must yield the same ultraviolet fixed points if the continuum limit is to be unique.

We have shown $\gamma(C)$ for six different values of C in Fig. 4.11, as obtained from the $O(3)$ Ka^2 and in Fig. 4.12 as obtained from the Padé approximated Ka^2. Note that these figures do not rediscover the dip. Considering the figures are obtained from the strong coupling expansion calculation of the string tension, that is not unexpected. However, we observe that the γ-function, for a fixed $\bar{\beta}$, gives smaller values as the critical endpoint is approached. We have also studied the γ-function along the lines parallel to the Wilson axis, where one observes that the γ-function for small values of $\bar{\beta}$ gives almost the same values for different lines. Nevertheless, as $\bar{\beta}$ is increased one obtains increasingly different values on different lines. Hence we conclude that the γ-function is suppressed by the presence of the first-order phase line and critical endpoint in the fundamental-adjoint plane. Thus, we expect a numerical calculation performed along a line in the negative adjoint plane to find either no dip or a smaller dip in the γ-function.

The $\gamma(C)$ has also been shown in Fig. 4.13 and Fig. 4.14 as obtained from the $O(3)$ ma and Padé approximated ma respectively. The value of $\gamma(C)$ along a particular line is lower than the $\gamma(C)$ obtained from the string tension along the same line.

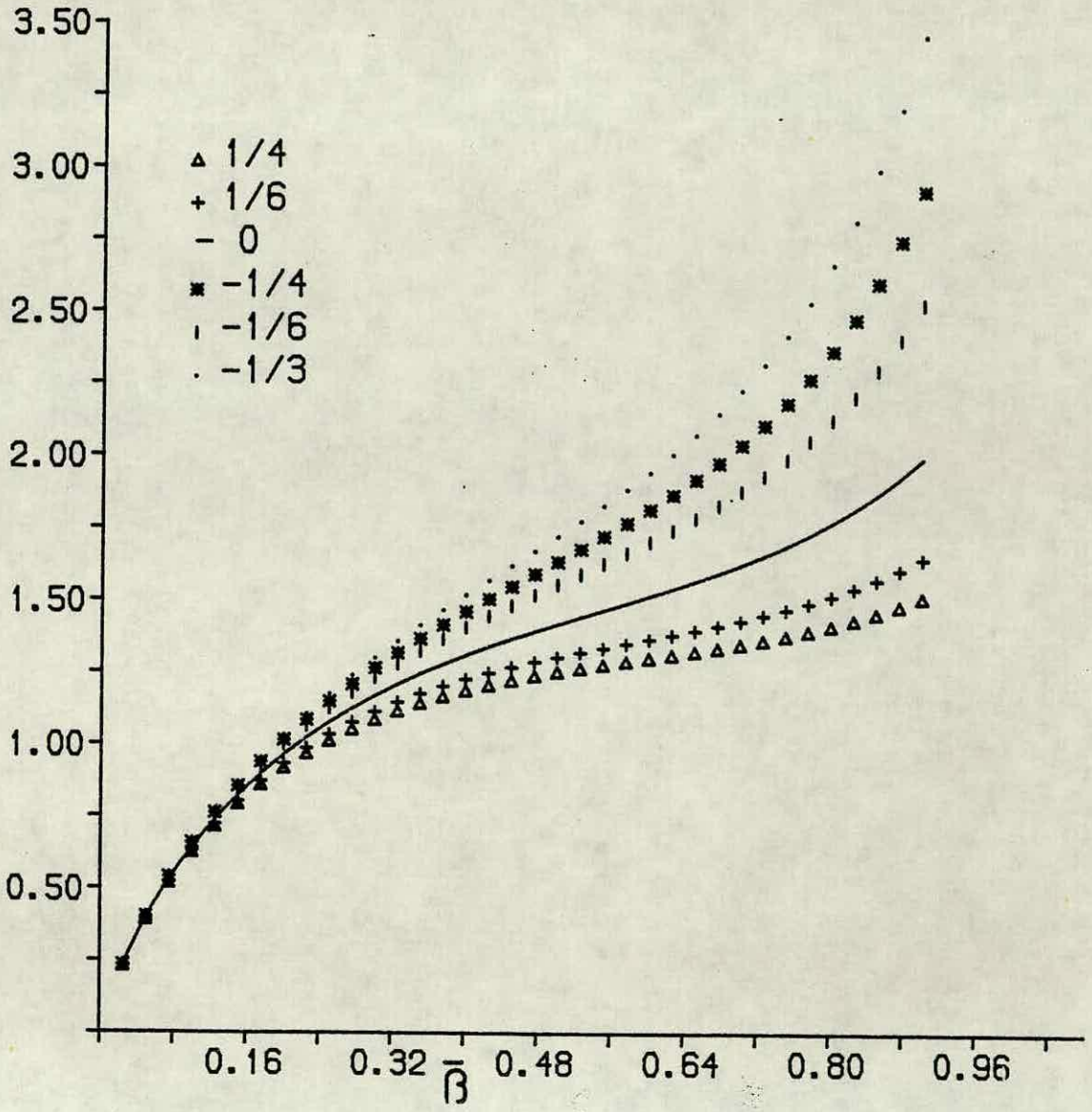

Fig. 4.11: $\gamma(C)$ as obtained from the O(3) Ka^2 along $C \equiv \bar{\beta}_A/\bar{\beta} = \frac{1}{4}, \frac{1}{6}, 0, -\frac{1}{6}, -\frac{1}{4}, -\frac{1}{3}$ lines in the fundamental-adjoint plane.

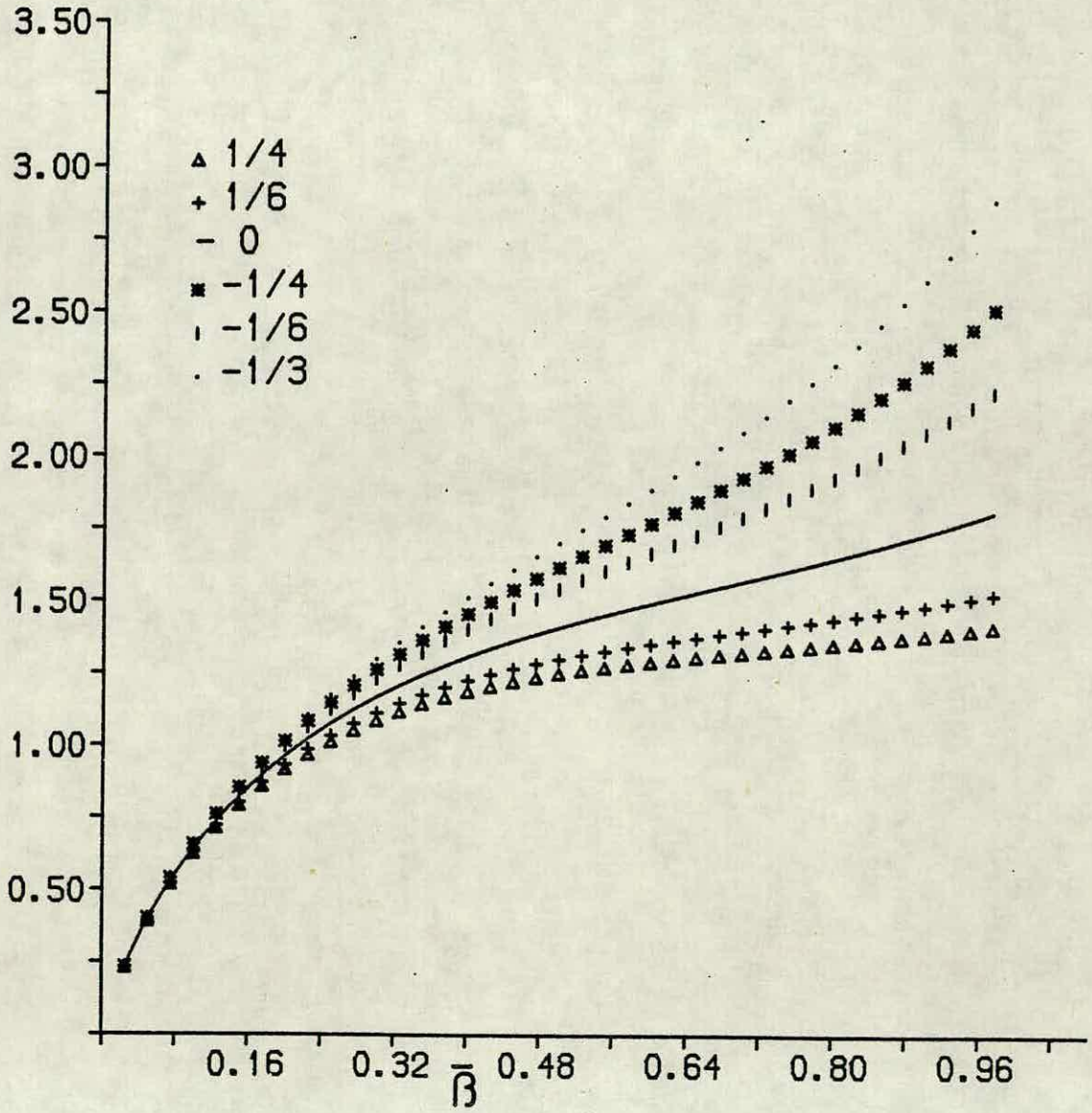

Fig. 4.12: As Fig. 4.11 but from the Padé approximated Ka^2.

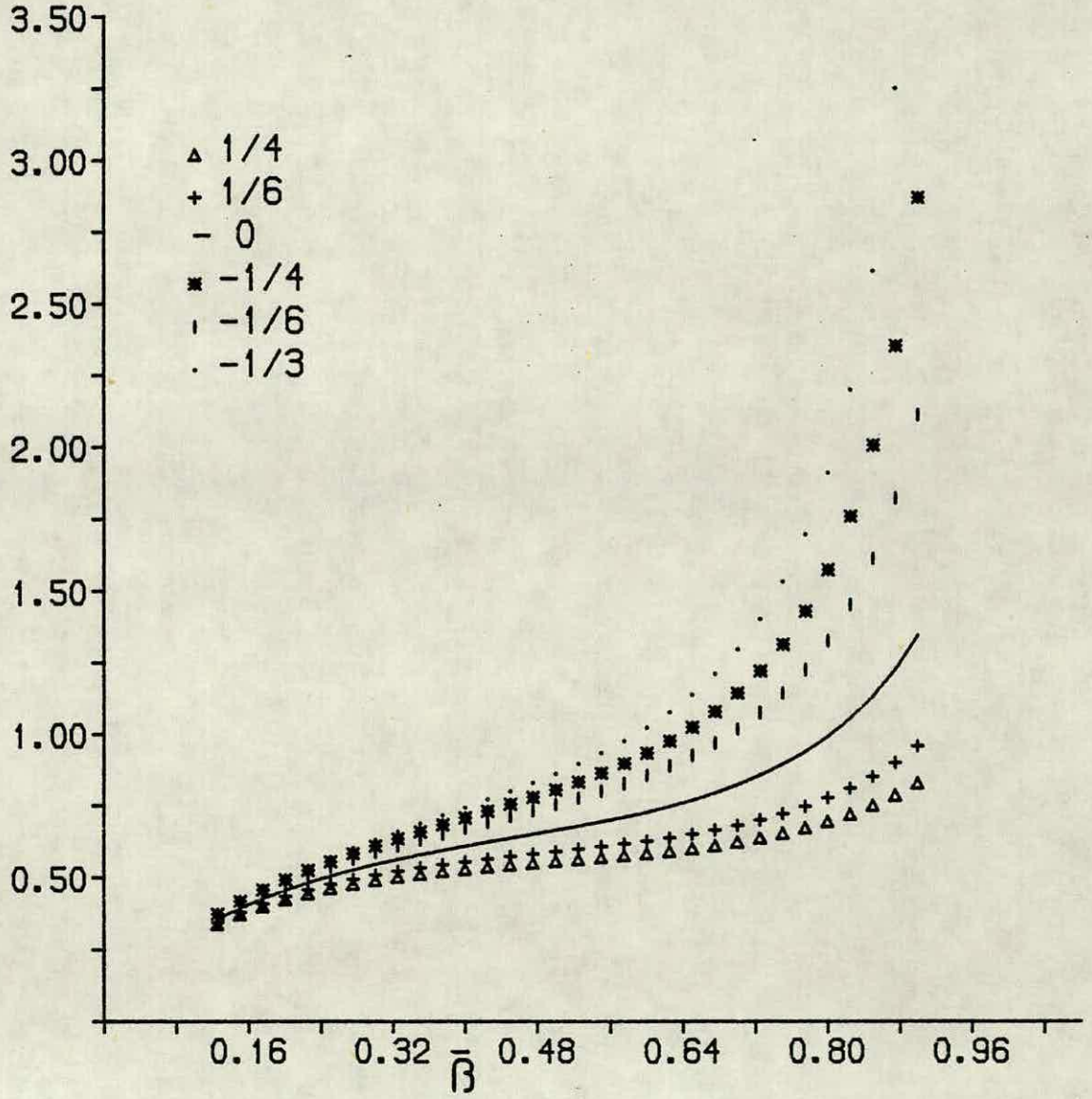

Fig. 4.13: $\gamma(C)$ as obtained from the O(3) ma along $C \equiv \bar{\beta}_A/\bar{\beta} = \frac{1}{4}, \frac{1}{6}, 0, -\frac{1}{6}, -\frac{1}{4}, -\frac{1}{3}$ lines in the fundamental-adjoint plane.

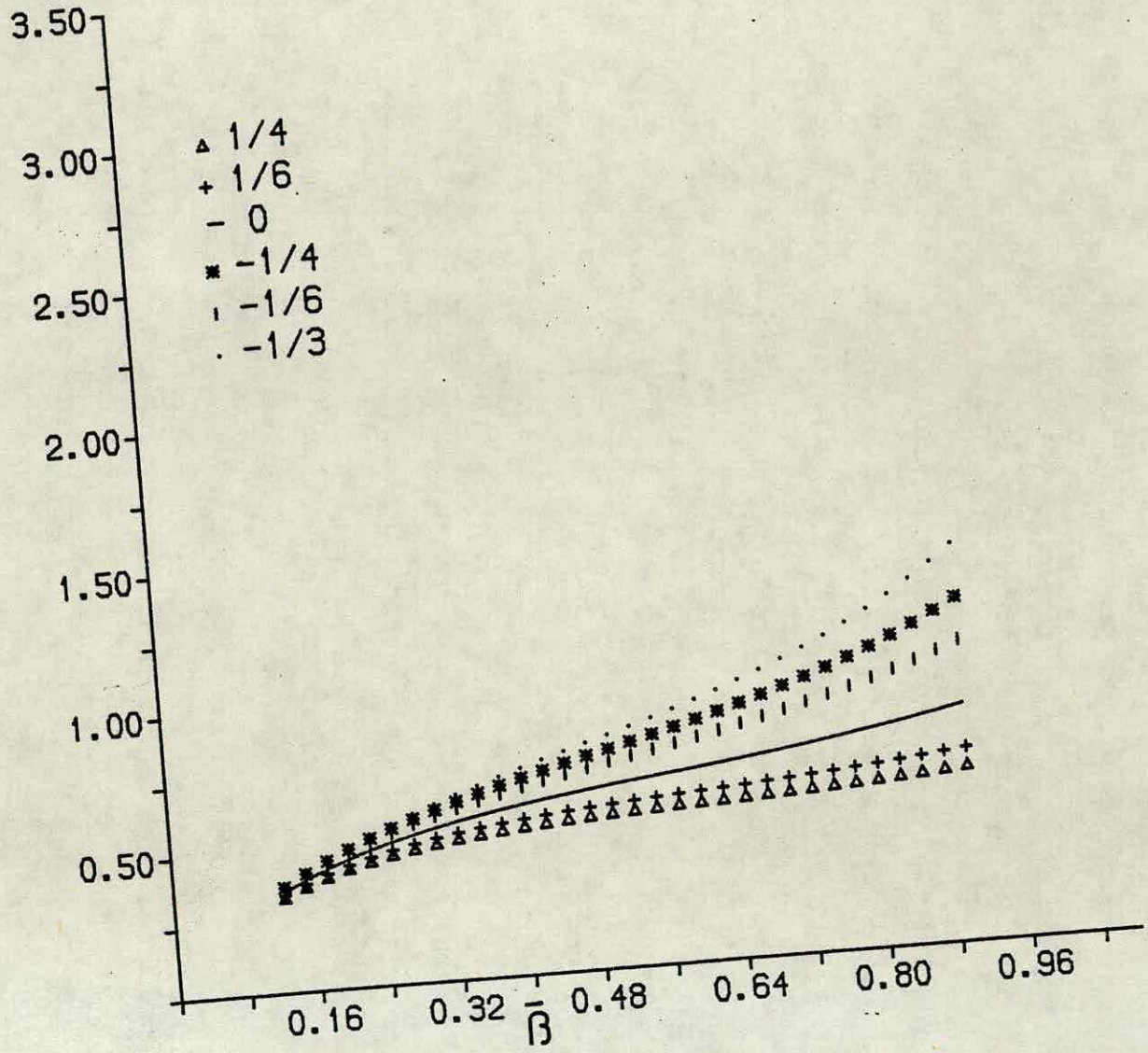

Fig. 4.14: As for Fig. 4.13 but from the Padé approximated ma.

That is because, in general, two different renormalization schemes give two different γ-functions. However, we still observe the suppression of the γ-function near the critical endpoint.

The renormalization group flows in the fundamental-adjoint plane have been studied [Bitar et al. (1984)] using the Migdal-Kadanoff transformation techniques. It is also possible to study the flows using the mixed action string tension and mass gap results. One defines two renormalization group functions:

$$\gamma_F = -a \frac{d\bar{\beta}}{da}$$

and

$$\gamma_A = -a \frac{d\bar{\beta}_A}{da} \quad , \tag{4.35}$$

which can be obtained by fixing the string tension and mass gap simultaneously. However, we will not go into the calculation.

4.6 Added Remark

After the completion of our work on the subject, an improved action Monte Carlo calculation of the string tension and mass gap has been published [Patel et al. (1986)]. They find that $m/\sqrt{K} = 3.1(3)$, in the negative adjoint plane, which is significantly higher than any previous Monte Carlo calculation has been done on the Wilson axis. The study also finds that $m/\sqrt{K}$ shows a better scaling in the negative adjoint plane than on the Wilson axis. Those results are in agreement with the observations we have made from the $m/\sqrt{K}$ plots.

CHAPTER 5

SUMMARY AND CONCLUSIONS

As was discussed in the introduction, gauge invariance is the crucial concept on which all the accepted field theories of elementary particles are based. Another important concept is the formulation of a quantum theory in terms of functional integration which enables us to understand the subject deeper, and provides us with a powerful mathematical method and a bridge between quantum theory and statistical physics.

Gauge theories, particularly non-abelian ones, need to be studied using non-perturbative methods. The lattice provides a regularized version of the theory which meets this requirement, through an elegant formulation which preserves the gauge invariance of the theory. It also provides a mathematically satisfactory definition of a gauge invariant quantum field theory in which rigorous results can be derived.

In Chapter 2 our concern was perturbative massive scalar electrodynamics to one-loop in d dimensions. It was seen that the infrared divergence problem can be overcome using a non-vanishing photon mass. As a part of the chosen renormalization scheme, the assigned photon mass had to be related to the scalar field mass, in fact equal to it, to preserve the Ward identity. Renormalization group related studies of the N component model in three dimensions have shown that the stability of the superconducting fixed point changes at $N = 229.6$, which is lower than

the ε-expansion estimate. The renormalization group flows in three dimensions were seen to behave in the same way as the flows near four dimensions. Hence, it was concluded that the one-loop perturbative calculation in three dimensions yields the same type of phase transition as the ε-expansion does near four dimensions. Even though it would be useful to calculate the higher contributions in perturbation theory, a full account of the subject can not be possible without a non-perturbative treatment.

A review of pure lattice gauge theories and the strong coupling expansion methods had been the subject in Chapter 3. Group integration on on the lattice was also introduced, and some integrals for the SU(3) gauge group were calculated.

In Chapter 4 our subject was pure SU(3) lattice gauge theory in the fundamental-adjoint plane. The string tension and the mass gap were calculated to O(8) and O(3) respectively, using the fundamental-adjoint action, as functions of the character expansion coefficients in the strong coupling expansion. The O(3) string tension and mass gap results, and their Padé approximations, as functions of the two coupling parameters were used to plot the constant string tension and mass gap lines in the fundamental-adjoint plane. These results were also used to study the behaviour of $m/\sqrt{K}$ and the renormalization group function along various lines in the fundamental-adjoint plane.

It was seen that the structure of the constant string tension lines from our calculations is in close agreement with the numerically estimated lines, and the constant mass gap lines display a very similar structure to the string tension ones.

The ratio $m/\sqrt{K}$ has shown universality along the lines in the negative half of the adjoint plane, but not in the positive half. The Wilson axis was found to lie outside the universality region. It was also seen that $m/\sqrt{K}$ behaves smoother along the lines in the negative adjoint region and scaling sets in earlier. As the critical endpoint is approached scaling is totally lost. In connection with the lack of universality in the non-negative adjoint plane, the value of $m/\sqrt{K}$ was found to be larger in the negative adjoint plane than it is in the positive adjoint plane and along the Wilson axis. A recent numerical study [Patel et al. (1986)], published after the completion of our work on the subject, finds a larger $m/\sqrt{K}$ and a better scaling in the negative adjoint plane, which is in agreement with our results.

The final part of the work in Chapter 5 was the study of the renormalization group function, and it was seen that both the renormalization group functions, as obtained from the string tension and the mass gap, are suppressed as the first-order phase line and the critical endpoint is approached. Consequently, we have argued that a numerical simulation in the negative adjoint plane should find either no dip or a smaller dip in the renormalization group function.

Those studies indicate that along the Wilson axis and in the positive adjoint plane one gets spurious effects, which we interpret as a consequence of the existence of a phase structure close by. However, the negative adjoint plane appears to be out of the reach of those spurious effects, hence the physics extracted in that region should be reliable. Consequently, we expect numerical simulations

which one performs in the negative adjoint plane using an improved action to exhibit no inconsistencies and to find more realistic results.

The strong coupling expansions which use the fundamental-adjoint mixed action seem to be more fruitful than the Wilson action ones, even at low orders. Although it would be interesting to perform the same analysis in Chapter 4, using a mass gap result at higher orders and our O(8) string tension result, it is not expected that the qualitative features we have drawn will change.

It is clear that strong coupling calculations, either analytic or numerical, are essential in the study of non-abelian gauge theories and in the applications of quantum field theory to the statistical physics problems.

APPENDIX

In this appendix we list the formulas used in Chapter 2 for the calculation of the renormalization constants. We refer the reader to 't Hooft and Veltman (1972) for a systematic discussion. The Feynman integral

$$\frac{1}{D_1^{a_1} D_2^{a_2} \cdots\cdots D_k^{a_k}} =$$

$$= \frac{\Gamma(a_1+a_2+ \cdots +a_k)}{\Gamma(a_1)\Gamma(a_2) \cdots \Gamma(a_k)} \int_0^1 \cdots \int_0^1 dx_1 \cdots dx_k \frac{\delta(1-x_1-\cdots-x_k)\, x_1^{a_1-1} x_2^{a_2-1} \cdots x_k^{a_k-1}}{(D_1x_1+D_2x_2+ \cdots + D_kx_k)^{a_1+a_2+\cdots+a_k}} \tag{A-1}$$

along with the following integral formulas in the Euclidean space enabled us to solve the integrals in Chapter 4:

$$\int_E \frac{d^dq}{(2\pi)^d} \frac{1}{(q^2+2p\cdot q+R^2)^A} = \frac{\Gamma(A-d/2)}{(4\pi)^{d/2}\,\Gamma(A)} \frac{1}{(R^2-p^2)^{A-d/2}} \tag{A-2}$$

$$\int_E \frac{d^dq}{(2\pi)^d} \frac{q^2}{(q^2+2p\cdot q+R^2)^A} = \frac{1}{(4\pi)^{d/2}\Gamma(A)} \left[p^2 \frac{\Gamma(A-d/2)}{(R^2-p^2)^{A-d/2}} + \frac{d}{2} \frac{\Gamma(A-1-d/2)}{(R^2-p^2)^{A-1-d/2}} \right] \tag{A-3}$$

$$\int_E \frac{d^dq}{(2\pi)^d} \frac{q_\mu}{(q^2+2p\cdot q+R^2)^A} = -\frac{\Gamma(A-d/2)}{(4\pi)^{d/2}\Gamma(A)} \frac{p_\mu}{(R^2-p^2)^{A-d/2}} \tag{A-4}$$

$$\int_E \frac{d^dq}{(2\pi)^d} \frac{q^4}{(q^2+R^2)^A} = \frac{\Gamma(A-2-d/2)}{(4\pi)^{d/2}\Gamma(A)} \frac{(d^2+2d)}{4} \frac{1}{(R^2)^{A-2-d/2}} . \tag{A.5}$$

REFERENCES

Arnison, G. et al. {UA1 collab.}, Phys. Lett. 122B (1983a) 103.

Arnison, G. et al. {UA1 collab.}, Phys. Lett. 129B (1983b) 273.

Arroyo, A., C.P. Korthals-Altes, J. Peiro and M. Perrottet, Phys. Lett. 116B (1982) 414.

Bagnaia, P. et al. {UA2 collab.}, Phys. Lett. 129B (1983) 130.

Balian, R. and G. Toulouse, Phys. Rev. Lett. 30 (1973) 544.

Balian, R., J. Drouffe and C. Itsykson, Phys. Rev. D11 (1975) 2098.

Banner, M. et al. {UA2 collab.}, Phys. Lett. 122B (1983) 476.

Barkai, D., M. Cruetz and K.J.M. Moriarty, Phys. Rev. D28 (1983) 2101.

Barkai, D., K.J.M. Moriarty and C. Rebbi, Phys. Rev. D30 (1984) 1293.

Becchi, C., A. Rouet and R. Stora, Phys. Lett. 52B (1974) 344.

Beg, M.A.B. and H. Ruegg, J. Math. Phys. 6 (1965) 677.

Berg, B. and A. Billoire, Phys. Lett. 113B (1982a) 65.

Berg, B. and A. Billoire, Phys. Lett. 114B (1982b) 324.

Berg, B. and A. Billoire, Nucl. Phys. B221 (1983a) 109.

Berg, B. and A. Billoire, Nucl. Phys. B226 (1983b) 405.

Bhanot, G., Phys. Lett. 108B (1982) 337.

Bhanot, G. and M. Cruetz, Phys. Rev. D24 (1981) 3212.

Bhanot, G. and R. Dashen, Phys. Lett. 113B (1982) 299.

Bitar, K.M., D.W. Duke and M. Jadid, FERMILAB Report No. 84/82-T(1984).

Bitar, K.M., S. Gottleib and C.K. Zachos, Phys. Rev. D26 (1982) 2853.

Bjorken, J.D., Phys. Rev. 179 (1969) 1547.

Bowler, K.C., D.L. Chalmers, A. Kenway, R.D. Kenway, G.S. Pawley and D.J. Wallace, Nucl. Phys. B240 [FS12] (1984) 213.

Bowler, K.C., A. Hasenfratz, P. Hasenfratz, U. Heller, F. Karsch, R.D. Kenway, H. Meyer-Ortmanns, I. Montvay, G.S. Pawley and D.J. Wallace, Nucl. Phys. B257 [FS14] (1985) 155.

Brézin, E., J.C. Le Guillou and J.C. Zinn-Justin, Phys. Rev. D8 (1973a) 434.

REFERENCES (Contd.)

Brezin, E., J.C. Le Guillou and J.C. Zinn-Justin, Phys. Rev. D8 (1973b) 2418.

Bricmont, J., J. Lebowitz and Ch. Pfister, On the surface tension of Lattice systems, Rutgers University preprint, New Brunswick (1979).

Callan, C., Phys. Rev. D2 (1970) 1541.

Cashwell, W.E., Phys. Rev. Lett. 33 (1974) 244.

Celik, T., J. Engels and H. Satz, Phys. Lett. 129B (1983) 323.

Chen, J.H., T.C. Lubensky and D.R. Nelson, Phys. Rev. B17 (1978) 4274.

Coleman, S. and E. Weinberg, Phys. Rev. D7 (1973) 1888.

Cruetz, M., J. Math. Phys. 19 (1978) 2043.

Cruetz, M., Phys. Rev. D21 (1980a) 2308.

Cruetz, M., Phys. Rev. Lett. 45 (1980b) 313.

Cruetz, M., Phys. Rev. Lett. 46 (1981) 1441.

Cruetz, M., Quarks, Gluons and Lattices, (Cambridge University Press) (1983).

Cruetz, M., L. Jacobs and C. Rebbi, Phys. Repts. 95 (1983) 201.

Cruetz, M. and K.J.M. Moriarty, Phys. Rev. D25 (1982a) 1724.

Cruetz, M. and K.J.M. Moriarty, Phys. Rev. D26 (1982b) 2166.

Dasgupta, C. and B.I. Halperin, Phys. Rev. Lett. 47 (1981) 1556.

Dashen, R., U. Heller and H. Neuberger, Nucl. Phys. B215 [FS7] (1983) 360.

De Forcrand, Ph., G. Schierholz, H. Schneider and M. Teper, Phys. Lett. 152B (1985a) 107.

De Forcrand, Ph., G. Schierholz, H. Schneider and M. Teper, Phys. Lett. 160B (1985b) 137.

De Witt, B.S., Phys. Rev. 162 (1967a) 1195.

De Witt, B.S., Phys. Rev. 162 (1967b) 1239.

Dirac, P.A.M., Physikalische Zeitschrift der Sowjetunion 3 (1933) 64.

Drouffe, J.M., Phys. Rev. D18 (1978) 1174.

Drouffe, J.M. and J.B. Zuber, Phys. Repts. 102 (1983) 3.

REFERENCES (Contd.)

Duncan, A. and H. Vaidya, Phys. Rev. D20 (1979) 903.

Elitzur, S., Phys. Rev. D12 (1975) 3978.

Ellis, R.K. and G. Martinelli, Frascati Preprint LNF-84/1(P) (1984).

Fadeev, L.D. and V.N. Popov, Phys. Lett. 25B (1967) 29.

Feynman, R.P., Rev. Mod. Phys. 20 (1948) 267.

Fisher, M.E., Phys. Rev. Lett. 30 (1973) 679.

Gastmans, M. and R. Meuldermans, Nucl. Phys. B63 (1973) 277.

Gell-Mann, M., Phys. Lett. 8 (1964) 214.

Gell-Mann, M. and F. Low, Phys. Rev. 95 (1954) 1300.

Glashow, S.L., Nucl. Phys. 22 (1961) 579.

Gross, D. and F. Wilczek, Phys. Rev. Lett. 30 (1973a) 1343.

Gross, D. and F. Wilczek, Phys. Rev. D8 (1973b) 3633.

Grossman, B. and S. Samuel, Phys. Lett. 120B (1983) 383.

Gupta, R., G. Guralnik, A. Patel, T. Warnock and C. Zemach, Phys. Lett. 161B (1985) 352.

Gutbrod, F. and I. Montvay, Preprint, DESY 83-112.

Gutbrod, F., P. Hasenfratz, Z. Kunszt and I. Montvay, Phys. Lett. 128B (1983) 415.

Halliday, I. and A. Schwimmer, Phys. Lett. 101B (1981) 327.

Halperin, B.I. and T.C. Lubensky, Solid State Commun. 14 (1974) 997.

Halperin, B.I., T.C. Lubensky and Shang-Keng Ma, Phys. Rev. Lett. 32 (1974) 292.

Hamber, H. and G. Parisi, Phys. Rev. Lett. 47 (1981) 1792.

Hasenfratz, A.E. and P. Hasenfratz, Nucl. Phys. B180 (1981) 353.

Hasenfratz, A.E., P. Hasenfratz, U. Heller and F. Karsch, Phys. Lett. 143B (1984) 193.

REFERENCES (Contd.)

Hasert, F.J. et al., Phys. Lett. 46B (1973) 138.

Higgs, P.W., Phys. Lett. 12 (1964a) 132.

Higgs, P.W., Phys. Rev. Lett. 13 (1964b) 508.

Higgs, P.W., Phys. Rev. 145 (1966) 1156.

Irving, A.C. and C.J. Hamer, Nucl. Phys. B230 (1984a) 361.

Irving, A.C. and C.J. Hamer, J. Phys. A14 (1984b) 1649.

Ishikawa, K., A. Sato, G. Schierholz and M. Teper, Z. Phys. C21 (1983) 167.

Ishikawa, K., G. Schierholz and M. Teper, Phys. Lett. 116B (1982) 429.

Itzykson, C., M. Peskin and J.B. Zuber, Phys. Lett. 95B (1980) 259.

Jona-Lasinio, G., Nuovo Cimento 34 (1964) 1790.

Jones, D.R.T., Nucl. Phys. B75 (1974) 531.

Jurkiewicz, J., C.P. Korthals-Altes and J.W. Dash, Nucl. Phys. B233 (1984) 457.

Karsch, F. and R. Petronzio, Phys. Lett. 139B (1984) 403.

Karsten, L.H. and J. Smit, Nucl. Phys. B183 (1981) 103.

Kawai, H. and R. Nakayama, Phys. Lett. 113B (1982) 329.

Kawamoto, N. and J. Smit, Nucl. Phys. B192 (1981) 100.

Kennedy, A.D., J. Kuti, S. Meyer and B.J. Pendleton, Phys. Lett. 155B (1985) 414.

Kimura, N., Prog. Theor. Phys. 64 (1980) 310.

Kogut, J.B., Rev. Mod. Phys. 51 (1979) 659.

Kogut, J.B., Rev. Mod. Phys. 55 (1983) 775.

Kogut, J.B. and D.K. Sinclair, Phys. Rev. D24 (1981) 1610.

Kogut, J.B. and L. Susskind, Phys. Rev. D11 (1975) 395.

Kogut, J.B., D.K. Sinclair and L. Susskind, Nucl. Phys. B114 (1976) 199.

Kogut, J.B., D.K. Sinclair, R.B. Pearson, J.L. Richardson and J. Shigemitsu, Phys. Rev. D23 (1981) 2945.

REFERENCES (Contd.)

La Rue, G.S., J.D. Phillips and W.M. Fairbank, Phys. Rev. Lett. 46 (1981) 967.

Lautrup, B. and Nauenberg, Phys. Lett. 95B (1980a) 63.

Lautrup, B. and M. Nauenberg, Phys. Rev. Lett. 45 (1980b) 1755.

Lawrie, I.D., J. Phys. C: Solid State Physics 15 (1982) L879.

Lüscher, M., Comm. Math. Phys. 54 (1977) 283.

Lüscher, M., G. Münster and P. Weisz, Nucl. Phys. B180 (1981) 1.

Mack, G. and V.B. Petkova, Ann. Phys. (N.Y.) 125 (1980) 117.

Manton, N.S., Phys. Lett. 96B (1980) 328.

Marinari, E., G. Parisi and C. Rebbi, Phys. Rev. Lett. 47 (1981) 1795.

Martin, O., K. Moriarty and S. Samuel, Phys. Lett. 153B (1985) 87.

Menotti, P. and E. Onofri, Nucl. Phys. B190 (1981) 288.

Michael, C. and I. Teasdale, Nucl. Phys. B215 [FS7] (1983) 433.

Moriarty, K.J.M., Phys. Lett. 106B (1981) 130.

Münster, G., Z. Phys. C6 (1980) 175.

Münster, G., Nucl. Phys. B180 [FS2] (1981a) 23.

Münster, G., Nucl. Phys. B190 [FS4] (1981b) 439.

Münster, G., Nucl. Phys. B200 [FS4] (1982a) 536.

Münster, G., Nucl. Phys. B205 [FS5] (1982b) 648.

Münster, G., Phys. Lett. 121B (1983) 53.

Osterwalder, K. and E. Seiler, Ann. Phys. (N.Y.) 110 (1978) 440.

Parisi, G., R. Petronzio and F. Rapuano, Phys. Lett. 128B (1983) 418.

Patel, A., R. Gupta, G. Guralnik, G.W. Kilcup and S.R. Sharpe, Phys. Rev. Lett. 57 (1986) 1288.

Politzer, H.D., Phys. Rev. Lett. 30 (1973) 1346.

REFERENCES (Contd.)

Salam, A., Elementary Particle Theory {ed. N. Svartholm} (Stockholm: Almquist, Forlag A.B.) (1968) 367.

Schwinger, J., Phys. Rev. 82 (1951) 914.

Seo, K., Nucl. Phys. B209 (1982) 200.

Seo, K. and A. Ukawa, Phys. Lett. 114B (1982) 329.

Sykes, M.F., D.S. Gaunt, P.D. Roberts and J.A. Wyles, J. Phys. A5 (1972) 640.

Symanzik, K., Commun. Math. Phys. 49 (1970) 424.

't Hooft, G. and M. Veltman, Nucl. Phys. B44 (1972) 189.

Tomboulis, E.T., Phys. Rev. Lett. 50 (1983) 12.

Villain, J., J. Phys. (Paris) 36 (1975) 581.

Wegner, F., J. Math. Phys. 12 (1971) 2259.

Weinberg, S., Phys. Rev. Lett. 19 (1967) 1264.

Weingarten, D., Phys. Lett. B109 (1982) 57.

Wilson, K.G., Phys. Rev. Lett. 28 (1972) 548.

Wilson, K.G., Phys. Rev. D10 (1974) 2445.

Wilson, K.G., New Phenomena in Subnuclear Physics {ed. A. Zichichi} (Plenum Press, N.Y.) (1977).

Wilson, K.G. and M.E. Fisher, Phys. Rev. Lett. 28 (1972) 240.

Wilson, K.G. and J.B. Kogut, Phys. Repts. C12 (1974) 75.

Yang, C.N. and R. Mills, Phys. Rev. 96 (1954) 191.

Zinn-Justin, J., Lectures delivered at the Cargése Summer School 1973. K. Symanzik, op. cit. and K.S.

Zweig, G., CERN report no. 8182/TH401 (1964).